# MICROYIELD PROPERTIES OF TELESCOPE MATERIALS

CONTRACT NAS 1-8851

FINAL REPORT

January 21, 1970



PREPARED FOR

NATIONAL AERONAUTICS AND SPACE ADMINISTRATION

LANGLEY RESEARCH CENTER

HAMPTON, VIRGINIA

AEROSPACE SYSTEMS DIVISION THE BOEING COMPANY SEATTLE, WASHINGTON

NASA CR-66886

# MICROYIELD PROPERTIES OF TELESCOPE MATERIALS

by

W. William Woods

FINAL REPORT

January 21, 1970



Prepared under Contract NAS 1-8851

by

Aerospace Systems Division
THE BOEING COMPANY
Seattle, Washington

for

NASA/LANGLEY RESEARCH CENTER

Hampton, Virginia

ABSTRACT

Torsional and axial measurements of yield strain in beryllium-0.2%-Fe alloy are compared and found to have good agreement in accordance with the octagonal stress theory. Silicic materials, including CER-VIT, fused silica, and ULE fused silica, were also tested and found to have no apparent yield up to 70 $MN/M^2$ stress when etched. With untreated ground surfaces, apparent yield approaching one microstrain is observed in torsion with the silicic materials. Time dependent strain characteristics for the four materials are presented and discussed.

TABLE OF CONTENTS

TABLE OF CONTENTS (CONCLUDED)

LIST OF ILLUSTRATIONS

LIST OF ILLUSTRATIONS ( CONCLUDED)

# 1.0 SUMMARY

The principal objective of this program, which is the correlation of torsional shear with tension and compression measurements in the micro-yield region, has been achieved, with comparison of both yield (nonrecoverable) and delayed elastic (viscoelastic) strain characteristics.

Materials tested include fused silica (Corning 7940), titanium-doped silica (Corning 7971), CER-VIT 101 (Owens-Illinois), and Beryllium-0.2% iron alloy.

The beryllium-iron alloy was the only material tested in this program exhibiting significant yield strain. The measured yield strain characteristic follows the Ramberg-Osgood relationship over four orders of magnitude of strain. The torsional shear yield, after correction for the solid rod geometry, was found to correlate well with the tensile and compressive yield values as predicted by the octagonal shear stress theory.

The absence of significant yield in the silicic materials after removal of surface damage by etching is at variance with previous work with unetched materials. Surface grinding damage has been established as the responsible factor for this apparent yield.

All materials tested in this program exhibit delayed elastic strain characteristics in accordance with the Nutting relationship. Representative curves are presented for each material.

## 2.0 INTRODUCTION

Large diffraction-limited space optics require structural strain stabilities of $10^{-8}$. A thorough understanding of candidate mirror substrate materials is essential; otherwise, an effective space mirror system will not be attainable. The object of this program is to determine the amount of permanent deformation that occurs in typical mirror substrates after they are subjected to various degrees of stress.

As a part of its inhouse research, The Boeing Company has developed the capability of testing materials for residual or nonrecoverable shear strain in the range of $10^{-6}$ to $10^{-10}$ after release of applied torsional stress. The equipment and test programs with which it has been used are described in references 1 and 2.

Most conventional structural test work is concerned with tensile yield measurements in the range of $10^{-3}$ or greater. This has been extended by several workers to the range of $10^{-6}$ strain, and by a few to $10^{-7}$, at which point severe problems with equipment and material stability have been encountered. The torsion test equipment mentioned above was designed to extend measurement capability by several orders of magnitude.

The sensitivity and stability obtained with the torsional apparatus have allowed the measurement and analysis of material properties previously unreported. Correlation with previously existing tension and compression data was very sketchy, owing to lack of reported measurements. The reported measurements (reference 3) appeared to correlate reasonably well, but the range of overlap was small, and only tension was reported.

As the mechanisms responsible for the effects noted in the high precision torsion tests (reference 1) were not fully understood, the relationship between the shear properties and linear strain properties of the materials in the same order of magnitude could not readily be established except by experiment. It was advisable, therefore, to perform tension and compression tests of as near comparable precision as possible to that of the established torsion capability so that a comparison and correlation of material properties could be made.

The inherent high mechanical amplification of strain motions and the first-order cancellation of linear expansion afforded by torsion apparatus allow measurements to be made with much more precision than in a linear tension-compression system. The strain precision limit of the tension-compression apparatus is of the order of $2 \times 10^{-8}$, as compared to the $5 \times 10^{-10}$ level attained with the torsion apparatus. This still allows a large overlap below and above the 1-microstrain ($1 \times 10^{-6}$) value.

The performance of this equipment in advancing the state of art cannot be regarded as a "breakthrough" but only application of good engineering design. The author wishes to express his appreciation of the excellent mechanical design work of Heinz Recker on this equipment.

## 3.0 EXPERIMENTAL APPARATUS

The experimental apparatus used in this program is basically that described in reference 1, with minor design refinements to improve performance. Apparatus for tension-compression measurements has been designed and constructed with precision measurement features similar to those of the torsion facility. Figure 1 is a photograph of the complete apparatus assembly.

### 3.1 THERMAL CONTROL

Two essentially identical double (two-zone) thermal enclosures (figures 2 and 3) have been constructed to allow close control of specimen thermal environment. An enclosure of expanded polystyrene 16 centimeters thick insulates the outer thermal control zone from room ambient temperature. Within this enclosure is another enclosure with walls 2.5 centimeters thick, containing the inner thermal control zone and the test apparatus. Axial fans driven by motors external to the enclosures circulate air in each control zone. A pasteboard windscreen enclosure around the extensometer shields against air turbulence.

Temperature within each enclosure is sensed by a pair of thermistors having a positive temperature coefficient of 12.5% per degree Kelvin. Two fixed resistors, whose value determines the balance temperature, complete the d.c. excited bridge circuit. Bridge unbalance is amplified, time-integrated, and applied to an electric heater, as described in reference 1.

The heavily insulated outer walls of the thermal enclosures were designed for operation at temperatures from 190°K to 340°K. Heat removal in the outer thermal control zone for operation at or below ambient can be controlled by release of liquid carbon dioxide. Operation at other than 306°K is not within the scope of this program, however, and was not implemented.

Steady-state thermal fluctuations within the inner thermal control zone were measured by a platinum resistance thermometer to be within $\pm$500 microdegrees Kelvin. Introduction of hydraulic fluid at laboratory ambient temperatures causes an indicated temperature transient of approximately 5 minutes' duration with limits of -4 and +2 millidegrees Kelvin. Effects of this transient on extensometer indication are not discernible.

The inner thermal control zone is set for a temperature of 306°K and has a steady state electrical power input between 600 and 1,000 milliwatts. The outer zone operates at 1.5°K below the inner zone, with an input of approximately 2.4 watts. Mechanical power input from each fan is estimated at 200 milliwatts. Repeatability of the set point from one run to the next is within $\pm$0.1°K.

The time to reach the set point from a cold start is 45 minutes. Full equilibration requires 12 hours.

## 3.2 TORSION APPARATUS

The torsion apparatus described in reference 1 has been modified to accept a specimen with a test section 5 centimeters long and to apply load hydraulically rather than by gears (figures 4 and 5). The extensometer cups, of one-piece lava construction, are cemented to low-stress shoulders on the specimen and employ four differential transformers to measure differential angular position (figure 6). The specimen (section 4.0) is loaded in torsion by nuts cemented to its threaded end sections. The lower nut is driven by a fork coupled to a universal joint, a strain-gaged lever arm, and a hydraulic cylinder actuator. Backlash in the fork coupling is adequate to ensure complete freedom of motion of the specimen when unloaded. The strain-gaged lever arm senses the torque couple applied by the hydraulic cylinder. With the specimens employed in this program, permissible loading torque is limited by the universal joint rating of 13 Newton-meters. Equivalent specimen outer fiber stress is 124 $MN/m^2$ (18000 psi).

The torsion extensometer has been standardized as in previous programs (reference 1) by optical measurement of angular deflection of the extensometer and by comparison with electrical resistance standards. Figure 7 shows a theodolite set up for autocollimator measurement with two first-surface mirrors attached to the extensometer cups.

The torsion lever-arm load cell was standardized by string-pulley dead weight loading. This was compared against electrical resistance standards which were utilized for equipment standardization at the beginning of each test.

## 3.3 TENSION-COMPRESSION APPARATUS

The tension-compression apparatus, shown in figures 8 through 10, is patterned after the torsion apparatus except for the direction of loading and sensing. Lava cups cemented to the specimen shoulders support four differential transformers to form an extensometer sensitive to axial extension. Spherical steel balls threaded and cemented to the ends of the specimen are restrained in spherical sockets to form ball joints for minimization of bending forces during loading. The lower ball joint is designed with a clearance or backlash of +1.8 mm for complete freedom of the specimen when unloaded. A hydraulic cylinder with a bore of 5.04 cm provides the loading force, which is measured by two strain-gage load cells in the columns of the loading apparatus. With a 6.9 $MN/m^2$ (1000 psi) hydraulic pressure supply, specimen stress of 460 $MN/m^2$ (67000 psi) in tension and 550 $MN/m^2$ (80000 psi) in compression may be produced. The load cells are rated to 8.9 kN (2000 lb) which corresponds to specimen stress of 175 $MN/m^2$ (26000 psi). The load cells may be over-ranged by 50% without damage.

Severe difficulty was experienced in providing reliably adequate core clearance on all four LVDT's during assembly. This problem was solved by providing threaded bushings for installation of the core support rods to the extensometer. Four sets of bushings are provided with 0, 0.13,

0.25, and 0.38 millimeter eccentric offset of the threaded hole. Axial position reference for the eccentric bushings is provided by springloading against the extensometer flange with a second bushing and a rubber O-ring.

The extensometer output was calibrated by deflection of one of the differential transformers with a micrometer over a range of 0.1 millimeter. The output was compared to that produced by resistance-standard signals inserted at the input to the preamplifier, as employed in the torsion system.

Load cells were standardized at a small fraction of their capacity by dead weight loading. Resistance standards, compared to this value, were used for standardization thereafter.

### 3.4 EXTENSOMETER MOUNTING

Mounting of the specimen to the extensometer requires secure attachment to eliminate the possibility of stick-slip operation. Mechanical clamping has been found to be unsatisfactory unless clamping forces approaching the fracture limit of silicic materials are used. These forces produce unacceptable side effects. Thermosetting adhesives do not allow convenient subsequent disassembly. The best alternative is a thermoplastic adhesive.

A commercial structural adhesive, a Phenoxy thermoplastic, was chosen after testing of several alternative cements. The Phenoxy is quite viscous at its softening temperature ($420^{o}K$), and requires a spring-loaded jig for assembly of extensometer to the specimen. Figure 11 shows the tension-compression extensometer mounted in one of the jig fixtures.

### 3.5 LOADING CONTROL SYSTEM

Loading control for both torsion and tension-compression systems was accomplished with simple electrohydraulic controls. An accumulator having a storage capacity of 2 liters, pressurized by a hand pump, serves as the power supply. Solenoid valves control the direction of flow of fluid to the loading cylinders. Pressure-compensated flow-control valves provide selection of constant loading rate independent of supply pressure and specimen load.

A pair of cam-operated switches on the load mechanism indicates direction of departure from the neutral no-load position. An interlock is provided so that when the specimen is under static load, the loading system will actuate only in the direction of decreasing load, thus preventing specimen overloading. The loading control system is presently operated with manual pushbuttons, which are depressed until the desired load or position is reached, as indicated by load and position displays.

The electrohydraulic loading control system was evaluated with specimen test section diameters of 7.1 and 15.2 millimeters. Loading rates from 1 to 100 $MN/m^2$ sec were easily set and controlled with the flow control valves. Load levels are maintained with negligible drift when load control valves are closed.

Transient response of the flow control valves initially caused some concern. The flow surges through the regulator portion of the valve when pressure across the valve is suddenly increased from zero to full supply. This turned out to be an advantage, however, because the flow surge takes up a major portion of the mechanical backlash of the loading system when the load is applied, thus reducing the delay between loading command and start of loading. Upon initiation of unload command, this surge feature unloads the specimen almost instantaneously, regardless of flow control setting. This allows optimum conditions for observation of the delayed elastic effect while retaining convenient control over recentering of the mechanical system.

### 3.6 ELECTRONIC READOUT

Signal processing for the extensometer differential transformers is handled by a solid-state carrier amplifier, designed and built specifically for this application. Voltage gain is variable, in steps of 20 dB, from 20 to 100 dB. The noise figure at the input of the preamplifier has been measured at 3 dB. This allows a close approach to the useful resolution limit of the differential transformers while providing indication over their full operating range.

A bank of relays mounted on the top of the loading structure allows separate monitoring of each differential transformer, two specimen bending modes, and the principal stress mode. The relays are operated by a remote selector switch located outside the enclosures.

Strain gage load cells excited by direct current are monitored with a multirange voltmeter. The output signal is also amplified and fed to a digital voltmeter and printer.

Upon release of load, the digital voltmeter-printer is switched to the extensometer output. The voltmeter-printer is triggered by a sequencer to furnish extensometer deflection readings at time intervals of 5, 50, 500, 5000, and 50000 seconds after load release, each interval length being repeated 9 times. The end of measurement cycle is presettable to any of the above times, stopping the print, and signaling readiness for the next load cycle.

## 4.0 TEST SPECIMENS

Test specimens, as shown in figure 12, have a conventional cylindrical test section terminated by low-stress shoulders to which the extensometer is cemented. Threaded, large cross-section ends allow secure gripping by both torsion and tension-compression loading mechanisms for interchangeability on either system. The ratio of cross section to length of the test section was sized to ensure column buckling stability in compression up to 250 $MN/m^2$ (36000 psi) stress for all candidate materials of this program.

Materials chosen for test were as follows:

| Material | No. of Specimens | Specimen Numbers |
|---|---|---|
| CER-VIT 101 Premium Grade | 4 | 101-104 |
| 7971 ULE Fused Silica Mirror Blank Quality | 4 | 111-114 |
| 7940 Fused Silica Mirror Blank Quality | 4 | 121-124 |
| Beryllium, Fine-Grained 0.2% Iron Alloy, Isostatic Cold Pressed and Sintered | 3 | 131-133 |

Test specimens were machined from each material by the respective material supplier. Upon receipt of the finished specimen, it was subjected to a heat treatment and acid etch prior to testing. Descriptions of the manufacture and treatment of the specimens are presented in Appendix A.

# 5.0 TEST PROGRAM

## 5.1 TEST PROCEDURES

As the fragility of the specimens allowed, each specimen was subjected to three test series: compression, tension, and torsion. Specimens were stress-relieved by an appropriate heat treatment after each test. Possible cumulative effects of sequential testing were evaluated by testing each of the three identical specimens of a given material in a different sequence (tension, compression, torsion) (torsion, tension, compression) (compression, torsion, tension).

For each test, specimens were subjected to unidirectional loads (previous torsion tests were bidirectional), increasing in geometric progression to a maximum stress level of 70 $MN/m^2$ (10 ksi) for the nonmetallic materials and maximum yield level of 30 microstrain for the metal. After the load was removed, the strain recovery was recorded before the subsequent load was applied. The stress level for the nonmetals was chosen to avoid fracture so that each specimen could be subjected to the complete sequence of tests. Duration of "hold" of each load was 30 seconds.

For tension and compression tests the loading strain and extraneous loading magnitudes were measured with the extensometer during loading and after the final viscoelastic decay measurement. Between each pair of load applications, the specimen was completely unloaded and observed for viscoelastic decay and yield strain. The extensometer output was automatically recorded at preselected intervals as described in Section 3.6 to yield sufficient data for determination of specimen return end point.

The deflection of the torsion extensometer under full scale loading conditions exceeds the measurement range of the differential transformer sensors. Measurement of load strain or bending indication is therefore limited to low load ranges.

The test temperature was maintained in all tests at $306^{\circ}K$ with a precision of $0.01^{\circ}K$ or better. A minimum soak time of 16 hours was employed after installation for specimen and apparatus to reach thermal equilibrium.

To reduce excessive breakage of the silicic materials in tension and torsion tests, a light etch was found necessary immediately before installation for each test. This procedure removes surface abrasions and microcracks resulting from handling and mounting in heat treatment fixtures.

Before the start of each test run, a 30-minute drift check was made on the extensometer indication. Indicated drift apparently results from thermal stresses induced in the assembly process, and may take from one half to 3 days to settle to insignificant rates. Where the test schedule permits (as over a weekend), the longer stabilization time was

utilized. In some tests, where the extensive stabilization delay was not practicable, the drift rate was extrapolated and used to compensate ensuing measurements. The minimum stabilization period was kept at 16 hours.

At the start of each test run, the load cell and extensometer readout circuits were standardized on all ranges by signal injection from resistance standards which had been compared previously to physical standards (Sections 3.3 and 3.4). Zero readings on each range were taken as well. The extensometer was generally brought to near-zero indication by adjustable signal injection or "buckout" ahead of the preamplifier, and the adjustment was locked for the entire test sequence.

## 5.2 DATA REDUCTION

Data from each test sequence consisted of a series of annotated number sequences on a paper tape from the printing digital voltmeter. These number sequences, together with additional information such as material type, specimen number, specimen diameter, and date were punched into cards for computer processing. The program used for this purpose is presented in Appendix B, together with a sample output. For further discussion of the procedures involved in the data reduction process, see reference 1.

## 6.0 RESULTS

In the following description of results, stress is expressed in metric units of meganewtons per square meter, A conversion factor the the English system is: 1 ksi = 6.89 $MN/m^2$.

### 6.1 MICROYIELD PROPERTIES

Of the materials tested in this program, only the beryllium alloy exhibited significant yield. The beryllium test results are therefore the logical choice for comparison of torsional and axial yield test methods, and are treated first.

#### 6.1.1 Beryllium -0.2% Iron

The initial torsion test on this material proved it to be surprisingly soft, with an apparent microyield shear strength less than 10 $MN/m^2$. On the suggestion of Dr. John Moberly, the specimen was retested after an aging treatment (Appendix A), and showed an increase of strength of a factor of 2. A conventional linear plot of these two tests is shown in figure 13. Note that when retested in the same direction as the previous load, but with lesser loading, the material exhibits what is termed "strain hardening". That this is applicable only to loads in one direction is demonstrated by reversing the load, whereupon a characteristic softer than that in the original test direction is noted. This effect is commonly termed the Bauschinger effect, and is seldom considered in connection with strain hardening. That this is not peculiar to torsional testing is demonstrated by the curves of figure 14, a and b. Figure 14a shows the annealed, strain-hardened, and Bauschinger axial characteristics for a maximum stress history of 56 $MN/m^2$; and figure 14b for 200 $MN/m^2$. Note that these are log-log plots, and cover several decades of strain. Both the strain-hardened and Bauschinger curves would presumably converge on the annealed curve if taken to higher stress levels.

In order to compare torsional yield to axial yield test data, two factors were applied. The solid rod geometry was compensated for by multiplying the yield data by a factor derived from the log-log slope of the yield curve (reference 1). The true outer fiber shear yield data thus obtained wad divided by $\sqrt{3}$ and the outer fiber shear stress multiplied by a factor of $\sqrt{3}$ to yield equivalent axial strain and axial stress, as derived by the octagonal stress theory (reference 4). The torsional data thus converted are plotted with the axial data in figures 15a, b, and c. The data plots well as a straight line according to Ramberg and Osgood (reference 5) up to a strain level of $10^{-5}$.

As each specimen was to be subjected to three successive tests in different orders, the strain level in each of the first two tests was limited to less than 100 microstrain, to decrease influence on subsequent testing. The final test was taken to the limit of the instrumentation capability, which is slightly greater than 1000 microstrain.

As shown in figure 15a, the effect of aging is to increase all stress

values for a given strain by a factor of 2. This is quite different from the above-mentioned strain hardening in that the hardness increase is nondirectional. The curves for the annealed condition appear to group quite well, except for a tendency of the torsional curves to have a different slope from the axial at the lower stress levels. A summary plot is shown in figure 16.

The present data correlates well with previously reported work, as shown in figure 17. Data from the present work on annealed material overlaps Maringer's work on low oxide beryllium (reference 7), and the aged material corresponds well with Moberly's results on 1% iron alloy (reference 6). Agreement between the earlier work by this author on HPI-40 (reference 2), Maringer on I-400 (reference 7) and Moberly on instrument grade beryllium (reference 6) is also quite reasonable, considering the variability of materials.

### 6.1.2 CER-VIT

The CER-VIT specimens were the first to be received, and consequently suffered the most from the process of learning to operate the revised equipment. Specimen 101, given a cursory test as received from the manufacturer, was broken in disassembly. Specimen 102 suffered from slipping grips in torsion, a fractured thread section in tension, and as a result, poor mounting alignment in compression. Specimen 103 was broken in tension, thus precluding compression and torsion tests. Results of the tests are presented in figure 18 (a through d). These figures and ensuing figures incorporate both positive and negative logarithmic abscissa to indicate nonrecoverable strains. Positive values indicate nonrecoverable strains were in the same direction as the applied stress and negative values indicate strains were opposite in direction to the applied stress. The negative offsets and scatter of the data were discouraging, considering the precision attained in the previous program (reference 3). Even with the reduced measurement precision, however, it was apparent that the yield effects previously measured (ibid) were not forthcoming.

Differences in precision were attributed to the change in end and shoulder geometry, leading to increased stresses at the extensometer cement line, causing yield in the cement. This would account for the sizable "negative yield" encountered. The change in the overall specimen characteristic outside this scatter could not readily be accounted for in this fashion. As the major change in test section treatment between this and the previous program was the removal of surface damage by etching, the etching was assumed responsible for the change in yield characteristic. The cursory results from specimen 101 (fig. 18a), which was given only a very brief etch by the manufacturer, strongly suggest this. To verify this postulate, Specimen 104 was reground, reducing the test section diameter by only enough to give grinding wheel contact over the entire test section. The thread relief between the end threads and the extensometer shoulders was reduced from 19.6 to 12.7 millimeters to reduce stresses at the cement line. As shown in figure 18e, this treatment yielded results similar to those in the previous test program. Re-etching to remove surface damage

restored the no-yield characteristic as shown in the same illustration.

### 6.1.3 ULE Silica

The ULE (titanium doped) silica specimen testing was marred only by the loss of specimens by fracture in test. Here again, as shown in figure 19 (a through c), were found the "negative yield" values, the relatively large data scatter, and the obvious lack of correlation with the previous work of reference 1. Specimen 114, which had not been received until all others had been tested, was reground in the same manner as 104 (Section 6.1.2) and retested. Results of these tests are shown in figure 19d. Regrinding of the test section without subsequent anneal or etch produces large offset, or apparent "yield".

### 6.1.4 Fused Silica

The fused silica tests were similar to the other silicic materials in that no consistent non-recoverable strain (yield) characteristic was found. Measurement data scatter was also comparable. Figure 20 (a through c) displays the results.

An additional test in torsion was run on Specimen 122 to compare the performance of the cement (dop wax) used in the previous program (reference 1) with that used in this program. The results, as shown in figure 20b, indicate the dop wax to be weaker and more susceptible to stress gradients in the specimen extensometer shoulder, but otherwise no significant differences in performance were found.

The first three specimens each completed all three tests (tension, compression and torsion). Specimen 124 therefore was not needed in the originally scheduled test program, and was available for additional tests. A torsion test of specimen 124 in the as-received condition yielded essentially the same results as the etched condition, as shown in figure 20d. After the test section was reground, the consistent yield characteristic appeared and was again removed by etching. Figure 20d shows these results.

## 6.2

Evaluation of the time-dependent strain characteristic of a material is very important to the measurement of non-recoverable (yield) strain in the submicrostrain region, as quite often the yield strain can be determined only by extrapolation of the viscoelastic (time dependent) strain curve. In the work of reference 1, the time-dependent strain was found to plot as a straight line versus time on log-log paper. This conforms with a general materials behavioral characteristic described by Nutting in 1921 (reference 8). This characteristic was employed in the data reduction computer program as presented in Appendix B. The computer program was developed from the one presented in reference 1 to provide extrapolation of time-dependcent strain to its end point. The data reduction and extrapolation process also makes the

time dependent strain available separate from the non-recoverable, or yield strain. The characteristics thus derived are presented in the following subsections in order of specimen testing.

### 6.2.1 CER-VIT

The straight line log-log characteristic was found to fit the CER-VIT performance quite well with very few surprises, as shown in figure 21. The major difference between this work and that of reference 1 is the change in slope from minus one-half to minus one for the etched specimens. That the difference is attributable to removal of surface grinding damage is shown by comparison of figure 21 (a through c) with figure 21d.

The viscoelastic, or time-dependent strain magnitude is seen to be directly proportional to stress in both torsional and axial modes. Although the proportionality constants for tension and compression are essentially identical, that for torsion is almost an order of magnitude greater.

### 6.2.2 Fused Silica and ULE Fused Silica

Extrapolation of the straight-line characteristic of time and viscoelastic (time-dependent) strain in log-log space to infinitesimal values of time would indicate that time-dependent strain increases without limit at time zero. It is obvious that this cannot be so, and the straight-line characteristic does not hold at small values of time. The performance of the etched silica specimens, as shown in figure 22, bear out this conclusion. The strain appears to vary almost linearly with time up to approximately 1 minute after load release, and thereafter as the reciprocal of a power of time, which produces the linear log-log characteristics. This behavior introduced difficulties into the computer reduction of yield data, as shown in figure 22a. In reducing the average curvature of the plotted data to near zero, positive curvature at large values of time was introduced to compensate for the negative values of curvature at small values of time. This led to errors in the extrapolated non-recoverable (yield) values related in Section 6.1. The errors were in general not greater than 30% of the reported values, however, and do not change the appearance of the plots significantly. Further manual reduction of the data produced the revised curve of figure 22a.

The characteristics of the fused silica (Corning 7940) and ULE fused silica (Corning 7971) were very similar in torsion, as may be seen by comparing b and c in figure 22. Compared with the CER-VIT torsion characteristic, they are of lower magnitude by a factor of 8 for equal stress loading.

The tension and compression viscoelastic (time-dependent) strain characteristics were difficult to evaluate, owing to the low strain values and the higher effective noise level of the axial test equipment.

Tension loads were limited by incipient fracture problems, and in general were insufficient to allow reasonable extrapolation. Compression tests on Specimens 113 and 121 yielded data as plotted in d and e, figure 22. Although the data from Specimen 113 was rather noisy, it appeared to duplicate the initial curvature of the torsion tests. Specimen 121, which was taken much higher in loading on its final (compression) test, had much less apparent curvature, and lesser final slope, with the exception of its maximum load. Although the axial slope and curvature characteristics appear somewhat inconsistent, the 1-minute time values of strain agree quite well with those of the torsion characteristics.

Regrinding the specimen without etch or anneal produces the torsional results shown in f and g, figure 22. The magnitude of viscoelastic (time-dependent) strain is grossly increased, and the slope of the line decreased. The increase effectively masks the curvature characteristic shown by the etched material. The topmost curve of 22g has a sharp drop at the end, which is typically indicative of a small uncorrected mechanical drift component.

### 6.2.3 Beryllium

Measurement of the beryllium time-dependent strain characteristic was complicated not so much by the absolute magnitude involved, as by the ratio of viscoelastic (time-dependent) to non-recoverable (yield) strain values. In general the yield strain exceeded the time-dependent strain by a factor of 10 at the minimum, and in most instances by a factor of a few hundred. The time-dependent strain therefore appeared insignificant and was not allowed to run to very long time intervals. The available data are plotted in figure 23. As opposed to the silicic materials, the time-dependent strain in beryllium is not linearly proportional to stress, but relates as some higher power. The torsional and axial values compare favorably.

Figure 23d shows the decay from the final loading on Specimen 133, allowed to run over a week-end. Note that this is a semilog plot. This plot was obtained after the specimen had been strained in tension to a yield of greater than 1000 microstrain and then yielded in compression back to near its original length. As the plot shows no evidence of curvature at the long-time end, it is inadequate for prediction of end point, or true yield. Extension to several weeks or months time interval would be required to acquire adequate data for this.

## 6.3 LOADING SYSTEM EXTRANEOUS MOTIONS

Although the extensometers in this program were designed for optimum sensitivity and stability of measurement along the principal loading direction, they were inherently capable of reading motions normal to the principal axis as well. At each load point, the principal deformation as well as the extraneous motions was measured. The extraneous motions were then interpreted as maximum outer fiber bending strain. Typical measurements are plotted in figure 24.

The extraneous loading motions in torsion are less than in axial testing, as expected from the basic design geometry. All three test methods begin to show saturation of the preamplifier above 1000 microstrain, and it is this which constitutes the upper limit of measurement at present. The tension test sequence shows greater bending loads than the compression. In compression testing, both ball joints are reseated at each load, whereas in tension testing, the upper ball is not reseated. A small angular offset of the upper bearing may thus be held against the tension alignment couple and cause minor bending stresses in the specimen. Lifting the upper ball off its seat in compression at the start of tension test sequence will reduce this effect but not eliminate it.

# 7.0 DISCUSSION

## 7.1 BERYLLIUM

The choice of the 0.2% iron alloy of beryllium for testing in this program was made after considerable discussion with fabricators of beryllium mirrors. The principal consideration was with the basic material manufacturing process (isostatic pressing). A secondary consideration was the use of alloying elements for strengthening.

The test of the annealed alloy show it to be quite soft, with characteristics near the lower limit of beryllium results produced by other investigators. Although prestraining the material increases its hardness considerably in the prestrained direction, the application of such a process to mirror usage appears questionable, as this "softens" the material for stresses in the opposite direction. A postulated mechanism for this behavior is the migration of dislocations by the applied stress field to crystal boundaries where they are prevented from further motion. Subsequent lesser stress fields of the same sign do not have the defects available for propagation. Increasing the stress field brings higher energy lattice defects into play, with a resulting net motion that is a function of the energy distribution of these defects. Reversal of the stress field allows the low-energy defects to propagate away from the boundary, giving the indication of a "soft" material again.

As the material was softer than expected, an aging treatment (Appendix A) was suggested by Dr. Moberly, to precipitate and immobilize low-energy lattice defects. This was proven to be beneficial for increasing hardness, bringing the yield characteristics very close to those measured by Moberly (reference 6) for the 1% iron alloy.

Correlation between tension and compression results appears quite good, showing essentially no effect of the order of testing. The torsion tests made the material appear slightly harder at low stress levels when compared to the axial tests. This was accompanied by a decided change in slope of the Ramberg-Osgood characteristic near 15 $MN/m^2$ equivalent axial stress. Above 15 $MN/m^2$, both the torsional and axial curves are essentially the same, continuing on up to the limits of the test equipment. A probable cause for the departure of the torsional data at low levels is surface oxidation during anneal, effectively strengthening the surface with respect to the body material. This would affect the torsional tests much more than the axial test, and could produce the differences displayed.

The torsional and axial test methods correlate very closely, validating the conversion of data from one system to the other, except where surface effects differ strongly from those of the body material. Further support for this position is lent by the excellent correlation between torsional and axial time-dependent characteristics of the beryllium specimens.

Although this beryllium alloy appears quite soft in the annealed condition, it is amenable to age-hardening to an appreciable extent. It has not been established whether this is the maximum hardening capability of the material although the specimen supplier tends to deprecate appreciable further hardenability.

The time-dependent strain characteristics are quite small compared to the yield values, thus emphasizing the stability of the material. Other alloys such as the 5% copper alloy appear superior to the one tested here and remain to be thoroughly investigated.

The long-term plot of time dependent strain in figure 23d does not appear to have great significance to the use of beryllium for mirror applications, except for the indication that the material should be thoroughly annealed after machining to remove the almost interminable creep engendered by large plastic strains. The plot points up some of the capability and versatility of the testing facility, as well as emphasizing the logarithmic time behavior of materials in the microstrain region. Also of note is the comparison of the curves in figure 17, wherein the data from the present facility cover more orders of magnitude of stress and strain than any other represented.

7.2 CER-VIT

The major differences in torsion between the characteristics of the test specimens as ground and after etching emphasize the importance of surface treatment to stability. The basic material is apparently without appreciable yield for short-term loading, although it does exhibit a relatively large viscoelastic, or time-dependent strain in proportion to stress. Although the removal of 0.1 mm of surface by etching completely suppresses the effects of grinding, the light etch employed by the specimen supplier to remove 0.025 mm is inadequate for this purpose.

The large ratio between the magnitude of time-dependent strain in torsion to that in axial testing would indicate that this characteristic is primarily a surface effect. With surface mechanical damage removed by etching, some other mechanism must be postulated.

The yield measurements for fully etched specimens in torsion indicate a scatter of approximately $\pm$ 0.003 microstrain, predominantly at the higher stress levels. This compares reasonably well to the goal of $\pm$ 0.001 microstrain set at the start of this program for this specimen geometry. The viscoelastic, or time-dependent strain characteristics indicate an unloaded stability of the order of $\pm$ 0.0003 microstrain. The thermal control and output-indicating equipment are thus shown to have the requisite stability. The remaining problem of extensometer attachment was alleviated by a change in specimen geometry, as shown by the final curves on Specimen 104.

The axial yield tests showed considerably lower precision, with an uncertainty approaching $\pm$ 0.1 microstrain. That this again is a problem of

specimen geometry as it affects extensometer attachment is apparent upon examination of the axial time-dependent strain characteristics. Here the precision is approximately $\pm$ 0.002 microstrain.

The process of determining yield of this material in the nanostrain region involves extended periods of data-taking to gather adequate information for extrapolation of the time-dependent strain. Small amounts of drift of the specimen or equipment will distort the extrapolations, altering the apparent yield values. The 16-hour minimum settling period utilized during the major portion of this program has in several cases proved inadequate for reduction of installation drift to insignificant values. This installation drift is most likely attributable to gradual relief of stresses in the extensometer cement line. A 40-hour settling period has been found more nearly adequate for this purpose.

## 7.3 FUSED SILICA AND ULE FUSED SILICA

With the silica specimens, as with the CER-VIT, a major difference in performance is apparent between the as-ground and the etched conditions. The etched material has no consistent yield characteristics, whereas the as-ground material in torsion consistently indicates an apparent yield. The values obtained for the apparent yield of as-ground specimens in torsion correlate well with those obtained in the previous program (reference 1) considering the difference in specimens diameters. The viscoelastic or time-dependent strain also shows major difference between the etched and as-ground conditions, with major changes in slope and magnitude. The as-ground time-dependent strain characteristics correlate quite well with those previously measured (reference 1).

The agreement between the shear and axial viscoelastic (time-dependent) strain characteristics, although somewhat rough, indicates the effect to be a body effect as opposed to a surface effect. It also negates the argument that this could be attributed to the dampers on the torsion system. The axial system has no appreciable damping external to the specimen.

The uncertainty band in the silica yield measurements is, as with the CER-VIT, much greater than in the time-dependent strain measurements. This again points to specimen geometry and extensometer attachment problems, which were alleviated in the final tests.

Time-dependent strain, or delayed elastic (viscoelastic) effects in glasses have been studied by several investigators (references 9, 10, and 11). Most of this work has been qualitative and associated with long term loading, creep, or thermal effects. Murgatroyd and Sykes attempt to fit the Nutting relationship to their data on silica, but find the extrapolated yield point to be unrealistically negative and thus tend to discard the relationship. As plotted, the slope of their silica Nutting curve is less than 0.1, as opposed to a near-unity slope for most of the silica data of this report. This difference may be a function of the loading period, which in their case was "prolonged."

Argon (reference 9) develops an energy spectrum for available motion centers in glass by thermal relaxation methods. By similar techniques, energy spectra may be developed from an exact knowledge of the shape of the time-dependent or delayed elastic strain curve at a single temperature. No attempt has been made here to develop such data.

The apparent yield in torsional measurements, which has been shown to be a surface effect from grinding damage, is very significant to the fabrication of telescope mirrors, where the grinding process is fully as severe and is followed only by a polishing process. The extent of removal of the grinding damage by polishing is uncertain and can be fully established only by further testing.

## 7.4 EXTRANEOUS BENDING MOTIONS

In each test made, the extraneous bending stresses are reasonably small, being less than 0.5% of the full scale principal stress. In general, the indicated bending stresses are represented by a fixed quantity plus a constant proportion of the principal stress. Whether the indicated proportional part of the load is actually present or merely a residual mismatch in the sensitivity of the opposed differential transformers is open to question. The precision of the differential transformer sensitivity balance was limited to approximately 0.5%. Further reduction of mismatch is possible over a restricted range, but is complicated by mismatch in nonlinearity when large dynamic ranges of 0.25mm or greater are attempted.

## 7.5 APPLICATIONS

It is pertinent at this point to discuss the application of the results of this test program to the fabricator of telescope mirrors. In particular, it is illuminating to postulate the response of a mirror to a stress which produces a given number of units of strain. In this case only short-term stress loading, of the order of 1 minute or less, must be specified, as the present test program did not investigate long-term loading effects.

If we assume a stress load that causes a 200-fringe distortion in a CER-VIT mirror, we can expect 0.3 fringe distortion to remain 6 seconds after load release, 0.06 fringes after 1 minute, and 0.008 fringes after 10 minutes.

For a silica mirror under the same conditions, we should expect 0.07, 0.015, and 0.003 fringes respectively. For the same stress levels, then, the silica exhibits roughly one fourth the time-dependent (viscoelastic) strain shown by the CER-VIT. For most applications, either would be minor. Permanent deformation should be negligible. This all assumes that surface effects are negligible; that is, all grinding damage has been removed by etching or polishing.

Beryllium mirrors are a different story altogether. As neither the yield (non-recoverable) nor the time-dependent (viscoelastic) strain is a linear function of stress, one cannot make generalizations as above. The time-dependent strain, generally small compared to the yield, can be ignored. The yield depends primarily upon the maximum stress level at any point in the structure and must be evaluated at all points of loading.

# 8.0 CONCLUSIONS AND RECOMMENDATIONS

## 8.1 CONCLUSIONS

1) The primary objective of this program, which was to establish the correlation of torsional shear with tension and compression measurements in the sub-microstrain region, has been accomplished. The results of torsion, tension and compression tests are shown to be equivalent, for the conditions of this program, when surface effects are negligible. When surface effects are significant, they will tend to dominate torsional test results.

2) The equipment employed in this test program has been shown to have a basic uncertainty of measurement of $\pm$ 0.0003 microstrain in torsion and $\pm$ 0.002 microstrain in tension and compression. Stresses in the joints of attachment of the extensometer to the specimen have been found responsible for appreciable degradation of this capability.

3) The silicic materials tested in this program show very strong surface effects from grinding. These surface effects influence both yield (non-recoverable) and time-dependent (viscoelastic) measurements in torsion and were significant in the results published from an earlier program (reference 1).

4) Removal of 0.1 MM of surface by acid etching eliminates virtually all surface effects from grinding. With surface effects removed, torsion and axial measurements correlate closely.

5) With surface effects removed, the silicic materials are essentially free of yield for short-term loads up to 200 $MN/m^2$.

6) After etching, the CER-VIT continues to show surface effects in the time-dependent (viscoelastic) strain characteristics. The vitreous silica materials do not show this.

7) The 0.2% iron alloy of beryllium exhibits significant yield at moderate values of stress. Surface effects are small compared to those of the basic material, so that basic material properties are well characterized by both axial and torsional testing.

8) Although quite soft in its annealed state, the 0.2% iron alloy of beryllium is amenable to age hardening. The limit of this hardening has not been established.

## 8.2 RECOMMENDATIONS

Although the tests in this program have established several material characteristics and effects thereon of various treatment, the materials tested and the conditions of test have been necessarily limited in scope. Recommended further investigations include the following:

1) Silicon. This material is being actively investigated for use as an optical mirror substrate. Tests of microyield and time-dependent strain properties are needed to provide adequate comparison with other mirror substrate materials.

2) Beryllium. Other alloys of beryllium, such as the 5% copper alloy, appear to be superior in hardness to the one tested in this program. Tests of the copper alloy should be made for comparison.

3) Polishing. Grinding of the surface of silicic materials, as employed in mirror fabrication, has been shown to cuase significant surface effects. The extent to which subsequent polishing operations remove the surface effects should be established by further testing.

4) Loading Period. The tests employed in this program all involved short-term (30 second) load intervals. Effects of longer term loads, as they affect both the time-dependent (viscoelastic) strain and the yield (non-recoverable strain), remain to be evaluated.

5) Environment. All tests in this program were run at a single temperature of 306$^{o}$K. Many of the materials characteristics could be expected to be temperature dependent. As most mirror applications involve a significant range of environmental temperatures, evaluation of characteristics over appropriate temperature ranges is needed.

# APPENDIX A

## SPECIMEN SPECIFICATION, FABRICATION, AND TREATMENT

### A.1 CER-VIT

Four specimens of CER-VIT were ordered from Owens-Illinois, Inc., with the following specification, wherein Sketch 11-042875B refers to the drawing of figure 12:

> "4 EACH CER-VIT Premium Grade C-101, microstrain test specimen per Boeing Sketch 11-042875B, threaded."

Specimens were "machined by diamond wheel to a 32 microinch rms finish" and etched to remove 12 micrometers of surface material. Manufacturer's inspection report was as follows:

> "Order filled from: Premium C-101 D11T3 M 111-1, Nos. 1, 2, 3, and 4. Chemical analysis shows that this melt meets composition specifications. Average linear thermal expansion coefficient (0-38° C): $-0.2 \times 10^{-7}/^{\circ}$ C.
>
> Sample Dimensions: On file in Quality Control Laboratory
> Seed Count: Less than $1/in^3$ per piece mean dia. 0.020
> Stress Retardation: None visible"

Upon receipt, Specimen 101 was given a cursory test as received to demonstrate equipment. Its subsequent fracture precluded further processing. Specimens 102, 103, and 104 were subjected to an etch solution of 10% HF/ 10% $H_2SO_4$ for a total surface removal of 0.1 millimeter. Figure A1 shows the surface appearance as received and after this latter etch. Between tests, specimens were subjected to heat treatment at 810° K for 1 hour. Specimen 104 was given an additional brief etch immediately preceding its installation for tension testing.

As it was the only surviving specimen, Specimen 104 was chosen for additional processing and testing. The test section was reground with a 120 grit diamond wheel to remove a minimum of 0.025 millimeters from all portions of the test section. The thread relief diameter on both ends was reduced from 19.6 to 12.7 millimeters. After torsion testing, the specimen was re-etched to a depth of 0.1 mm and retested in torsion.

Test section diameter measurements were made initially with a micrometer caliper. This was shortly proven to be undesirable, as the tension fracture of Specimen 103 was directly traceable to minute scratches left by this process. Figure A2 shows the resulting fracture. Subsequent test section diameter measurements were made with an optical comparator.

A.2 FUSED SILICA (CORNING 7940)
ULE SILICA (CORNING 7971)

Four specimens each of the two grades of fused silica were ordered from Corning Glass Works with the following specification, wherein Drawing 15588B and Sketch 11-042875B refer to the drawing of figure 12:

> "4 EACH 7940 Fused Silica, Mirror Blank Quality Microstrain Test Specimen per Corning Glass Works, Drawing 15588B, Rev. 1, threaded, per Boeing Sketch 11-042875B.
>
> 4 EACH 7971 Corning ULE Fused Silica, Mirror Blank Quality Microstrain Test Specimens per Corning Glass Works, Drawing 15588B, Rev. 1, threaded, per Boeing Sketch 11-042875B."

The manufacturer's report on fabrication and quality control of these specimens was as follows:

> "ULE MICROSTRAIN TEST SPECIMENS
>
> 1. Boule used for order - #313-907
>
> 2. Boule in block form
>
>  a. Glass was Blanchard ground top and bottom with 60 grit wheel to 4.08 thickness. Glass was Tysaman sawed to length and width of 4.830 x 4.08.
>
>  b. Maximum stress for block was 3 mu/cm.
>
>  c. Average thermal expansion coefficient for these specimens from 5 degrees to 35 degrees C is $-.014 \times 10^{-6}$ in/in/C°.
>
>  d. Avg. # seed/$in^3$ - .07
>  Max. # seeds/$in^3$ - 5
>  Max. Mean Diameter Seed - .010
>
> 3. Specimens were core drilled parallel with long dimension 4.830 and surfaces were ground with standard metal bonded diamond wheels to tolerances as listed on inspection sheet. The specimens were then threaded.
>
> 4. Striae is parallel with length of specimen. The specimens were annealed separately after machining and max. stress is included on inspection sheet."

"FUSED SILICA MICROSTRAIN TEST SPECIMENS

1. Boule used - 243-814

2. Boule in Block Form

   a. Glass was Blanchard ground top and bottom to 4.08 thickness with 60 grit wheel. Glass was Tysaman sawed to length and width to 4.830 x 4.08.

   b. Max. stress for block - 2 mu/cm

   c. Avg. # seeds/$in^3$ - 1.03
      Max. # seeds/$in^3$ - 8
      Max. Mean Diameter Seed - .016

3. Specimens were core drilled parallel to long dimension 4.830 and surfaces were ground with standard metal bonded diamond wheels to tolerances as listed on inspection sheet.

4. Striae is parallel with length of specimens. The specimens were annealed separately after machining and the maximum stress is included with the inspection sheet."

Upon receipt, all specimens with the exception of Specimens 114 and 124 were etched with a 50% HF solution to remove 0.1 millimeter of surface material. Surface characteristics before and after etch are shown in figure A3.

Specimen 124 was given a low-level torsion test as received, and both 114 and 124 were reground and subjected to additional testing, etching, and retesting. In the regrind process, a minimum of 0.025 millimeters was removed from the test sections with a 120 grit diamond wheel, and the relief between the threaded end and extensometer shoulder on both ends was reduced from 19.6 to 12.7 millimeters.

Between tests, specimens were heat treated at 810° K for 1 hour and furnace cooled. In the latter portions of the testing program, specimens were given a light etch after heat-treat to remove minor abrasions from the holding fixture.

Measurements of the test-section diameter after etch were made with an optical comparator.

The following is a communication from Dr. Chas. F. DeVoe, Staff Scientist, Optical Projects Department, Corning Glass Company, Corning, New York.

"In general, HF acid fortification is utilized to increase glass strength via check removal. Typically, a ground glass surface consists of hills and valleys of rough glass. A high number of glass checks (cracks) are present in such a ground surface; the number and depth of these checks is a function of the grinding operation (i.e., grit size and type, pressure, etc.)

"As in most chemical reactions, acids tend to attack sharp corners at a faster rate than flat areas. In fortification, the hydrofluoric acid goes after and dissolves the sharp peaks and rounds out the valleys. Initially the valleys are filled with small bits of glass particles and are not as noticeable as they are after a short acid rinse. As fortification continues, the surface becomes flatter and flatter with the eventual elimination of all glass checks.

"The strength of such a check-free surface approaches that virgin glass, however, subsequent handling tends to reduce this high strength as checks are reintroduced in the glass surface.

"The mixed acid system, often called a polishing acid, utilized the etch reaction products as a sludge blanket to prevent excessive etching of the valleys. In the $H_2SO_4$ mixed acid, the sulfates formed often are glutinous and provide protection for the glass valleys. However, in the fused silica systems, all reaction products are completely soluble and no sludges are formed with or without the $H_2SO_4$.

"The attached photomicrographs* were all taken with incident lighting at 100X, and show the various Code #79-0 Fused Silica surfaces before and after etching. Each photomicrograph is labeled as to acid treatment and glass takeoff. All acid fortification was accomplished in stagnant acid solutions at 71-73 degrees F.

"We strongly recommend that a 20 minute treatment in 50% HF (as received) be used as the minimum fortification cycle for the samples as finished. A beeswax/resin mixture resists acid attack and can be used as a coating to protect the ends of the sample from acid attack."

*See figure A4

## A.3 BERYLLIUM

The choice of beryllium material to be tested in this program was made on the recommendation of Mr. Wm. Goggin of Perkin-Elmer Corp., as one of the principal investigators in the fabrication and testing of beryllium mirrors. Accordingly, the following specification was sent to Dr. John Moberly of Stanford Research Institute, Menlo Park, California, for fabrication of three test specimens. The referenced Sketch 11-042875B refers to the drawing of figure 12.

> "3 each Microstrain Test Specimen, Beryllium, fabricated from fine grained low oxide beryllium powder, 0.2% iron by weight, per Boeing Sketch 11-042875B"

With the specimens, the following was received from Dr. Moberly.

> "Three microstrain tensile specimens have been fabricated and machined to specifications. The samples were fabricated from Kawecki-Berylco P-50 grade beryllium powder, Lot R-7080. The chemical and particle size analyses of the powder, as given by the supplier, are listed below:

TABLE I: CHEMICAL ANALYSIS OF P-50 BePOWDER, LOT R-7080

| | wt% |
|---|---|
| Be | |
| BeO | |
| C | 0.18 |
| Fe | 0.141 |
| Al | 0.038 |
| Ni | 0.015 |
| Si | 0.030 |
| Mg | 0.020 |
| Mn | 0.008 |
| Cr | 0.265 |

TABLE II: PARTICLE SIZE DISTRIBUTION (BY COULTER COUNTER) OF P-50 Be, POWDER, LOT R-7080

| | | |
|---|---|---|
| Minus | 35 Microns | 98% |
| Minus | 20 Microns | 72% |
| Minus | 15 Microns | 57% |
| Minus | 10 Microns | 39% |
| Minus | 5 Microns | 14% |

"Kawecki-Berylco does not give the BeO level, but we estimate it to be about 4 wt %. We added 0.2 wt % iron powder (99% pure) to the beryllium powder. After mixing the iron and beryllium powders, dense billets were obtained by the Stanford Research Institute pressureless-sintering technique. Each sample was prepared independently, i.e., the tensile samples were not machined out of a single billet. The powder was hydrostatically pressed at 27,000 psi and then sintered for 5 hours at 1200 degrees C. in a vacuum of 10 microns. The density of each specimen is given below:

| | |
|---|---|
| A-161 | 1.85 g/cc |
| A-162 | 1.86 g/cc |
| A-164 | 1.85 g/cc |

"The specimens were not stress relieved. I would recommend the samples be chemically etched before further heat treatment. Etching of 0.003 to 0.005 in. of metal off each surface is sufficient to remove the heavily damaged surface layer, but will not remove all residual stresses; 0.010 in. is probably needed. This added depth may not be necessary if the samples are stress relieved after etching. This, however, has not been verified. Our current procedure for our beryllium samples is:

1. Machine

2. Chemically etch 0.010 in. from all surfaces

3. Stress relieve at 1600 degrees f., one hour, in vacuum

"The sample is slowly cooled, 200 degrees F./hour, after the 1600 degrees F. heat treatment.

"The 40% $HNO_3$-5% HF solution should be satisfactory for the chemical etching. One precaution: don't allow the acid temperature to exceed 40 degrees C. (100 degrees F.). The etching reaction is very exothermic and the acid will, if not cooled, continue to heat up. Higher temperatures will increase the removal rate, but will also produce poorer surface finish."

The specimens were etched as recommended, removing 0.25 millimeters of material. No problem was encountered with heating of the bath, but the narrow test section of the specimen was found to heat up, causing non-uniform etching unless care was exercised to keep each incremental etching interval under 1 minute.

After etch and before each test, specimens were annealed as recommended in a high vacuum furnace. Although the pressure was kept below $5 \times 10^{-5}$ Torr, appreciable discoloration occurred during anneal, indicating surface oxidation. Specimen surface characteristics before and after etch are shown in figure A4. Several surface pits are shown in the photograph, and apparently result from residual porosity of the pressing operation. A semiquantitative evaluation of the pitting in the test section is as follows:

| | No. of Pits Greater than 0.08 mm | |
|---|---|---|
| Specimen No. | Before etch | After etch |
| 131 | 0 | 48 |
| 132 | 13 | 101 |
| 133 | 2 | 41 |

Although the pits are apparent by close, unaided visual inspection of the specimens, their influence upon the results of testing is considered to be negligible.

After its initial torsion test, Specimen 131 was subjected to a heat treatment of 570°K for 1 hour in air with oven cooling. This was intended as an aging treatment to determine whether the specimen would harden. After retesting in torsion, the standard annealing procedure was followed.

## APPENDIX B

## DATA REDUCTION COMPUTER PROGRAM

This program accepts the printed digital voltmeter output of standardization data and test data, together with the simulated stress and strain values associated with the standardization data, and provides the reduction to meaningful stress, yield strain, and time dependent strain output. A log-log printer plot of the time dependent strain is provided for rapid evaluation of the quality of results.

Job control cards, with the exception of the initial job card, are provided for operation of this program on an IBM 360 computer. Reference to external subprograms, except those generally supplied with the computer, have been eliminated from the program.

The program is written in the Fortran IV(G) language, and consists of one main and five subroutines.

The main program sets up the printer plot axis construction and labeling arrays, followed by the test title array, which is represented by the real variable MATL. The balance of the main program is the calling of the subroutines in sequence, followed by an input-stream-controlled recycle instruction as to whether the ensuing data is additional time dependent strain data, a new test sequence, or data end. The corresponding value of NN is 1, 3, and 2, respectively.

Subroutine CALTIT titles the first page of printout for a test sequence and sets up the calibration values of the various readout channels. The variable MODE is given a value of 1, 2, or 3 for torsion, tension, or compression testing respectively, and governs the application of the specimen test section diameter to the calibration of stress and strain channels. The diameter variable, DIAM, is in inches. Stress and strain channels are given gain numbers as follows:

| | | |
|---|---|---|
| 10 | load, or stress | Extensometer secondary modes |
| 11 | "X" bending | |
| 12 | "Y" bending | |
| 01 | | Extensometer prinicpal strain mode, four gain ranges |
| 02 | | |
| 03 | | |
| 04 | | |

The gain number, positive standardization readout, zero, negative standardization readout, and standardization value in terms of $MN/m^2$ and per unit strain (referred to principal strain) are read in for each channel. Sensitivity and zero figures are printed out for each channel.

To terminate the CALTIT subroutine cycle, an integer greater than 20 (the value 30 is customary) is coded into the GAIN field of the next card.

Subroutine INVAL, as the comment states, computes and prints out stress, load strain, load bending strain, and terminal unloaded residual strain values without extrapolation. The input variables are as follows:

| | |
|---|---|
| GAIN | Gain value of extensometer channel |
| LOADV | Load cell channel output voltage |
| EXV | Terminal extensometer voltage |
| ELV | "X" bending voltage (under load) |
| EWV | "Y" bending voltage (under load) |
| E1V | Extensometer output under load (gain of 1) |

The remaining variables are fairly obvious. To terminate the INVAL subroutine, a value greater than 20 is again coded in the GAIN field. The value 30 is customary.

The subroutine LODVAL performs the titling and fixed value data reduction for the following DATPRO subroutine. The load stress is computed and inserted into the title MATL before print-out.

The subroutine DATPRO accepts time sequence extensometer output and determines the amount of yield strain (TNRS) which, when subtracted from the time sequence strain data, produces a zero average curvature plot of the resulting data in log-log space. The initial printer data and equivalent strain data are printed out to enable rapid checking for coding and keypunch errors in the input stream. The iterations of data adjustment are printed to allow inspection of the covergence procedure. These variables and the following columnar print-out variables are defined as follows:

| | |
|---|---|
| F | Convergence factor, adjusted to give rapid convergence |
| SUM | Additive factor for adjusting TNRS |
| A | One minute (time) intercept ($\log_e$) of resulting curve |
| B | Slope of log-log curve |
| C | Average curvature of curve |
| TIME | Time after load release (minutes) |
| DATA | Indicated strain as a function of time |
| RS | Time dependent strain (DATA-TNRS) |
| RSBAR | Points on the fitted straight line equivalent to RS |

The subroutine DAPLOT takes the logarithmic values of time and time-dependent strain (X and Y), converts them to base 10, and plots them on a log-log plot for visual inspection of the quality of the extrapolation. The plot is titled with the MATL array, which contains the stress value inserted by the LODVAL subroutine.

A listing of the program deck with the plot axis arrays and a sample data deck is presented on the following pages, followed by a representative computer print-out of results.

```
//FOR       EXEC PGM=IEYFORT,REGION=140K
//SYSPRINT  DD SYSOUT=A,UNIT=SYSDA,                                    X
//            DCB=(LRECL=120,RECFM=FBA,BLKSIZE=1680)
//SYSLIN    DD DSNAME=&LOADSET,DISP=(MOD,PASS),UNIT=SYSDA,
//            DCB=(LRECL=80,BLKSIZE=400),SPACE=(400,(1200))
//SYSIN     DD *
C REDUCTION OF MICROYIELD CORRELATION DATA 7/7/69
      INTEGER SAMPLE,GAIN
      REAL SENS(20),ZERO(20),TIME(50),EV(50),STRN(50,4),X(50),Y(50)
      REAL TITLL(50),ANUML(51),TITLB(30),AXB(30),ANUMB(30),MATL(20)
      READ(5,1) BLANK,DOT,STAR
1     FORMAT(3A1)
      READ(5,2) TITLL,ANUML,TITLB,AXB,ANUMB
2     FORMAT(50A1/20A4/20A4/11A4/20A4/10A4/20A4/10A4/20A4/10A4)
5     READ(5,6) MATL
6     FORMAT(20A4)
      CALL CALTIT(MATL,SENS,ZERO)
      CALL INVAL(SENS,ZERO)
10    CALL LODVAL(SENS,ZERO,STRESS,MATL)
      CALL DATPRO(STRN,SENS,TIME,ZERO,STRESS,YIELD,N,MATL,X,Y)
      CALL DAPLOT (X,Y,N,BLANK,DOT,STAR,TITLL,ANUML,TITLB,AXB,ANUMB,
     XMATL)
      READ(5,15) NN
15    FORMAT(I2)
      GO TO (10,20,5),NN
20    CONTINUE
      STOP
      END
      SUBROUTINE CALTIT(MATL,SENS,ZERO)
      REAL MATL(20),SENS(20),ZERO(20),LMULT
      INTEGER SAMPLE,GAIN
10    READ(5,15) MODE,DIAM
20    WRITE(6,30) (MATL(I),I=1,14),DIAM
15    FORMAT(I2,10X,F6.0)
30    FORMAT(1H1,14A4,10X,16HSAMPLE DIAMETER= ,F8.4,7H INCHES /1H0)
      IF(DIAM.GT.0.0) GO TO 60
      WRITE(6,40)
40    FORMAT(45H DIAMETER VALUE IMPROPER. PROGRAM TERMINATED. )
      CALL EXIT
60    IF(MODE.GT.1) GO TO 100
70    EXMULT=DIAM/0.28
80    LMULT=(0.28/DIAM)**3
90    GO TO 120
100   EXMULT=1.0
110   LMULT=(0.28/DIAM)**2
120   CONTINUE
125   WRITE (6,126) LMULT,EXMULT
126   FORMAT(7H LMULT= ,1PE10.3,10X,7HEXMULT= ,E10.3)
130   READ(5,140)GAIN,CALP,CALO,CALM,CALV
140   FORMAT(I2,10X,4(F8.0,4X))
      IF(GAIN.GT.0) GO TO 150
      WRITE(6,145) GAIN
145   FORMAT(25H IMPROPER VALUE OF GAIN =,I6)
      CALL EXIT
```

```
150    IF(GAIN.NE.10)GO TO 210
160    SENS(10)=LMULT*CALV/(CALP-CALM)*2.0
170    ZERO(10)=CALO*SENS(10)
180    WRITE(6,190)SENS(10),ZERO(10)
190    FORMAT(20H LOAD SENSITIVITY = ,1PE10.4,14H  LOAD ZERO = ,E10.4)
200    GO TO 130
210    IF(GAIN.GT.20) GO TO 250
220    SENS(GAIN)=EXMULT*CALV*2.0/(CALP-CALM)
230    ZERO(GAIN)=CALO*SENS(GAIN)
       WRITE (6,235) GAIN,SENS(GAIN),ZERO(GAIN)
235    FORMAT(13H GAIN NUMBER= ,I4,10X,12HSENSITIVITY= ,1PE11.4,10X,
      15HZERO= ,E11.4)
240    GO TO 130
250    CONTINUE
       RETURN
       END
       SUBROUTINE INVAL(SENS,ZERO)
       REAL SENS(20),ZERO(20),LSTRN,LBEND,LOADV
       INTEGER GAIN
C COMPUTE SINGLE POINT (NOT EXTRAPOLATED) VALUES
285    WRITE (6,286)
260    READ(5,270) GAIN,LOADV,EXV,ELV,EWV,E1V
270    FORMAT(I2,10X,5(F7.0,5X))
280    IF(GAIN.GT.20) GO TO 370
286    FORMAT(1HO,20X,36HSINGLE POINT VALUES-NO EXTRAPOLATION/1HO/19X,5HY
      XIELD,6X,4HLOAD,8X,5HLONG.,7X,7HLATERAL/6X,6HSTRESS,6X,6HSTRAIN,6X,
      26HSTRAIN,6X,7HBENDING,5X,7HBENDING/1H )
290    STRESS=LOADV*SENS(10)-ZERO(10)
300    YIELD=EXV*SENS(GAIN)-ZERO(GAIN)
       IF(E1V.EQ.0.0) GO TO 335
310    LBEND=(ELV*SENS(11)-ZERO(11))/12.
320    WBEND=(EWV*SENS(12)-ZERO(12))/12.
330    LSTRN=E1V*SENS(1)-ZERO(1)
       GO TO 340
335    LBEND=0.0
       WBEND=0.0
       LSTRN=0.0
340    WRITE(6,350) STRESS,YIELD, LSTRN,LBEND,WBEND
350    FORMAT(1H ,2X,5(1PE12.3))
360    GO TO 260
370    RETURN
       END
       SUBROUTINE LODVAL(SENS,ZERO,STRESS,MATL)
       REAL SENS(20),ZERO(20),LSTRN,LBEND,LOADV,MATL(20)
       INTEGER GAIN
370    READ(5,380) LOADV,ELV,EWV,E1V
380    FORMAT(6(F7.0,5X))
390    STRESS=LOADV*SENS(10)-ZERO(10)
       WRITE(0,12) STRESS
12     FORMAT(F8.1)
       READ(0,13) (MATL(I),I=17,18)
13     FORMAT(2A4)
       WRITE(6,31) (MATL(I), I=1,20)
31     FORMAT(1H1,10X,20A4/1HO)
```

```
400     IF(ELV.EQ.0.0) GO TO 450
410     LBEND=(ELV*SENS(11)-ZERO(11))/12.
420     WBEND=(EWV*SENS(12)-ZERO(12))/12.
430     LSTRN=ELV*SENS(1)-ZERO(1)
440     GO TO 510
450     LBEND=0.0
460     WBEND=0.0
470     LSTRN=0.0
480     WRITE(6,490)STRESS
490     FORMAT(1H0,4X,7HSTRESS=,1PE12.3,25H NEWTONS PER SQUARE METER)
500     GO TO 530
510     WRITE(6,520)STRESS,LSTRN,LBEND,WBEND
520     FORMAT(1H0,4X,7HSTRESS=,1PE12.3,5H N/M2,4X,12HLOAD STRAIN=,1PE12.3
       1/4X,28HLONGITUDINAL BENDING STRAIN=,1PE12.3,4X,23HLATERAL BENDING
       2STRAIN=,1PE12.3)
530     RETURN
        END
        SUBROUTINE DATPRO(NR,SENS,TIME,ZERO,STRESS,TNRS,N,MATL,X,Y)
        REAL NR(50,4),SENS(20),ZERO(20),TIME(50),X(50),Y(50),MATL(20)
        REAL EV(50),INC
        INTEGER GAIN
        READ(5,1)N,GAIN,TIME(1)
1       FORMAT(2(I2,10X),F6.0)
        IF(N.GT.0) GO TO 30
        WRITE(6,118) N
118     FORMAT(22H IMPROPER VALUE OF N =,I6)
        CALL EXIT
30      IF(N.GT.50) GO TO 28
        READ(5,2)(EV(I),I=1,N)
2       FORMAT(6(F7.0,5X))
        WRITE(6,125) (EV(I),I=1,N)
125     FORMAT(11H EV READOUT/(5X,6(1PE12.4)))
        DO 3 I=2,N
        TIME(I)=TIME(I-1)+10.**( INT(ALOG10(TIME(I-1))))
3       CONTINUE
        DO 4 I=1,N
        NR(I,1)=EV(I)*SENS(GAIN)-ZERO(GAIN)
        TIME(I)=TIME(I)/12.
4       CONTINUE
        WRITE(6,126) (NR(I,1),I=1,N)
126     FORMAT(12HOSTRAIN DATA /(5X,6(1PE12.4)))
        WRITE(6,127)
127     FORMAT(1H0)
C INTRODUCE INITIAL OFFSET
        J=0
        TEMPA=NR(1,1)-NR(N,1)
        TEMPO=TEMPA/ABS(TEMPA)
        INC=-NR(N,1)
5       INC=INC+TEMPO*1.E-8
        TNRS=-TEMPO*INC
        J=J+1
        IF(J.LT.10) GO TO 6
        WRITE(6,55)
55      FORMAT(1H0//52H STUCK IN DATA ADJUSTING LOOP. PROCEDURE TERMINATED
```

```
      X.)
       RETURN
 6     CONTINUE
       DO 7 I=1,N
       TEMP=TEMPO*(NR(I,1)+INC)
       IF(TEMP.GT.0.0) GO TO 66
       INC=-NR(I,1)
       GO TO 5
 66    NR(I,4)=TEMP
 7     CONTINUE
 113   FORMAT(1H ,2X,3HJ= ,I3,4X,4HNRS= ,1PE10.3)
       SUMA=1.0
       SUM=0.0
       F=3.2E-9
       C=1.0
       A2=0.0
       A1=0.0
       BB=0.0
       DO28 K=1,30
C CHANGE TO LOGLOG
       DO21 J=1,N
       IF(TIME(J).GT.0.) GO TO 19
       WRITE(6,114)J,TIME(J)
 114   FORMAT(1H ,2X,3HJ= ,I3,4X,6HTIME= ,1PE9.3)
       TIME(J)=0.05
 19    IF(NR(J,4).GT.0.) GO TO 20
       WRITE(6,113)J,NR(J,4)
       NR(J,4)=1.0E-9/1.5**J
 20    X(J)=ALOG(TIME(J))
 21    Y(J)=ALOG(1.0E10*NR(J,4))
C LEAST SQUARES POLYNOMIAL CURVE FIT TO DEGREE TWO
       S1=0.0
       S2=0.0
       S3=0.0
       S4=0.0
       T1=0.0
       T2=0.0
       T3=0.0
       DO22 J=1,N
       S1=S1+X(J)
       S2=S2+X(J)*X(J)
       S3=S3+X(J)**3
       S4=S4+X(J)**4
       T1=T1+Y(J)
       T2=T2+X(J)*Y(J)
 22    T3=T3+X(J)*X(J)*Y(J)
       C1=C
       FN=FLOAT(N)
       C=((S1*T1-FN*T2)*(S1*S2-FN*S3)-(S2*T1-FN*T3)*(S1*S1-FN*S2))/((S1*
      1S2-FN*S3)**2-(S2*S2-FN*S4)*(S1*S1-FN*S2))
       B=((S1*T1-FN*T2)-C*(S1*S2-FN*S3))/(S1*S1-FN*S2)
       A=(T1-C*S2-B*S1)/FN
       A1=1.0E-10*EXP(A2)
       TEMP=C/C1
```

```
      IF (TEMP.LT.0.8) GO TO 222
      F=2.*F
      GO TO 225
  222 IF (TEMP.GE.0.) GO TO 23
      F=0.5*F
  225 WRITE(6,115) F
  115 FORMAT(1H ,2X,3HF= ,1PE9.3)
   23 IF(SUMA.GE.2.0E-11) GO TO 25
C PRINT OUT DATA
   24 WRITE(6,116)TNRS,A1,BB,(TIME(J),NR(J,1),NR(J,2),NR(J,3),J=1,N)
  116 FORMAT(1H0,5X,6HTNRS= ,1PE10.3,6X,4HA1= ,E10.3,6X,3HB= ,E10.3/
     11H0/10X,4HTIME,15X,4HDATA,15X,2HRS,17X,5HRSBAR/1H /
     2(10X,0PF8.3,11X,3(1PE10.3,6X)/)/1H  )
      K=40
   25 IF(K.EQ.30) GO TO 24
      DO26 J=1,N
   26 NR(J,3)=1.0E-10*EXP(A+B*X(J))
      TNRS=TNRS+SUM
      SUM=F*C*EXP(A)
      SUMA=ABS(SUM)
      WRITE(6,117)TNRS,SUM,A,B,C
  117 FORMAT(1H ,5X,6HTNRS= ,1PE10.3,6X,5HSUM= ,E10.3,9X,3HA= ,
     1E10.3,12X,3HB= ,0PF6.3,15X,3HC= ,1PE10.3)
      A2=A
      BB=B
C ADJUST DATA
      CRIT=(NR(N,4)-SUM)/NR(N,4)
      IF(CRIT.GT.0.) GO TO 27
      SUM=0.5*NR(N,4)
      F=0.5*F
      WRITE(6,115)F
   27 DO28 J=1,N
      NR(J,2)=NR(J,4)
      NR(J,4)=NR(J,4)-SUM
      IF(NR(J,4).GT.0.) GO TO 28
      WRITE(6,120) J,NR(J,4)
  120 FORMAT(3X,36HADJUSTED DATA POINT NON-POSITIVE. J= ,I4,5X,
     18HNR(J,4)= ,E10.4)
      NR(J,4)=1.0E-9/1.5**J
   28 CONTINUE
      RETURN
      END
      SUBROUTINE DAPLOT (LOGET,LOGES,NPT,BLANK,DOT,STAR,TITLL,ANUML,
     XTITLB,AXB,ANUMB,TITLT)
      REAL LOGET(50),LOGES(50),TITLL(50),ANUML(51),TITLB(30),AXB(30)
      REAL ANUMB(30),LINE(112,50),TITLT(20)
      WRITE(6,50)TITLT
   50 FORMAT(1HL,20X,20A4)
      DO 100 I=1,112
      DO 100 J=1,50
      LINE(I,J)=BLANK
  100 CONTINUE
      DO 300 I=1,NPT
      J=IFIX((0.4343*LOGET(I)+1.3)*26.)
```

```
      K=51-IFIX((0.4343*LOGES(I)-1.)*13.)
      IF(J .LE.0 .OR. J .GT. 112 .OR. K .LE. 0 .OR. K .GT. 50)GO TO 300
      LINE(J,K)=STAR
300   CONTINUE
      DO 400 I=1,50
      WRITE(6,350)TITLL(I),ANUML(I),DOT,(LINE(J,I),J=1,112)
350   FORMAT(1H ,A1,1X,A4,1X,A1,112A1)
400   CONTINUE
      WRITE(6,450)ANUML(51),AXB,ANUMB,TITLB
450   FORMAT(3X,A4,1X,30A4/7X,30A4//8X,30A4)
      RETURN
      END
/*
//LKED     EXEC PGM=LINKEDIT,COND=(5,LT),REGION=140K
//SYSPRINT DD SYSOUT=A,UNIT=SYSDA,                                    X
//         DCB=(LRECL=121,RECFM=FBA,BLKSIZE=1573)
//SYSLIB   DD DISP=SHR,DSNAME=SYS1.FORTLIB
//         DD DISP=SHR,DSNAME=ENG.D2EB.BSLIB
//SYSLMOD  DD UNIT=SYSDA,DISP=(,PASS),DSNAME=&&PDS(MEMB),
//            SPACE=(1024,(200,10,1),RLSE),DCB=BLKSIZE=1024
//SYSUT1   DD UNIT=SYSDA,SPACE=(3250,(250,5),RLSE),DCB=BLKSIZE=1024
//SYSLIN   DD DSNAME=&LOADSET,DISP=(OLD,DELETE)
//GO       EXEC PGM=*.LKED.SYSLMOD,COND=(5,LT,LKED)
//FT05F001 DD DDNAME=SYSIN
//FT06F001 DD SYSOUT=A,UNIT=SYSDA,                                    X
//         DCB=(LRECL=130,RECFM=FBA,BLKSIZE=1430)
//SYSIN    DD *
 .*
          STRAIN - UNITS OF ONE MICROSTRAIN
            5                2                1              0.5
 0.2              0.1              0.05             0.02             0.01
    .005                .002             .001
                                         TIME AFTER LOAD RELEASE - MINUTES

I.....I.....I.....I.....I.....I.....I.....I.....I.....I.....I.....I.....I.
0.05    0.1     0.2      0.5      1        2        5       10       20       50
      100     200      500     1000
 DATE 11/03/69 ULE SILICA 114 REGROUND TORSION          STRESS=          MN/M2
01          0.2666
10          1.0000      0.0         -0.9652     91.5
11          0.0206      0.0         -0.0206     0.00001
12          0.0234      0.0028      -0.0182     0.00001
01          0.0256      0.0046      -0.0156     0.00001
02          0.2180      0.0042      -0.2070     0.00001
03          2.2220      0.0020      -2.2000     0.00001
04          2.3220      0.0280      -2.3220     0.000001
30
04          0.1081      0.0280      0.0019      0.0119      0.4191
04          0.1599      0.0261      0.0019      0.0159      0.5399
04          0.1499      0.0320      -0.0009     0.0159      0.7255
04          0.1870      0.0657      -0.0002     0.0147      1.0610
04          0.2367      0.1338      0.0         0.0199      1.5047
04          0.3159      0.3214      -0.0008     0.0199      1.8677
```

```
04          0.3794      0.4460      -0.0022     0.0399      2.0121
01          0.0         0.0058      0.0006      0.0032      0.0058
30
0.1081      0.0019      0.0119      0.4191
19          04          2.01
0.0819      0.0632      0.0568      0.0554      0.0511      0.0475
0.0448      0.0421      0.0394      0.0376      0.0331      0.0320
0.0299      0.0295      0.0290      0.0308      0.0283      0.0286
0.0280
01
0.1599      0.0019      0.0159      0.5399
19          04          2.01
0.1090      0.0926      0.0826      0.0740      0.0675      0.0620
0.0580      0.0500      0.0526      0.0420      0.0370      0.0343
0.0326      0.0324      0.0309      0.0300      0.0298      0.0294
0.0261
01
0.1499      -0.0009     0.0159      0.7255
19          04          2.01
0.1600      0.1336      0.1164      0.1040      0.0940      0.0866
0.0804      0.0760      0.0720      0.0569      0.0496      0.0460
0.0434      0.0410      0.0400      0.0387      0.0389      0.0387
0.0320
01
0.1870      -0.0002     0.0147      1.0610
19          04          2.01
0.3022      0.2550      0.2232      0.2020      0.1844      0.1712
0.1612      0.1520      0.1451      0.1150      0.1016      0.0930
0.0879      0.0894      0.0820      0.0790      0.0780      0.0748
0.0657
01
0.2367      0.0         0.0199      1.5047
19          04          2.01
0.5000      0.4220      0.3730      0.3390      0.3142      0.2942
0.2790      0.2664      0.2554      0.2090      0.1896      0.1764
0.1749      0.1656      0.1607      0.1560      0.1542      0.1494
0.1338
01
0.3159      -0.0008     0.0199      1.8677
20          04          2.01
1.0200      0.8440      0.7570      0.7000      0.6560      0.6222
0.5950      0.5730      0.5550      0.4804      0.4394      0.4190
0.4047      0.3943      0.3849      0.3778      0.3714      0.3670
0.3348      0.3214
01
0.3794      -0.0022     0.0399      2.0121
35          04          3.01
1.4220      1.2940      1.2080      1.1440      1.0942      1.0552
1.0234      0.9960      0.8810      0.8209      0.7866      0.7635
0.7468      0.7324      0.7197      0.7115      0.7027      0.6499
0.6250      0.6078      0.5957      0.5876      0.5799      0.5735
0.5686      0.5631      0.5360      0.5209      0.5018      0.4867
0.4729      0.4596      0.4569      0.4466      0.4460
02
```

DATE 11/06/69 CFP-VIT 104 BEGROUND TOESTEN SAMPLE DIAMETER= 0.2577 INCHES

LMULT= 1.283E-00 EXMULT= 9.204E-01
LOAD SENSITIVITY = 1.1363E 02 LOAD ZERO = 7.7268E 00
GAIN NUMBER= 11 SENSITIVITY= 4.4C36E-04 ZERO= 1.8936E-06
GAIN NUMBER= 12 SENSITIVITY= 4.3827E-04 ZERO= 1.9722E-06
GAIN NUMBER= 1 SENSITIVITY= 4.4248E-04 ZERO= 2.2124E-06
GAIN NUMBER= 2 SENSITIVITY= 4.2947E-05 ZERO= 2.3191E-07
GAIN NUMBER= 3 SENSITIVITY= 4.1229E-06 ZERO= 2.4737E-08
GAIN NUMBER= 4 SENSITIVITY= 3.9416E-07 ZERO= 4.2175E-09

SINGLE POINT VALUES-NO EXTRAPOLATION

| STRESS | YIELD STRAIN | LOAD STRAIN | LONG-BENDING | LATERAL BENDING |
|---|---|---|---|---|
| 6.647E 00 | 5.578E-08 | 2.336E-04 | 1.321E-07 | 5.624E-07 |
| 8.681E 00 | 1.786E-08 | 2.872E-04 | 2.569E-08 | 4.894E-07 |
| 1.448E 01 | 5.554E-08 | 4.634E-04 | -2.202E-08 | 9.277E-07 |
| 1.740E 01 | 8.029E-08 | 5.682E-04 | -1.468E-08 | 5.850E-07 |
| 2.337E 01 | 1.405E-07 | 7.305E-04 | -1.798E-07 | 5.624E-07 |
| 3.029E 01 | 2.322E-07 | 8.289E-04 | -4.037E-08 | 6.209E-07 |
| 3.765E 01 | 3.814E-06 | 8.939E-04 | -5.872E-08 | 5.624E-07 |
| 0.0 | 3.628E-07 | 8.850E-07 | 2.936E-08 | 4.383E-08 |

```
DATE 11/06/69 CFR-VIT 104 REFROUND TORSION                STRESS=     6.6 MN/M2


      STRESS=   6.647E 00 N/M2     LOAD STRAIN=   2.336E-04
   LONGITUDINAL BENDING STRAIN=   1.321E-07    LATERAL BENDING STRAIN=   5.624E-07
  EV READOUT
       1.0400E 00  6.3200E-01  4.6700E-01  3.7600E-01  3.1820E-01  2.7700E-01
       2.4660E-01  2.2320E-01  2.0440E-01  1.2900E-01  9.4000E-02  7.8700E-02
       6.8000E-02  6.0000E-02  5.5400E-02  5.1600E-02  4.9000E-02  4.6400E-02
       3.5000E-02

  STRAIN DATA
       4.0571E-07  2.4489E-07  1.7985E-07  1.4399E-07  1.2120E-07  1.0496E-07
       9.2982E-08  8.3758E-08  7.6348E-08  4.6623E-08  3.2933E-08  2.6803E-08
       2.2585E-08  1.9432E-08  1.7619E-08  1.6121E-08  1.5096E-08  1.4071E-08
       9.5780E-09

      TNRS= -4.220E-10      SUM=  1.403E-07      A=  6.505E 00      B= -0.855      C=  6.557E-02
   E= 1.600E-09
      TNRS=  4.578E-09      SUM=  2.171E-08      A=  6.445E 00      B= -0.936      C=  2.155E-02
   E= 8.000E-10
   E= 4.000E-10
      TNRS=  7.078E-09      SUM= -7.766E-09      A=  6.442E 00      B= -0.987      C= -3.093E-02
   E= 2.000E-10
      TNRS= -6.880E-10      SUM=  8.991E-09      A=  6.509E 00      B= -0.851      C=  6.700E-02
   E= 1.000E-10
      TNRS=  8.304E-09      SUM= -5.572E-09      A=  6.475E 00      B= -1.012      C= -8.591E-02
   E= 5.000E-11
      TNRS=  2.732E-09      SUM=  1.375E-09      A=  6.464E 00      B= -0.903      C=  4.248E-02
      TNRS=  4.107E-09      SUM=  8.805E-10      A=  6.449E 00      B= -0.929      C=  2.786E-02
      TNRS=  4.988E-09      SUM=  4.943E-10      A=  6.442E 00      B= -0.944      C=  1.543E-02
      TNRS=  5.472E-09      SUM=  2.276E-10      A=  6.439E 00      B= -0.954      C=  7.272E-03
      TNRS=  5.700E-09      SUM=  9.492E-11      A=  6.439E 00      B= -0.958      C=  3.032E-03
      TNRS=  5.795E-09      SUM=  3.666E-11      A=  6.438E 00      B= -0.960      C=  1.173E-03
      TNRS=  5.831E-09      SUM=  1.384E-11      A=  6.438E 00      B= -0.961      C=  4.426E-04

      TNRS=  5.831E-09      A1=  6.253E-08      B= -9.607E-01

        TIME          DATA          RS          RSBAR
       0.167      4.057E-07     3.999E-07     3.480E-07
       0.251      2.449E-07     2.391E-07     2.361E-07
       0.334      1.799E-07     1.740E-07     1.792E-07
       0.417      1.440E-07     1.382E-07     1.447E-07
       0.501      1.212E-07     1.154E-07     1.215E-07
       0.584      1.050E-07     9.913E-08     1.048E-07
       0.667      9.298E-08     8.715E-08     9.220E-08
       0.751      8.376E-08     7.793E-08     8.235E-08
       0.834      7.635E-08     7.052E-08     7.443E-08
       1.667      4.663E-08     4.080E-08     3.826E-08
       2.501      3.283E-08     2.700E-08     2.592E-08
       3.334      2.680E-08     2.097E-08     1.966E-08
       4.167      2.259E-08     1.675E-08     1.587E-08
       5.001      1.943E-08     1.360E-08     1.332E-08
       5.834      1.762E-08     1.179E-08     1.149E-08
       6.667      1.612E-08     1.029E-08     1.010E-08
       7.501      1.510E-08     9.265E-09     9.022E-09
       8.334      1.407E-08     8.240E-09     8.154E-09
      16.667      9.578E-09     3.747E-09     4.190E-09

      TNRS=  5.845E-09      SUM=  5.120E-12      A=  6.438E 00      B= -0.961      C=  1.638E-04
```

DATE 11/06/69 CEP VII 194 BEGROUND TEPSICN
STRESS= 6.6 MN/M2
STRESS RELAXATION, MN/M2
0.5
0.2
0.1
0.05
0.02
0.01
0.005
0.002
0.001
0.05
0.1
0.2
0.5
1
2
5
10
20
50
100
200
500
1000
TIME AFTER LOAD RELEASE - MINUTES

## REFERENCES


1. Eul, William A. and Woods, W. William: Shear Strain Properties to $10^{-10}$ of Selected Optical Materials. NASA Contractor Report NASA CR-1257.

2. Woods, W. W. and Recker, H., Nanostrain Materials Testing. Document D2-113501-1, The Boeing Company, January 1967.

3. Moberly, J. W., Goggin, William R., and Sedlacek, Rudolf: Hydrostatic Ring Test for High Precision Strain Measurements. RSI Vol. 39 No. 6 pp 835-837, June 1968.

4. Shanley, F. R.: Strength of Materials, pp 186-195. McGraw-Hill Book Company, Inc., New York, 1957.

5. Ramberg, Walter, and Osgood, William R.: Description of Stress-Strain Curves by Three Parameters. NACA Technical Note No. 902, April 8, 1943.

6. Moberly, John W.: Microstrain Behavior of Beryllium and Beryllium Alloys. Stanford Research Institute, Menlo Park, California. Unpublished Report.

7. Maringer, R. E.: The Effects of Processing on the Dimensional Stability of Beryllium Mirrors. Battelle Memorial Institute, Columbus Laboratories, Columbus, Ohio. Presented at the Workshop on Optical Telescope Technology - NASA Marshall Space Flight Center, Huntsville, Alabama, April 29-May 1, 1969.

8. Nutting, P. G.: A New General Law of Deformation. Journal of the Franklin Institute, Vol. 191, p. 679 (1921).

9. Argon, A. S.: Delayed Elasticity in Inorganic Glasses. Dept. of Mech. Engrg., M.I.T., Cambridge, Mass. Preprint 888, March 12, 1968.

10. Murgatroyd, J. B. and Sykes, R.F.R.: The Delayed Elastic Effect in Silicate Glasses at Room Temperature. J. Soc. Glass Technol. Vol. 31 p.17, 1947.

11. Pearson, S.: Creep and Recovery of a Mineral Glass at Normal Temperatures. J. Soc. Glass Technol. Vol. 36 p.105, 1952.

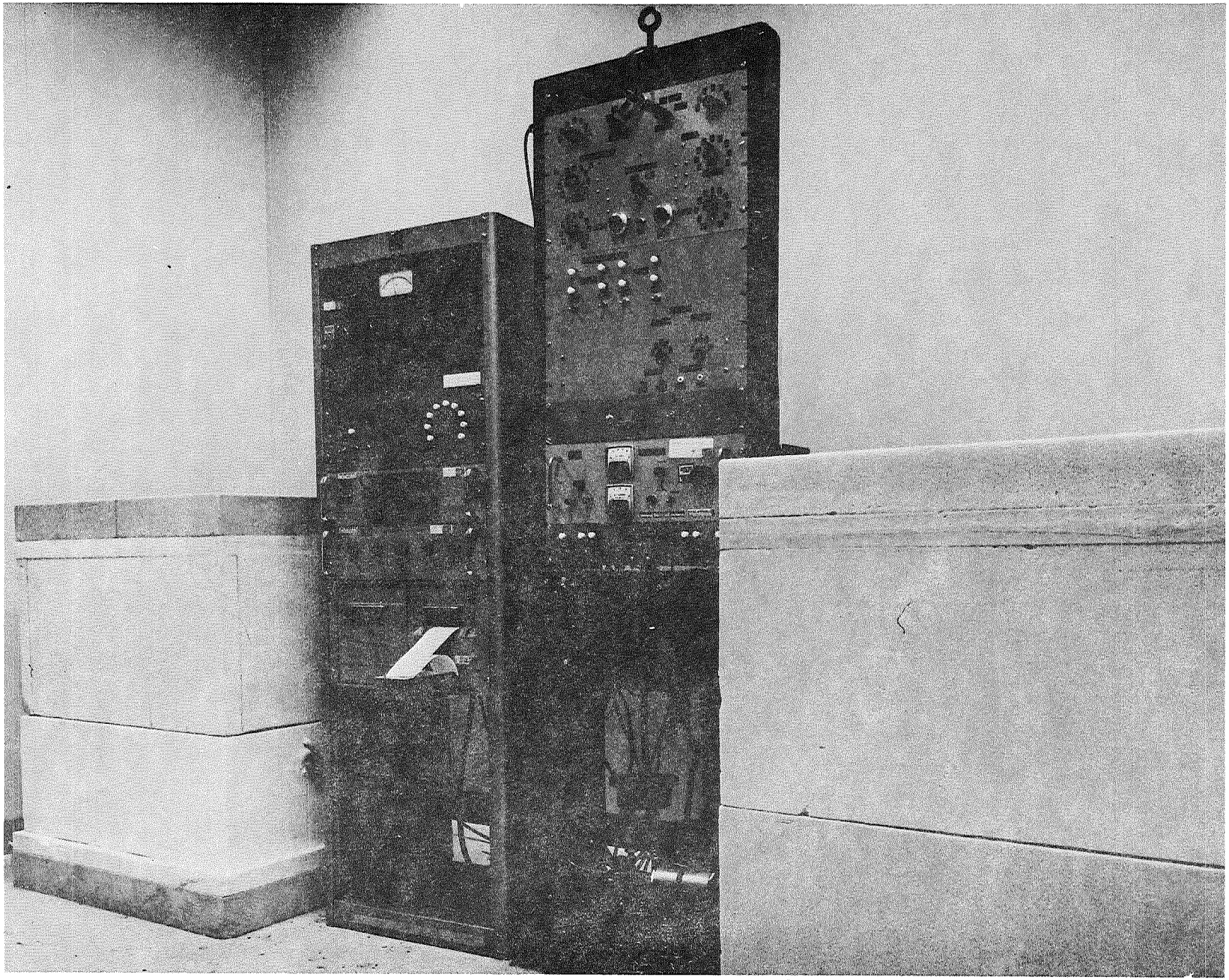

Figure 1: TEST APPARATUS ASSEMBLY

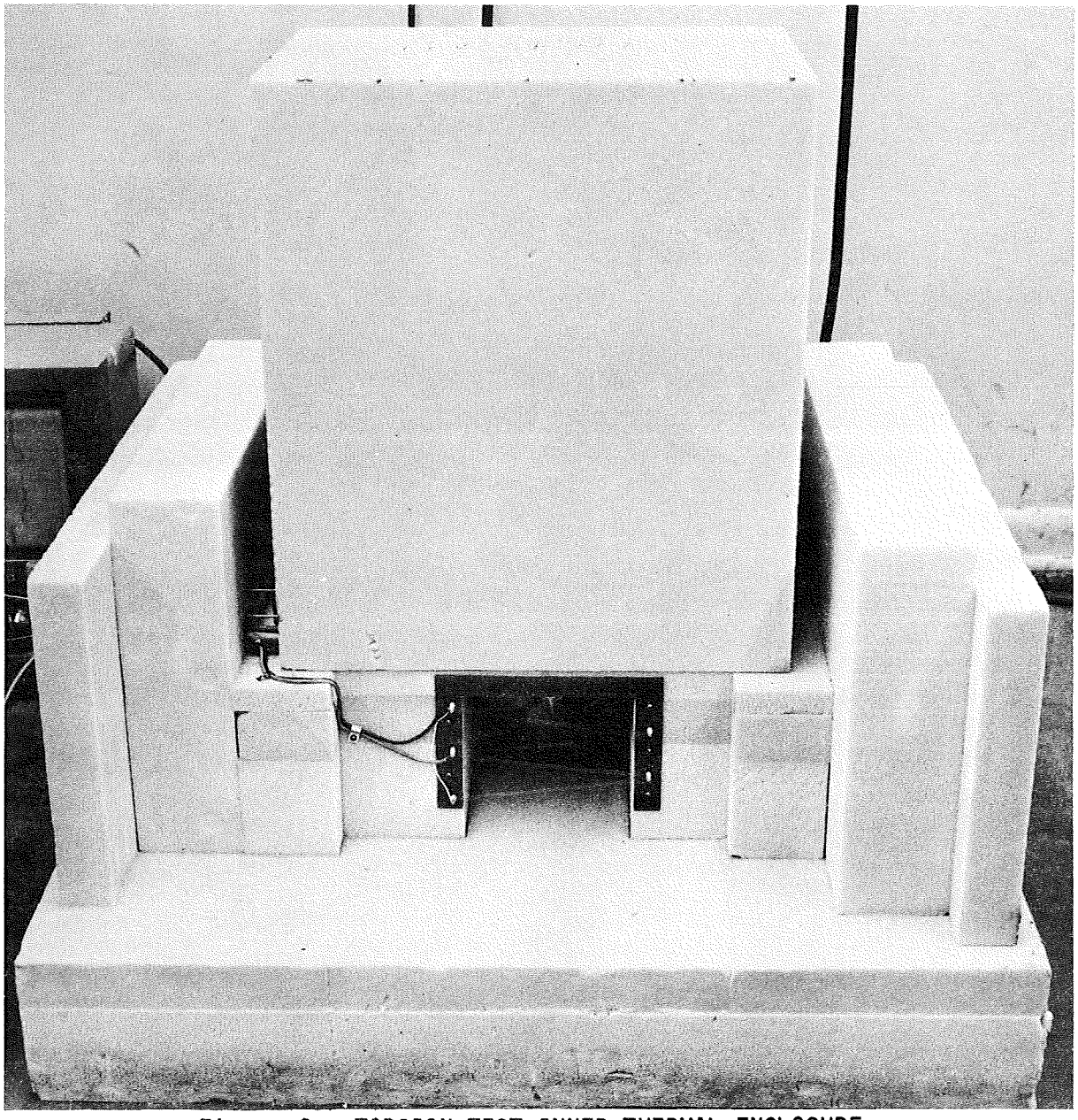

Figure 2: TORSION TEST INNER THERMAL ENCLOSURE

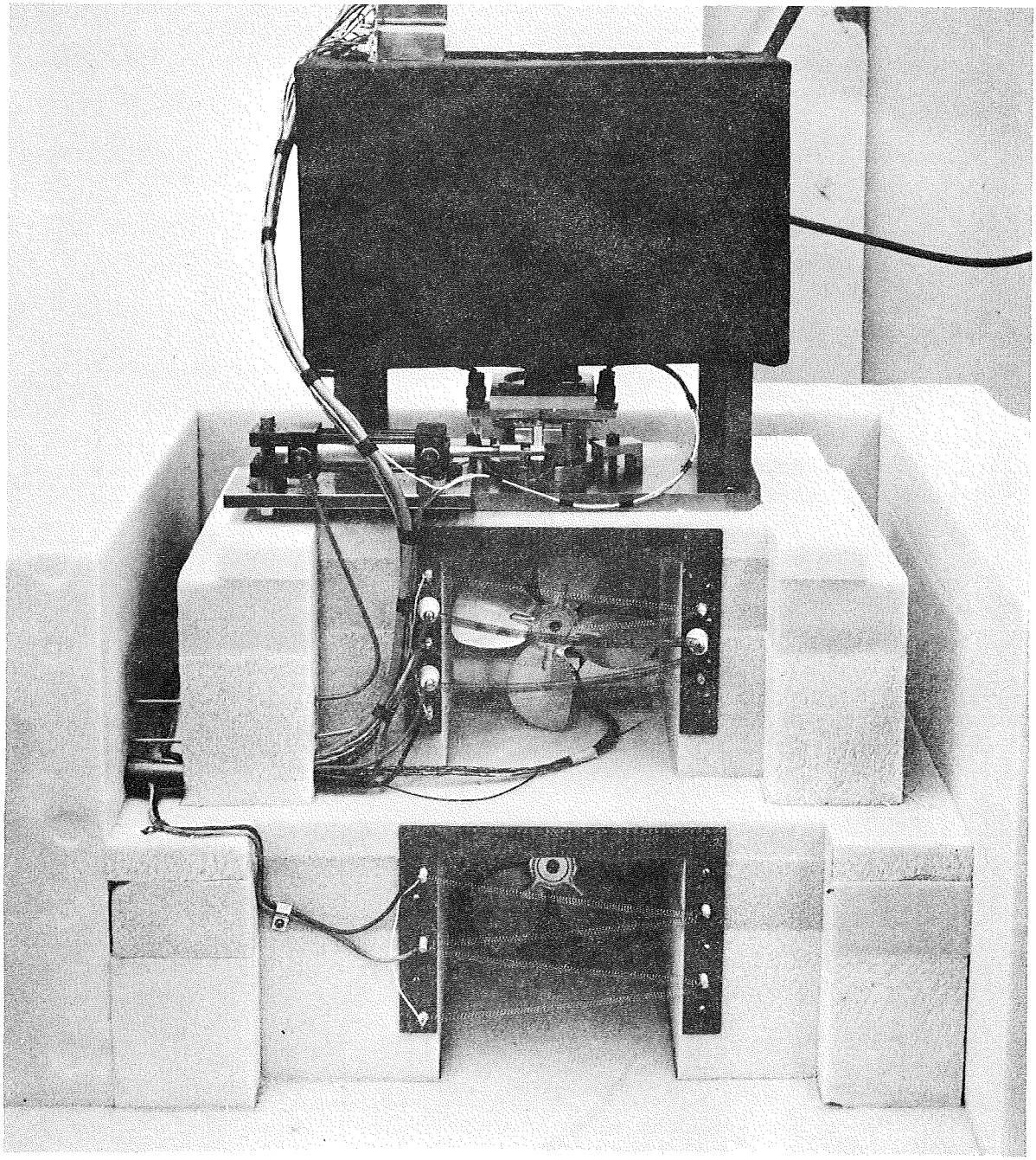

Figure 3: TORSION TEST WINDSCREEN

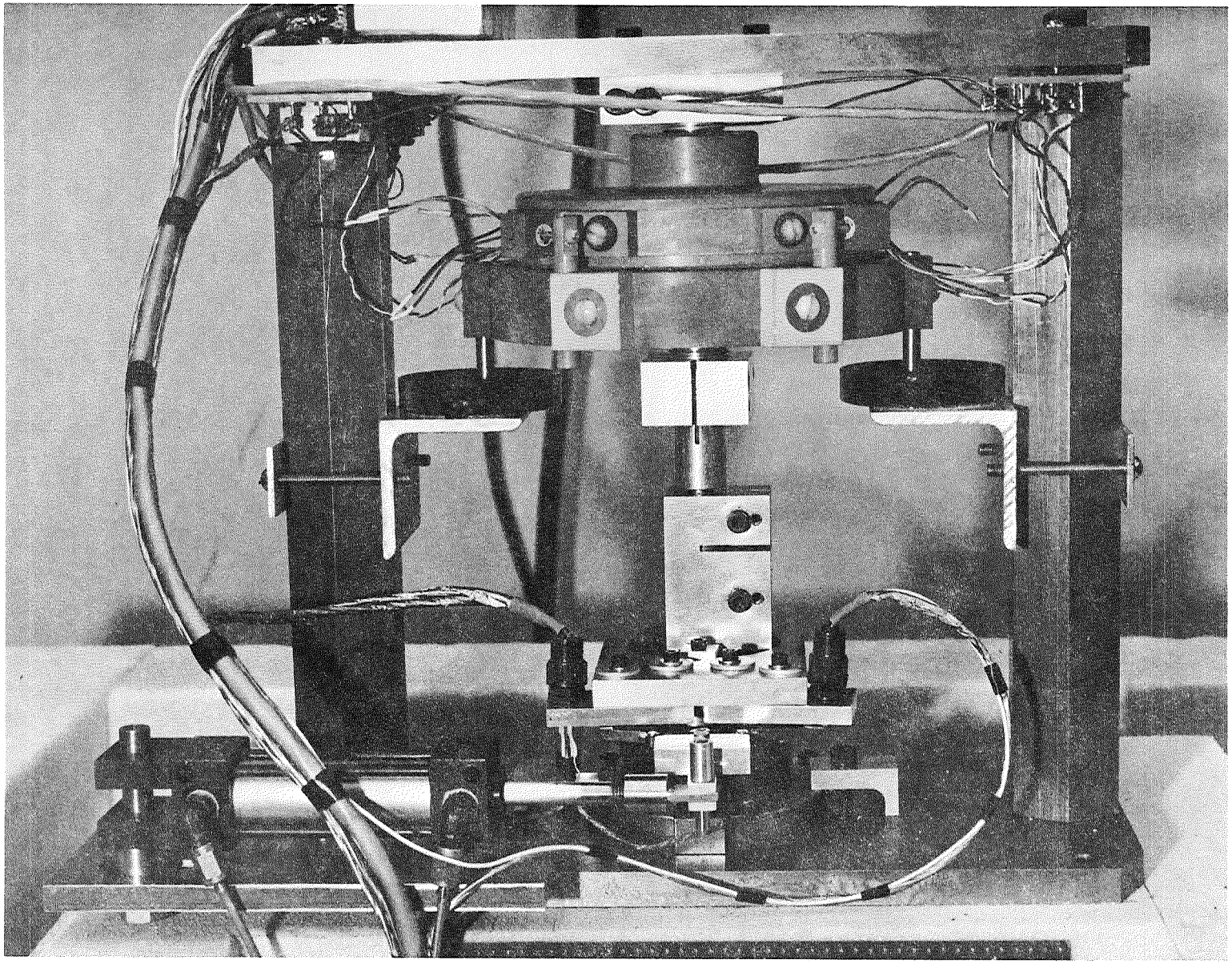

Figure 4: TORSION TEST APPARATUS

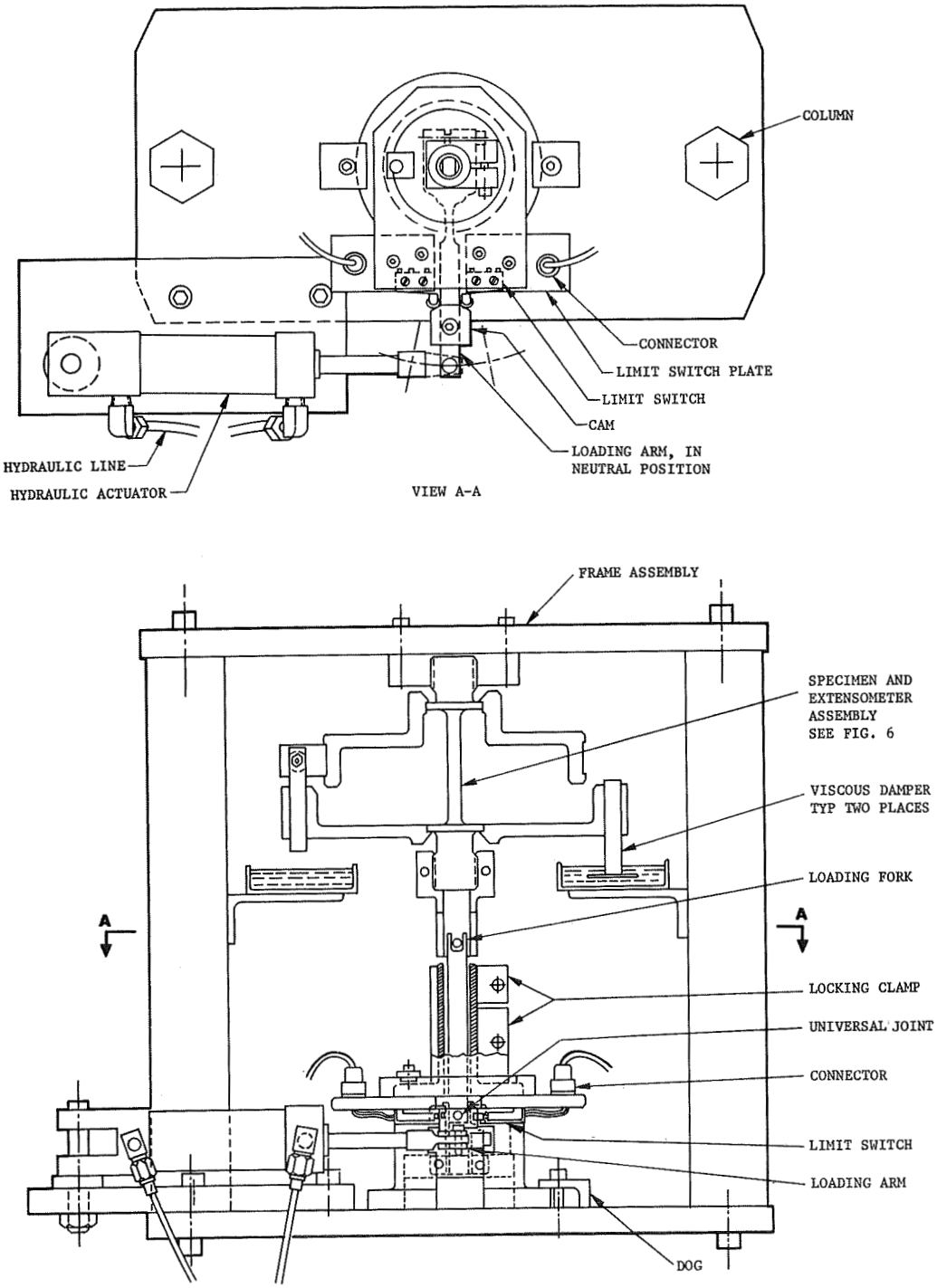


NOTE: FOR CLARITY SOME PARTS OF THE ASSEMBLY ARE SHOWN OUT OF THEIR TRUE LOCATION.

Figure 5: TORSION ASSEMBLY

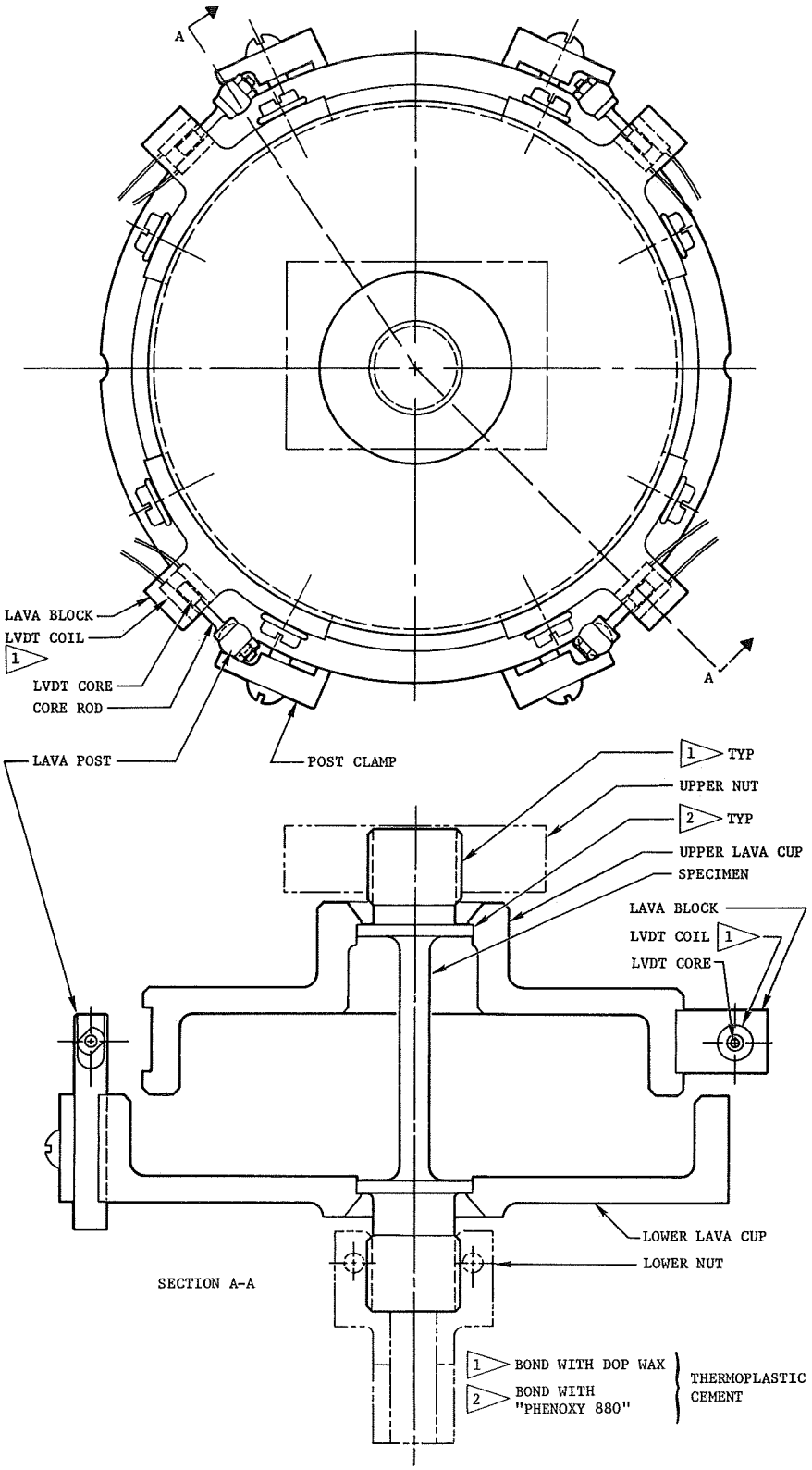


Figure 6: SPECIMEN AND TORSION EXTENSOMETER ASSEMBLY

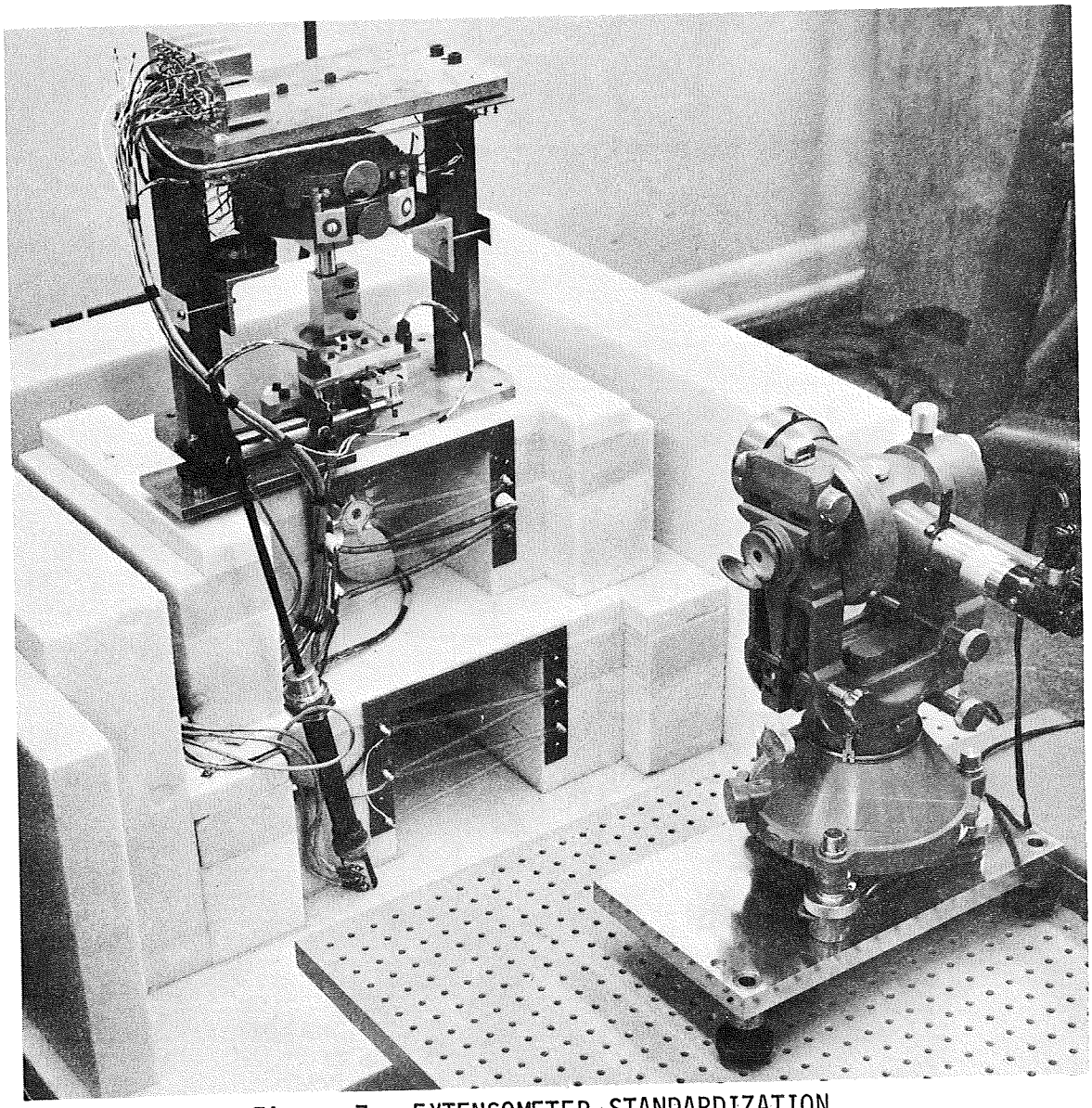

Figure 7: EXTENSOMETER STANDARDIZATION

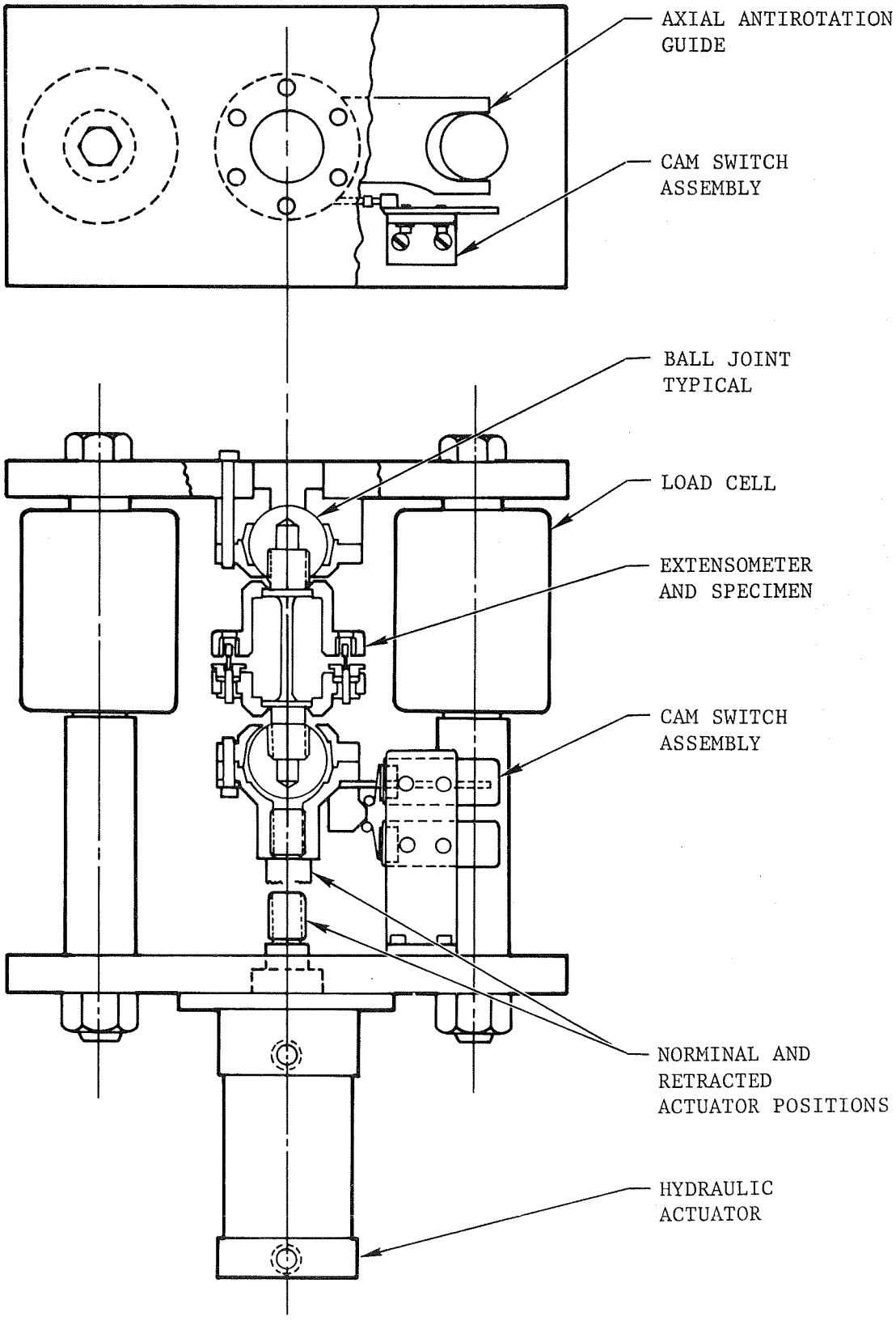


Figure 8 : TENSION-COMPRESSION ASSEMBLY

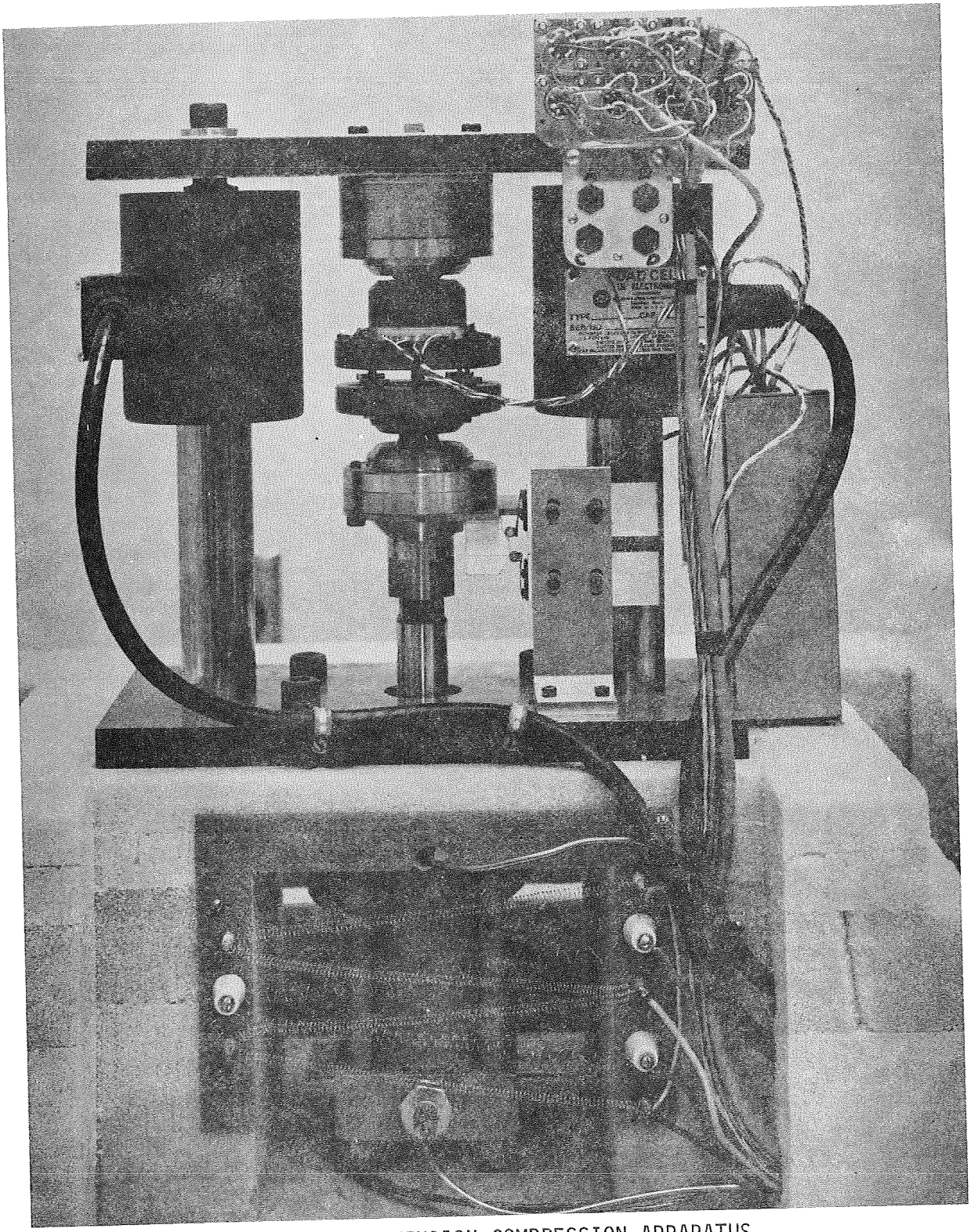

Figure 9: TENSION-COMPRESSION APPARATUS

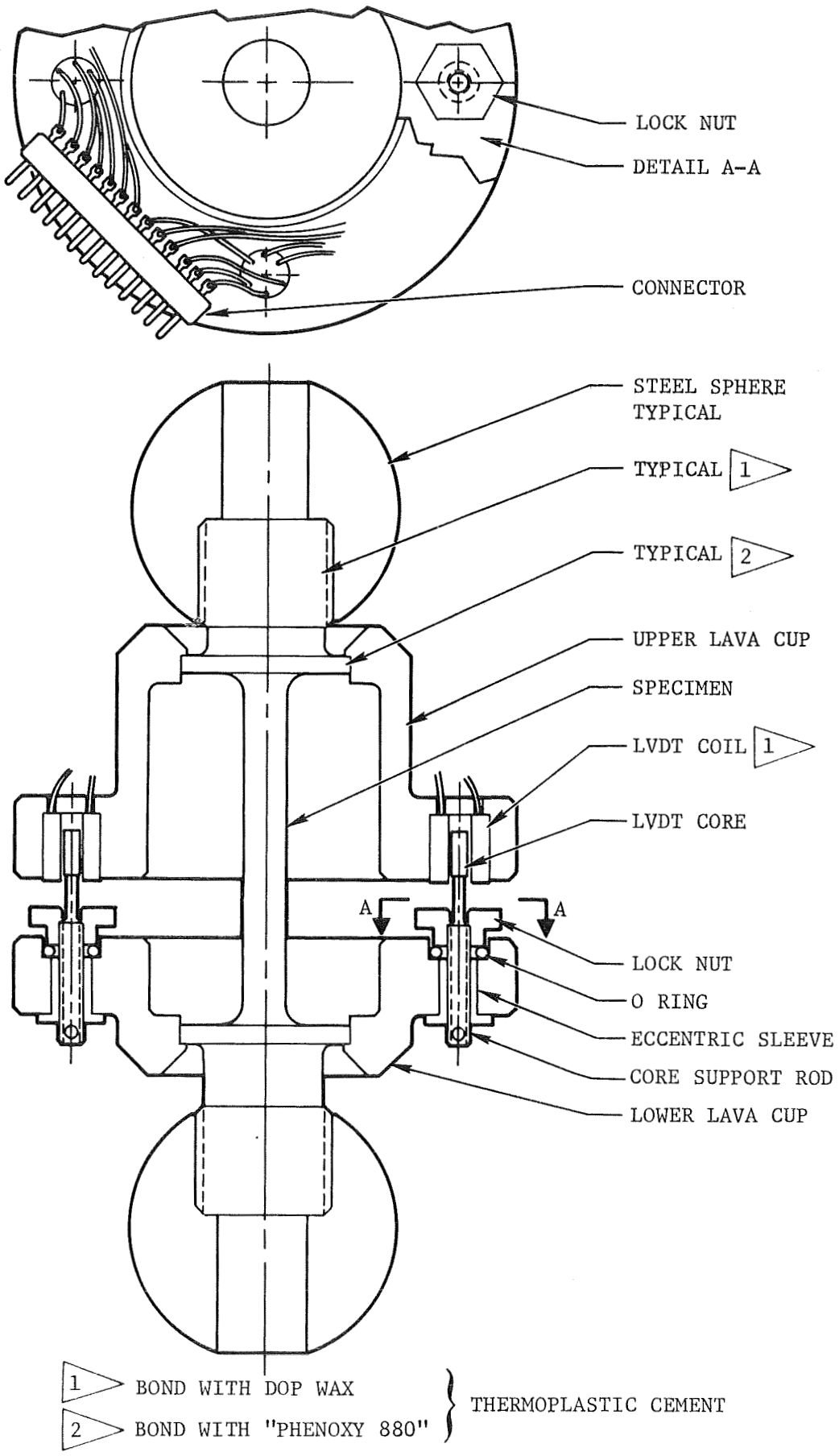


Figure 10: AXIAL EXTENSOMETER ASSEMBLY

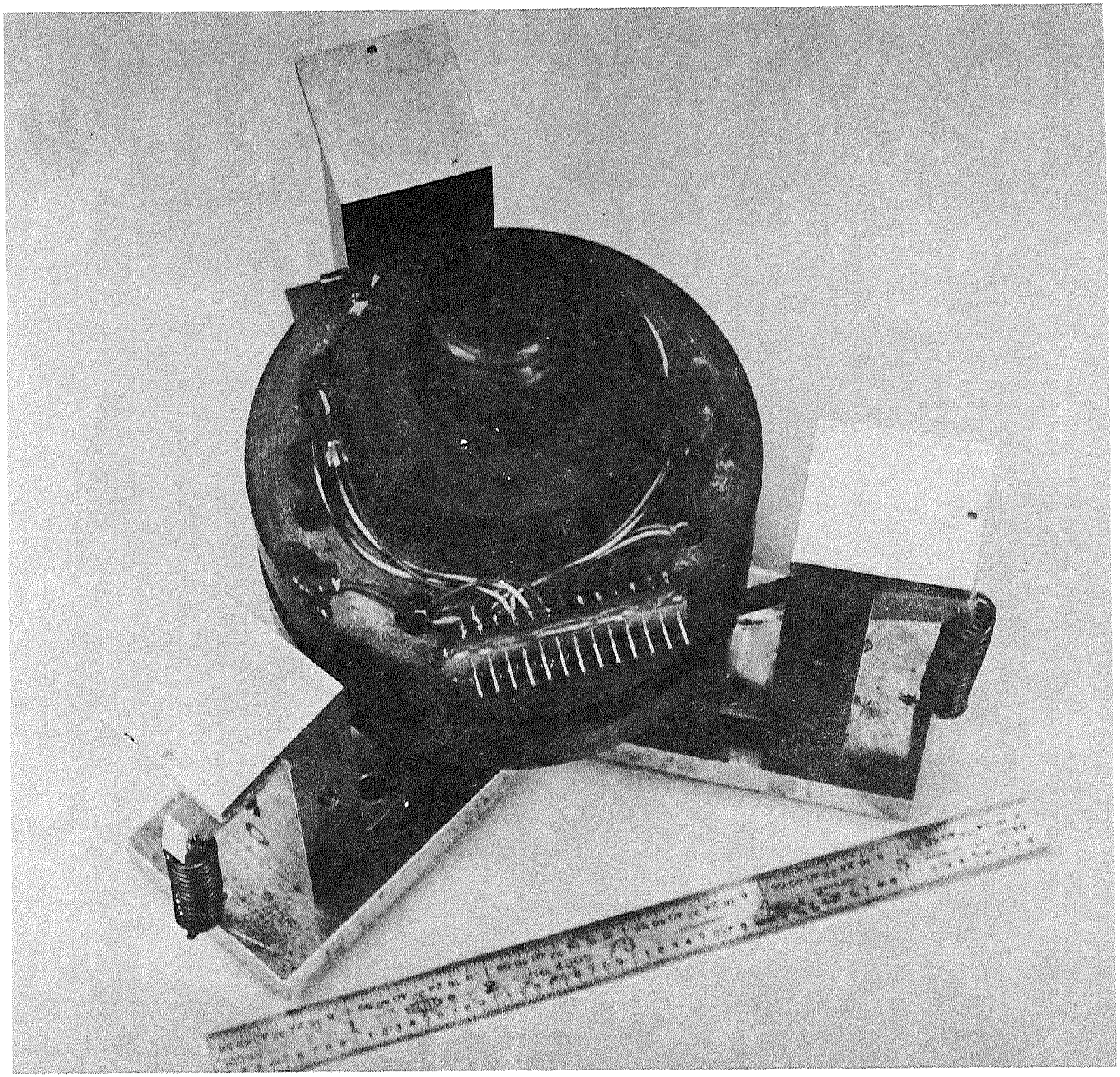

Figure 11: AXIAL EXTENSOMETER IN ASSEMBLY JIG

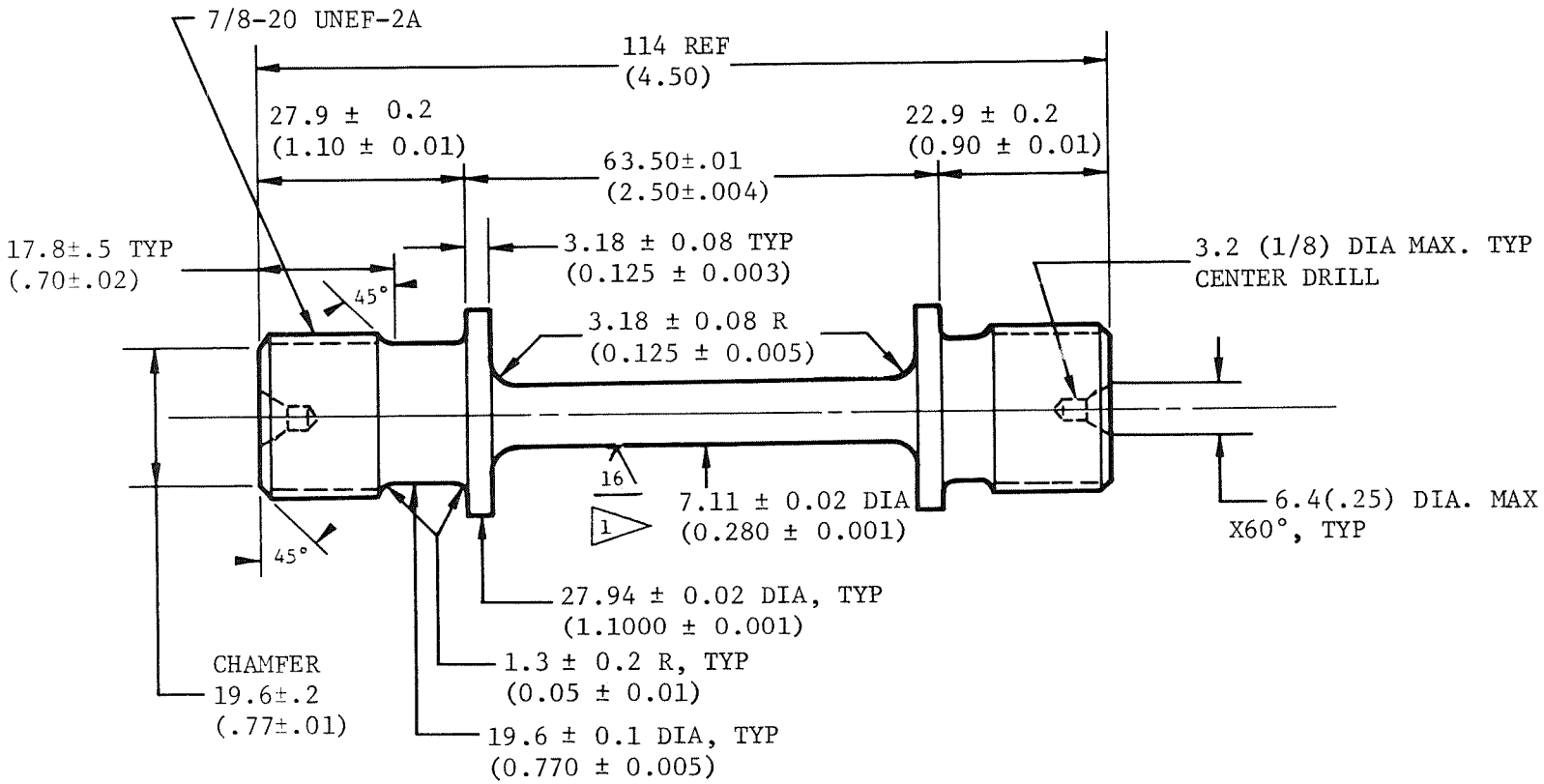


PART TO BE STRESS RELIEVED BEFORE AND AFTER MACHINING.

BREAK ALL CORNERS 0.1 to 0.2 R (0.005 TO 0.010)

ALL DIAMETERS TO BE CONCENTRIC, WITH END CENTERS WITHIN 0.02 TIR. (0.001)

$\overline{32}$ FINISH EXCEPT AS NOTED

1 $\overline{16}$ FINISH TO EXTEND APPROX 2.5 MM ALONG 3.2 R FILLETS

ALL DIMENSIONS IN MILLIMETERS (INCHES)

Figure 12: DIMENSIONED SPECIMEN SKETCH

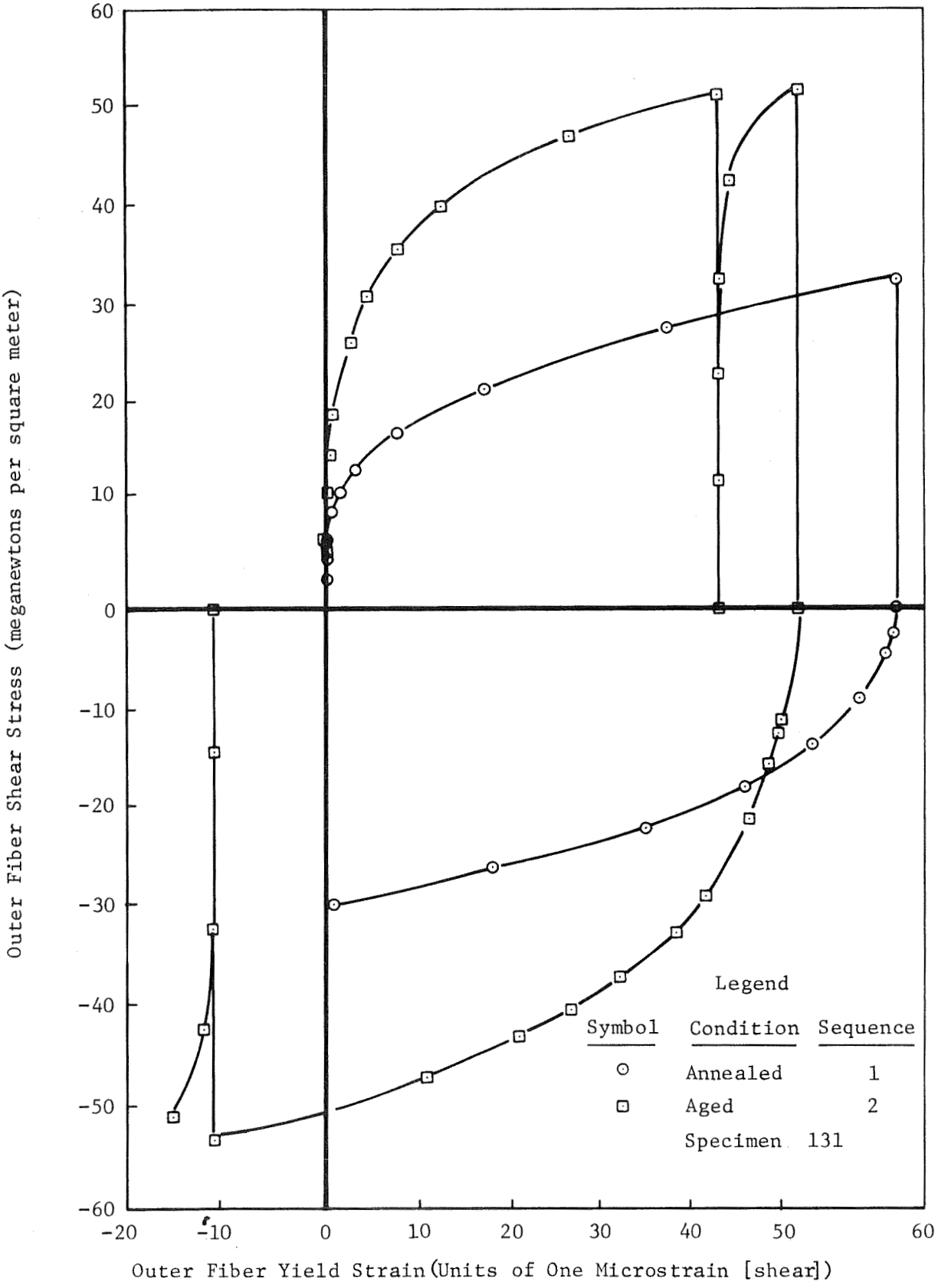


Figure 13: LINEAR PLOT OF TORSIONAL YIELD MEASUREMENTS ON BERYLLIUM

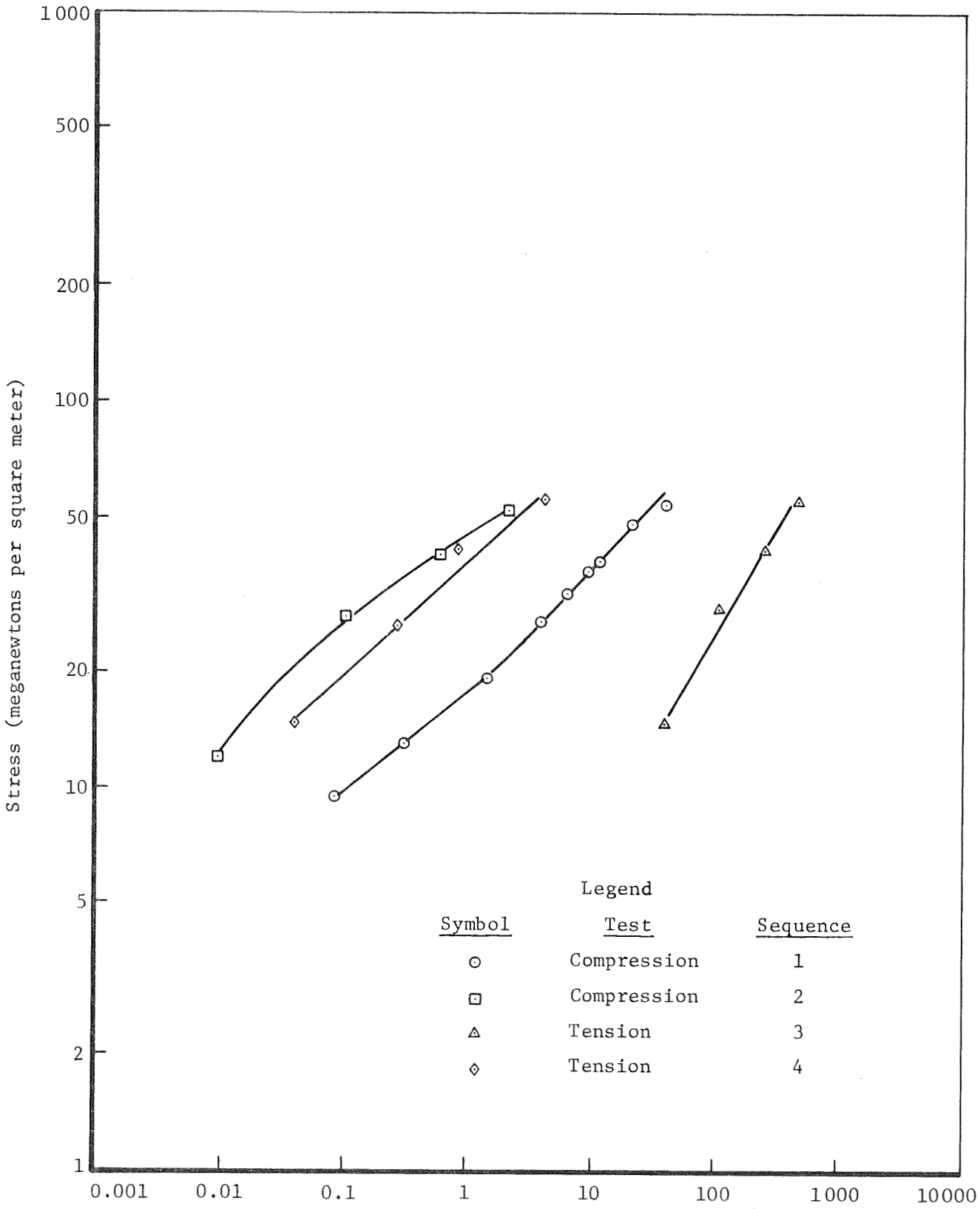


(a) SPECIMEN 133 COMPRESSION TEST

Figure 14: EFFECT OF PRESTRAIN ON YIELD MEASUREMENTS OF BERYLLIUM

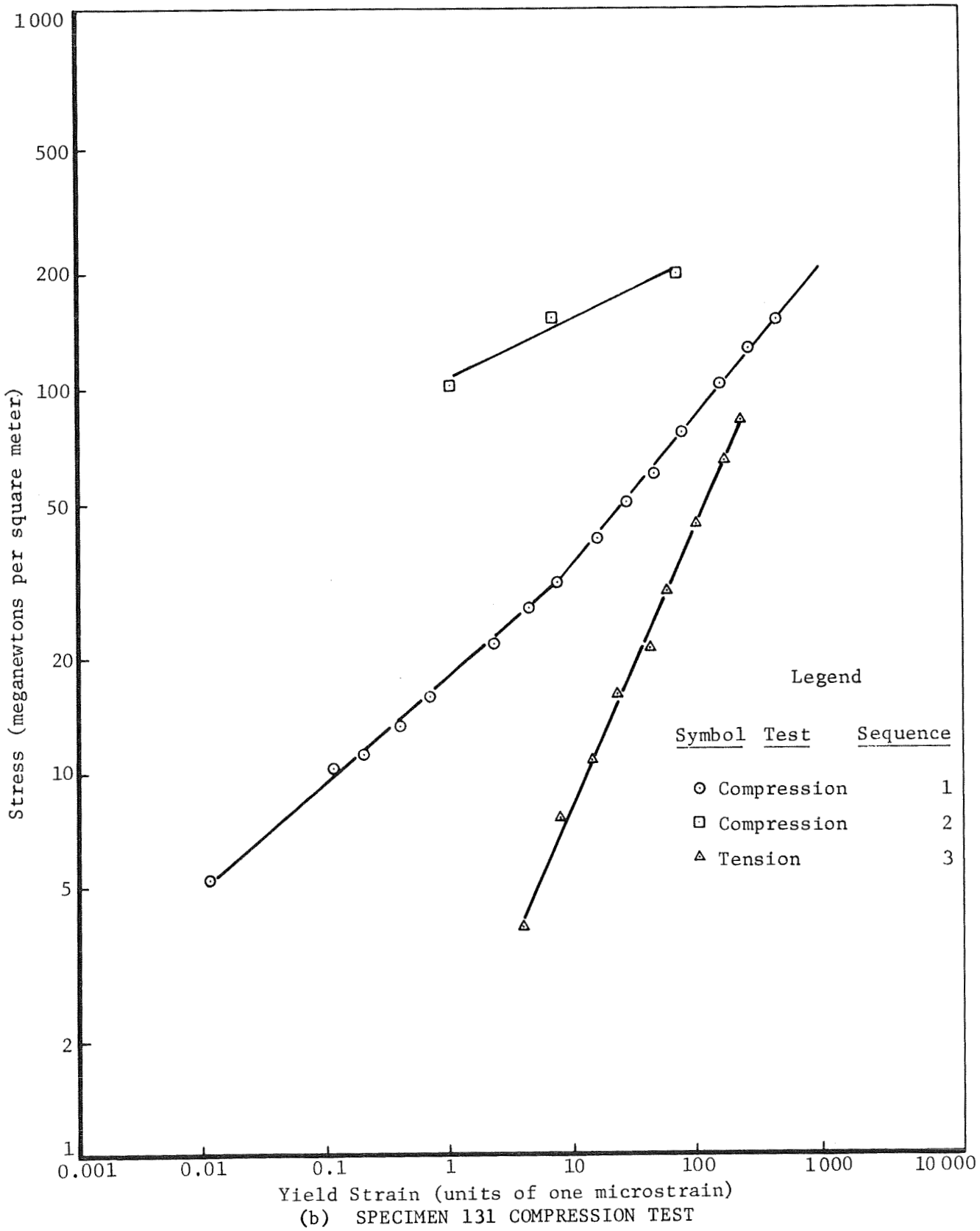


(b) SPECIMEN 131 COMPRESSION TEST

Figure 14: (Concluded)

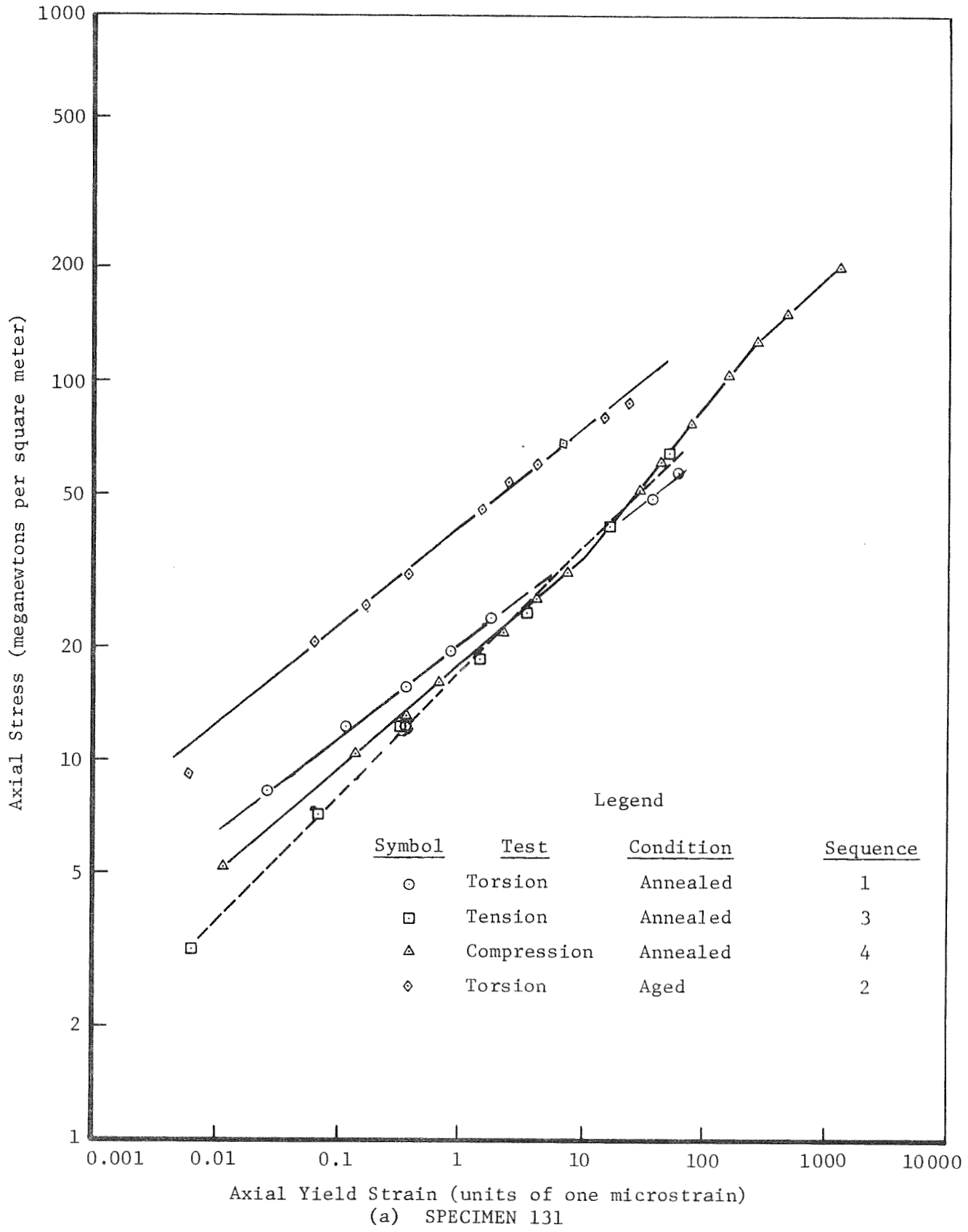


(a) SPECIMEN 131

Figure 15: COMPARISON OF AXIAL AND TORSIONAL MEASUREMENTS ON BERYLLIUM

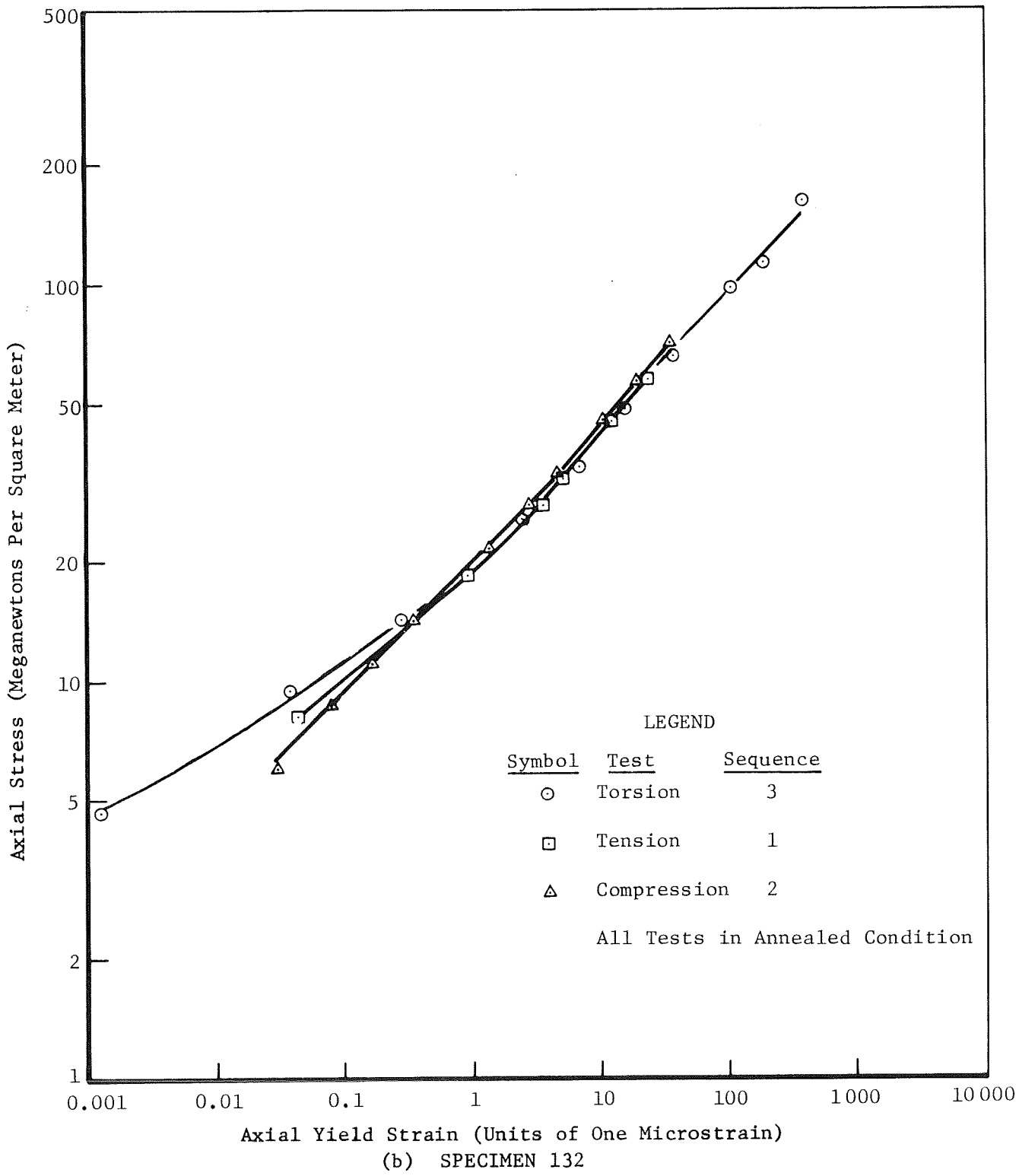


(b) SPECIMEN 132

Figure 15: (Continued)

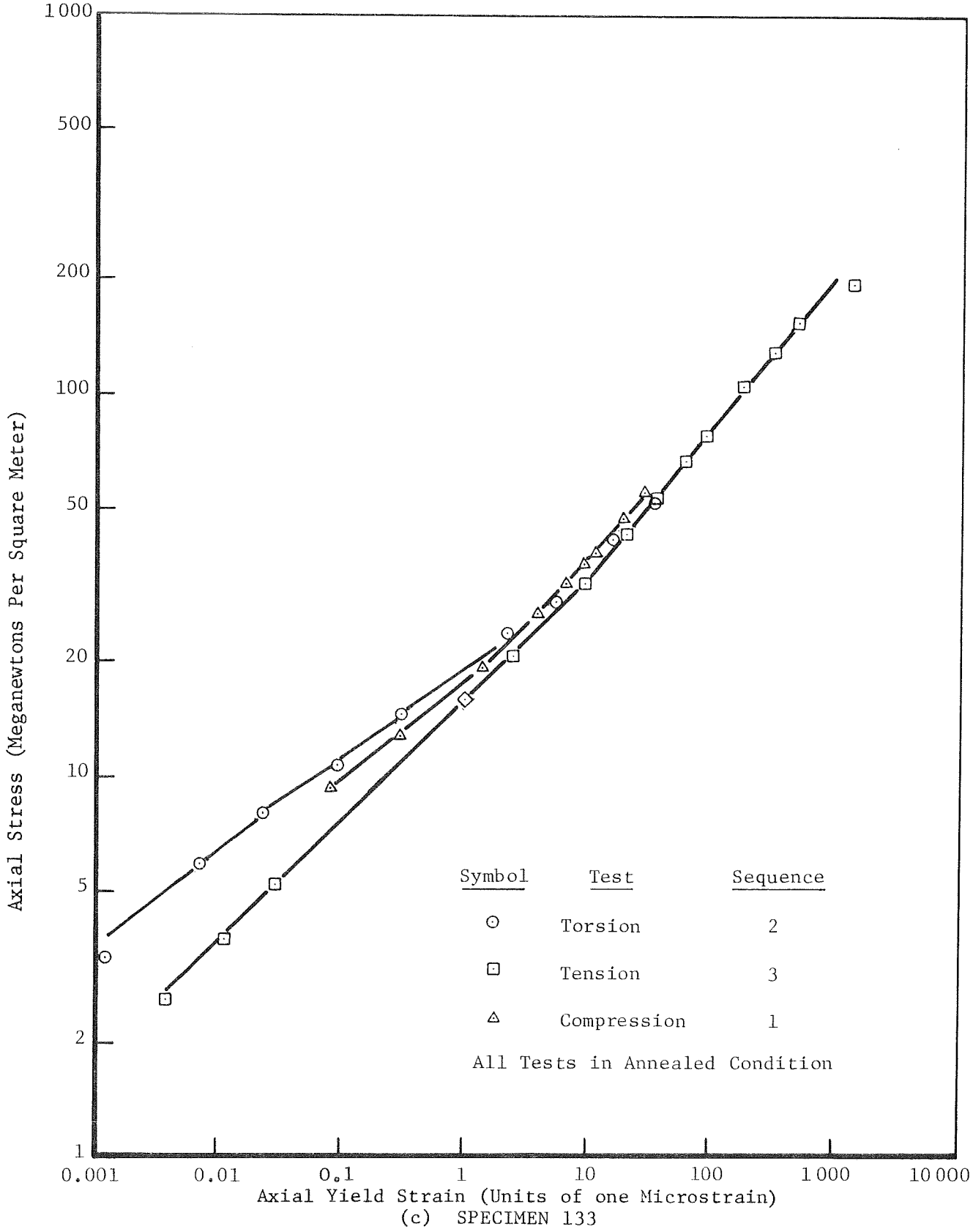


(c) SPECIMEN 133

Figure 15: (Concluded)

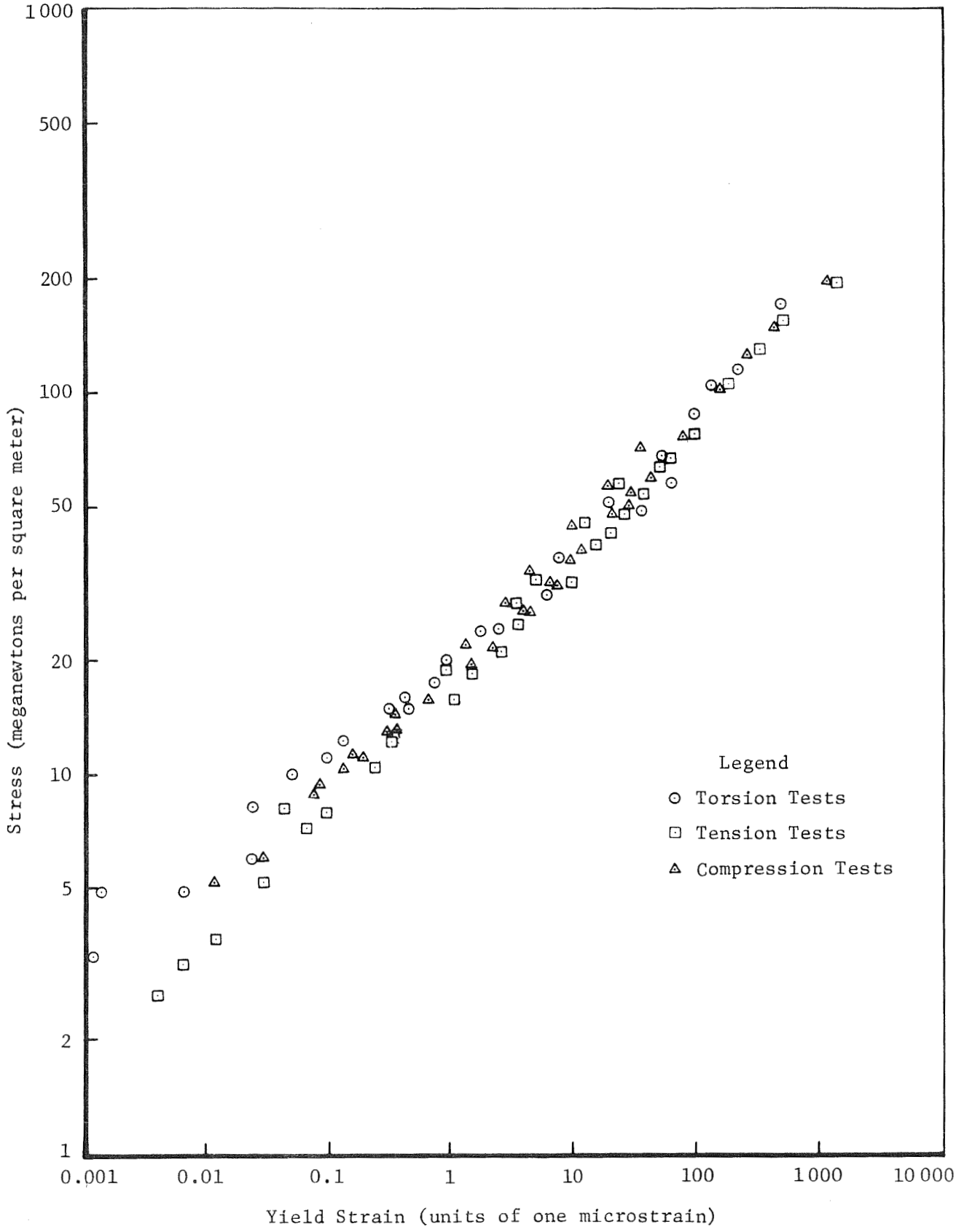


Figure 16: SUMMARY PLOT OF YIELD MEASUREMENTS ON ANNEALED BERYLLIUM SPECIMENS

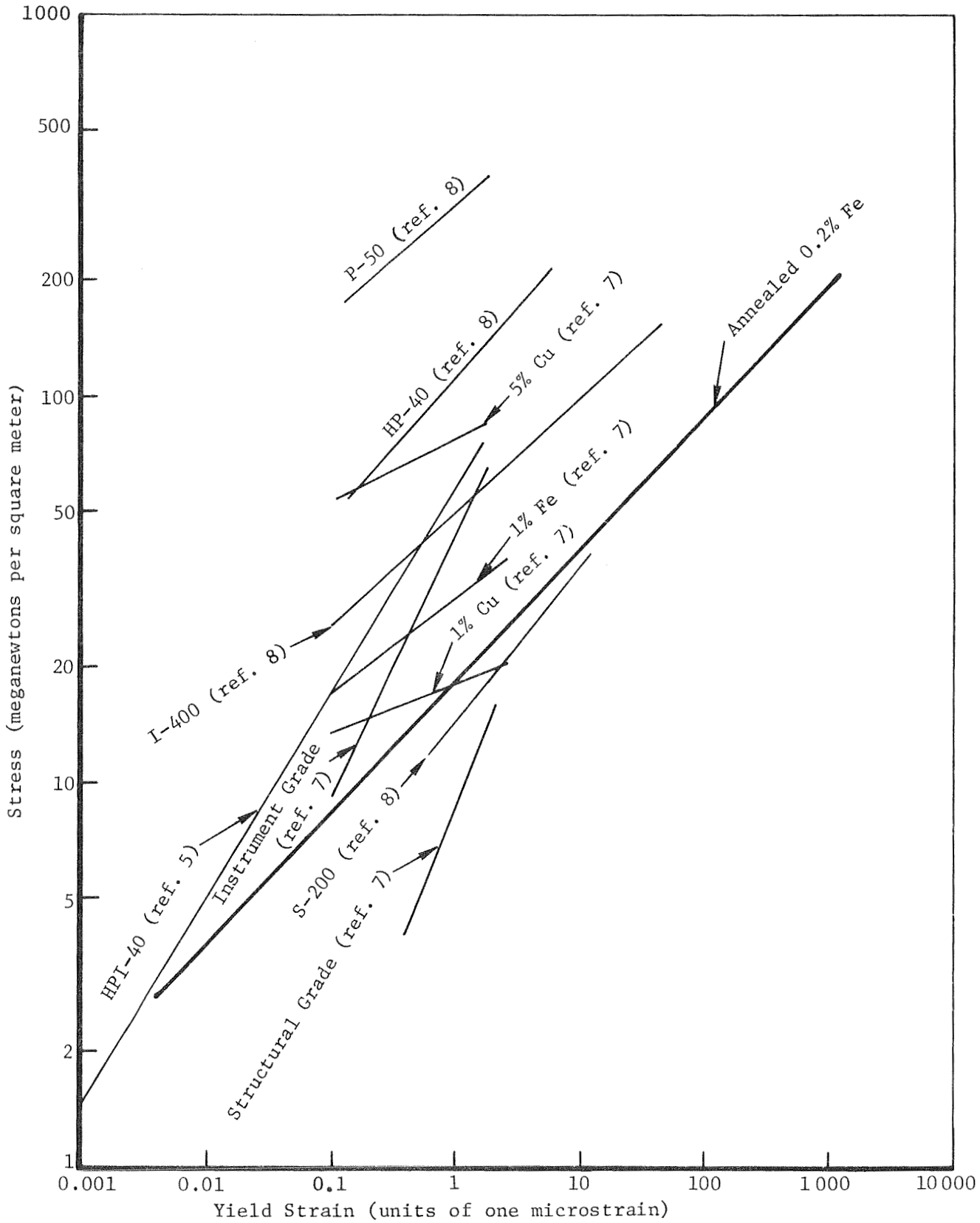


Figure 17: COMPARISON OF BERYLLIUM YIELD MEASUREMENTS WITH PREVIOUS WORK

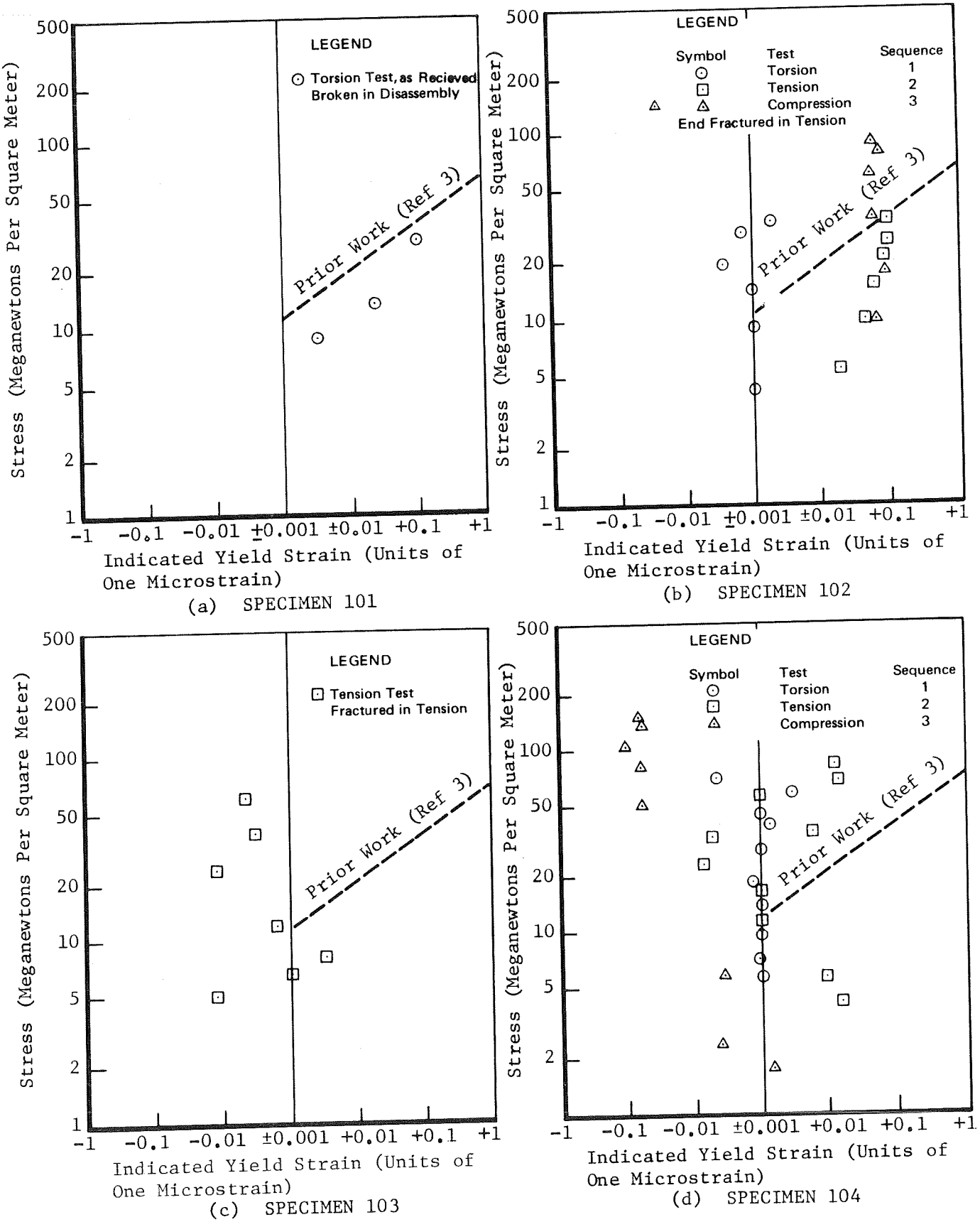


Figure 18: CER-VIT YIELD MEASUREMENTS

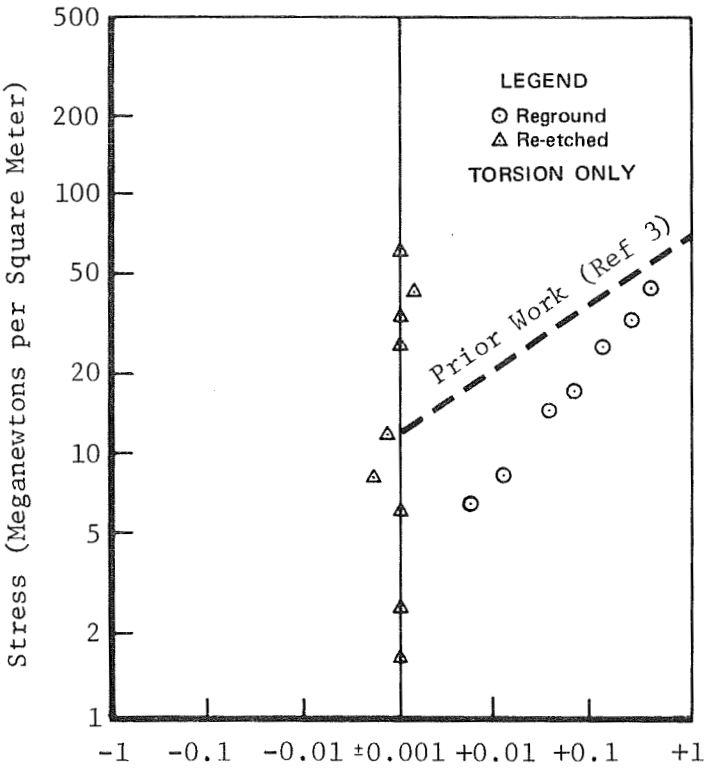


(e) SPECIMEN 104 REGROUND

Figure 18 (Concluded)

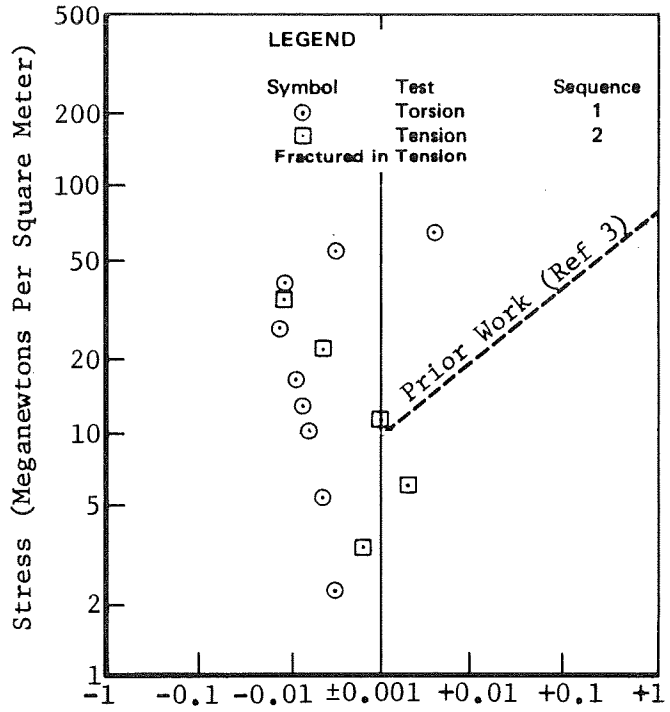


(a) SPECIMEN 111

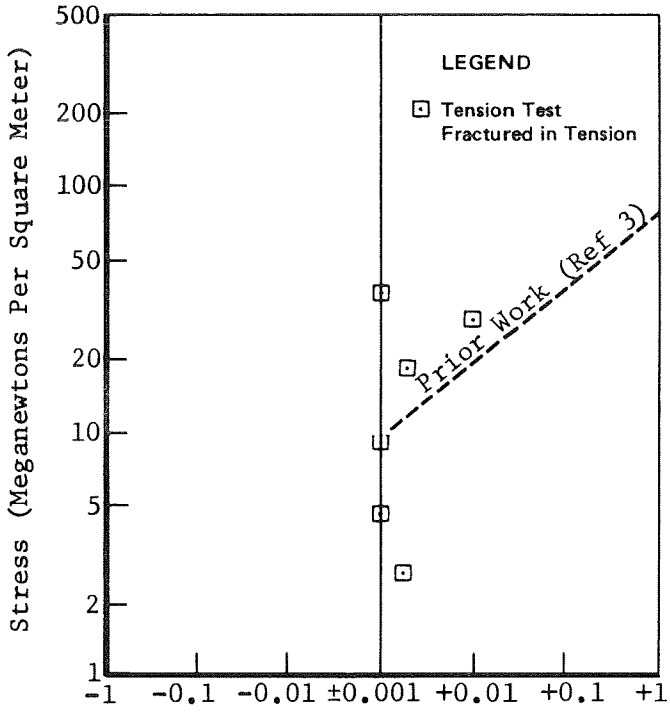


(b) SPECIMEN 112

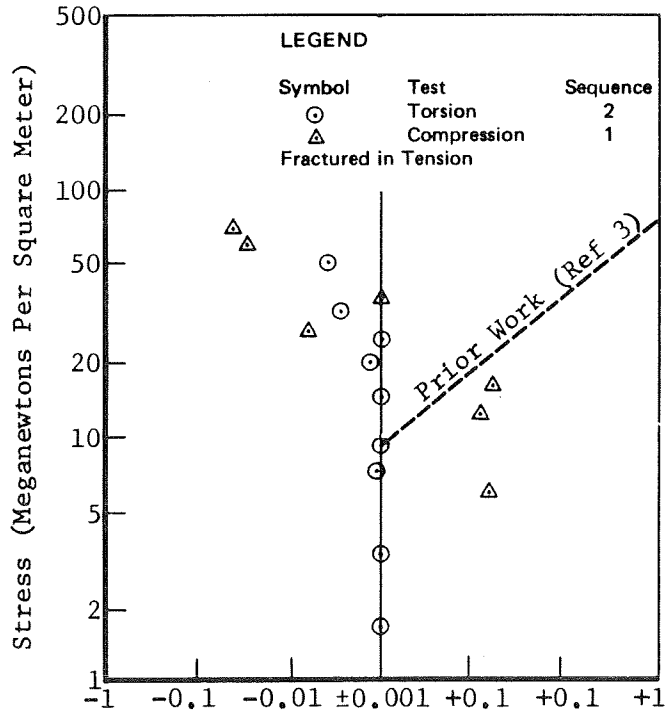


(c) SPECIMEN 113

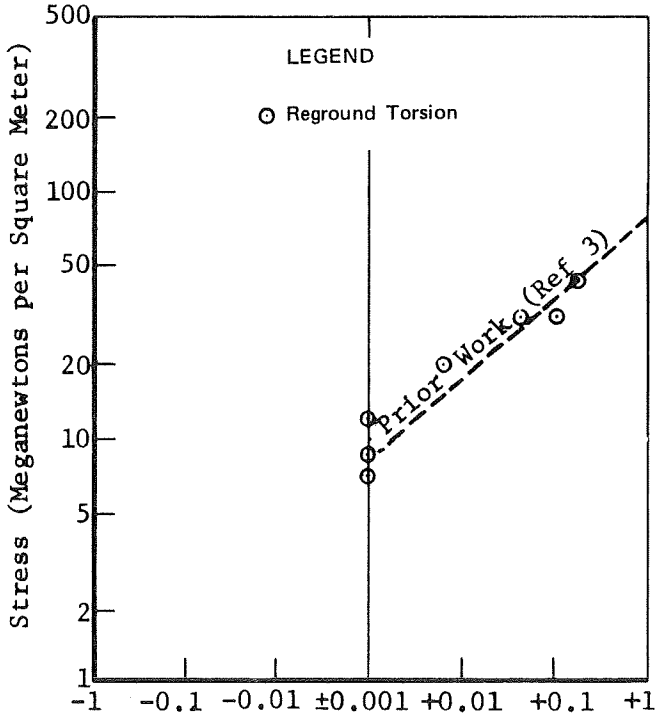


(d) SPECIMEN 114

Figure 19: ULE SILICA YIELD MEASUREMENTS

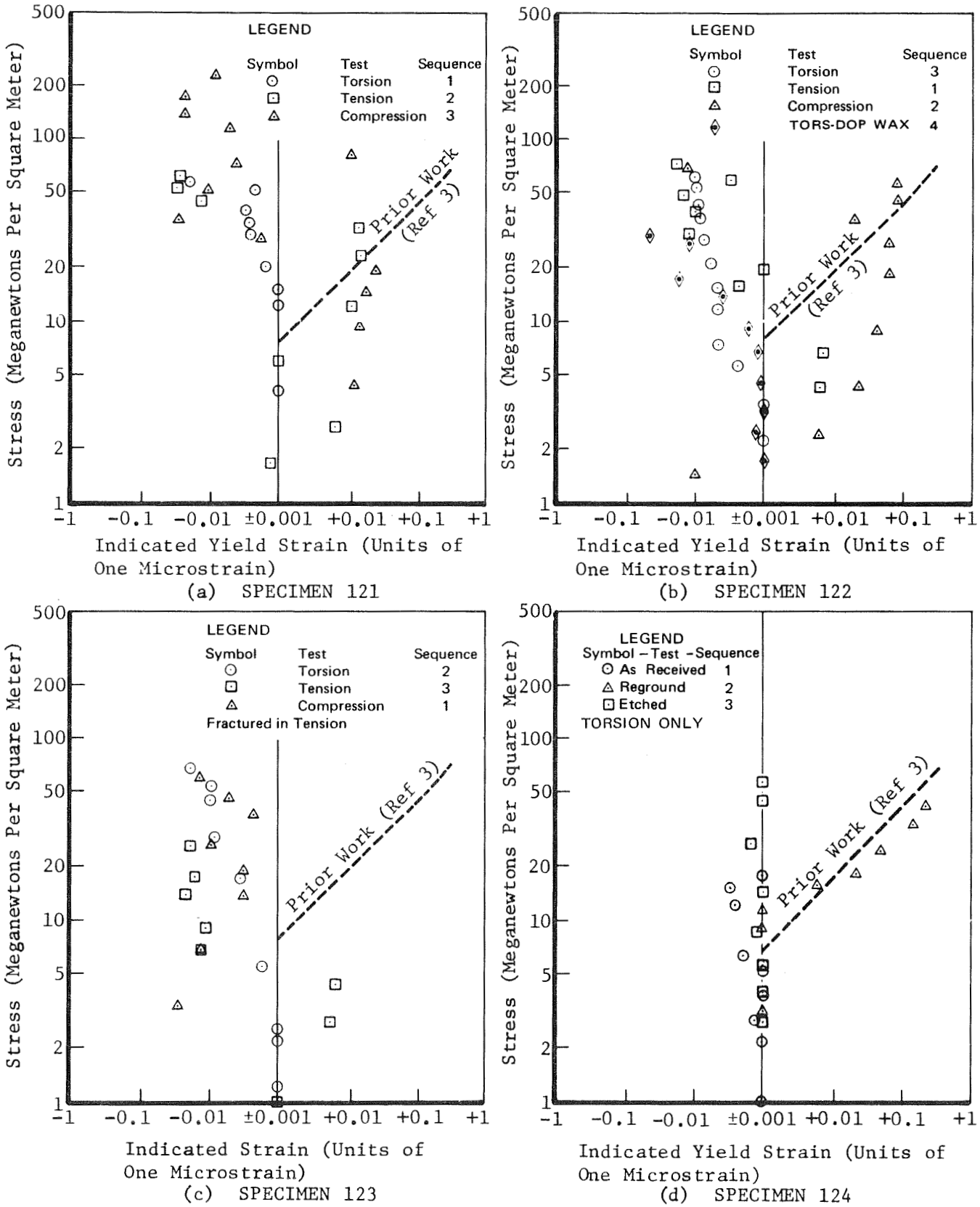


Figure 20: FUSED SILICA YIELD MEASUREMENTS

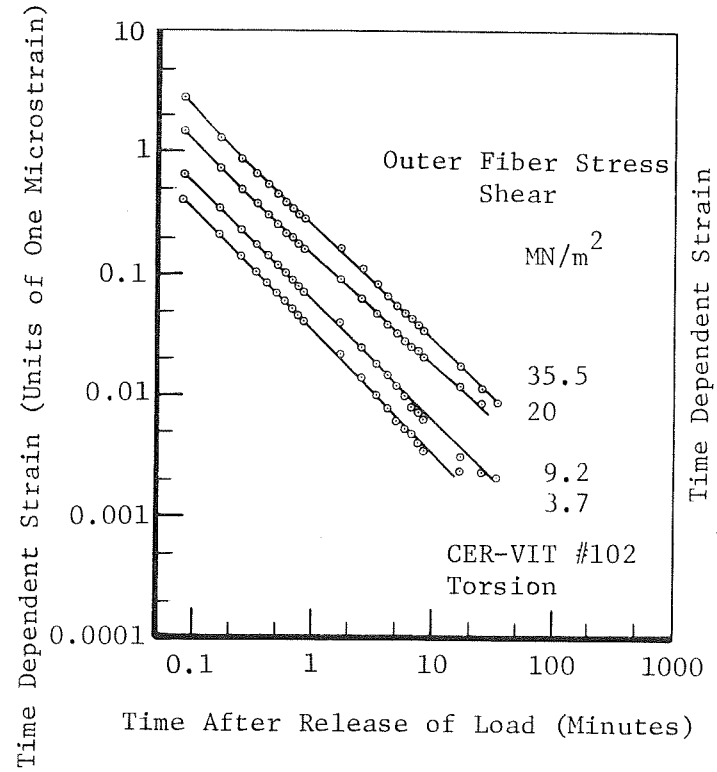


(a) SPECIMEN 102 TORSION

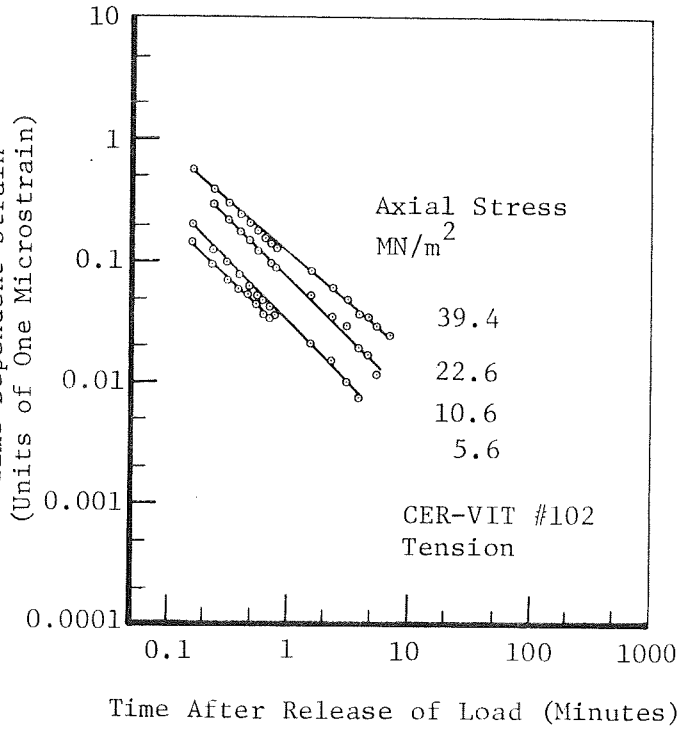


(b) SPECIMEN 102 TENSION

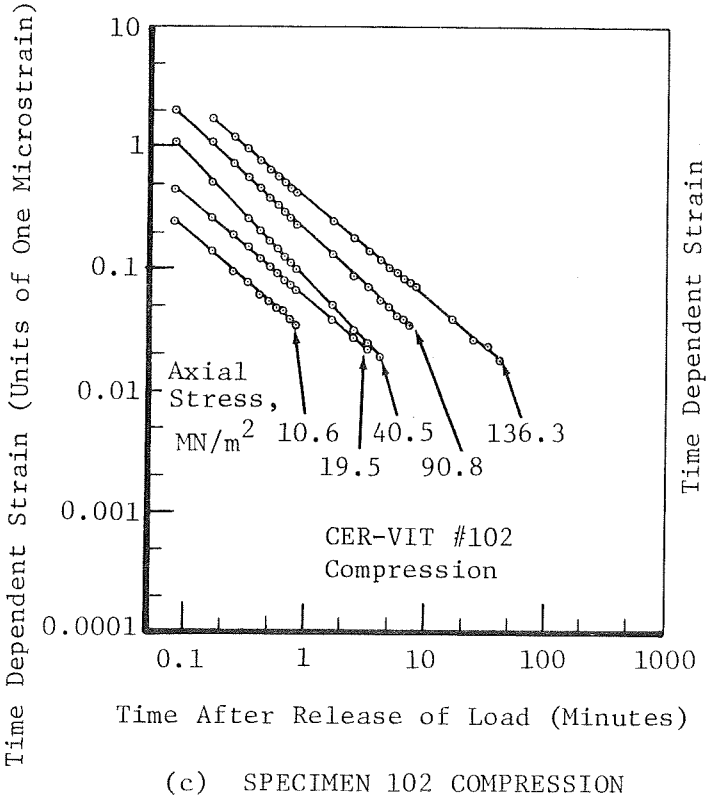


(c) SPECIMEN 102 COMPRESSION

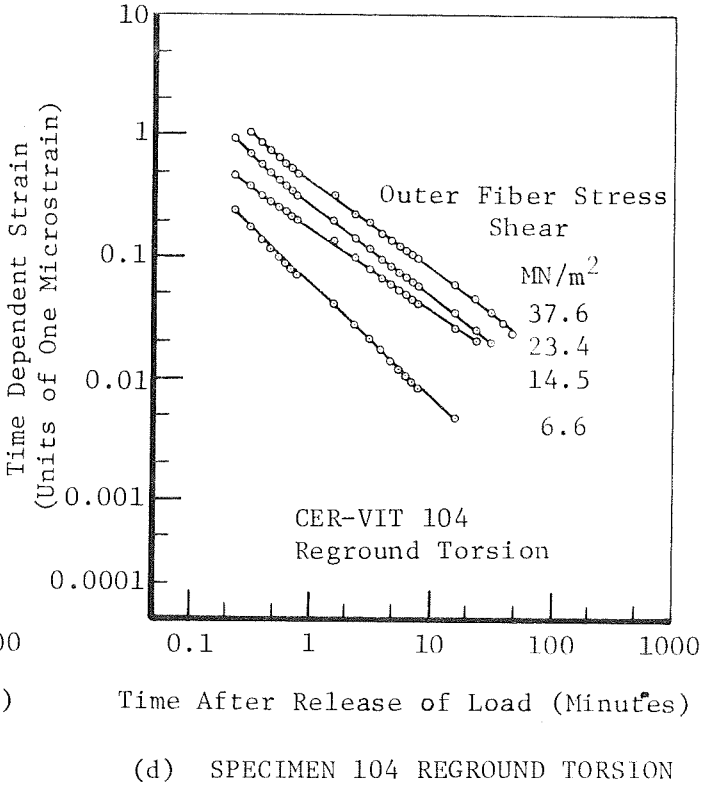


(d) SPECIMEN 104 REGROUND TORSION

Figure 21: CER-VIT TIME DEPENDENT STRAIN

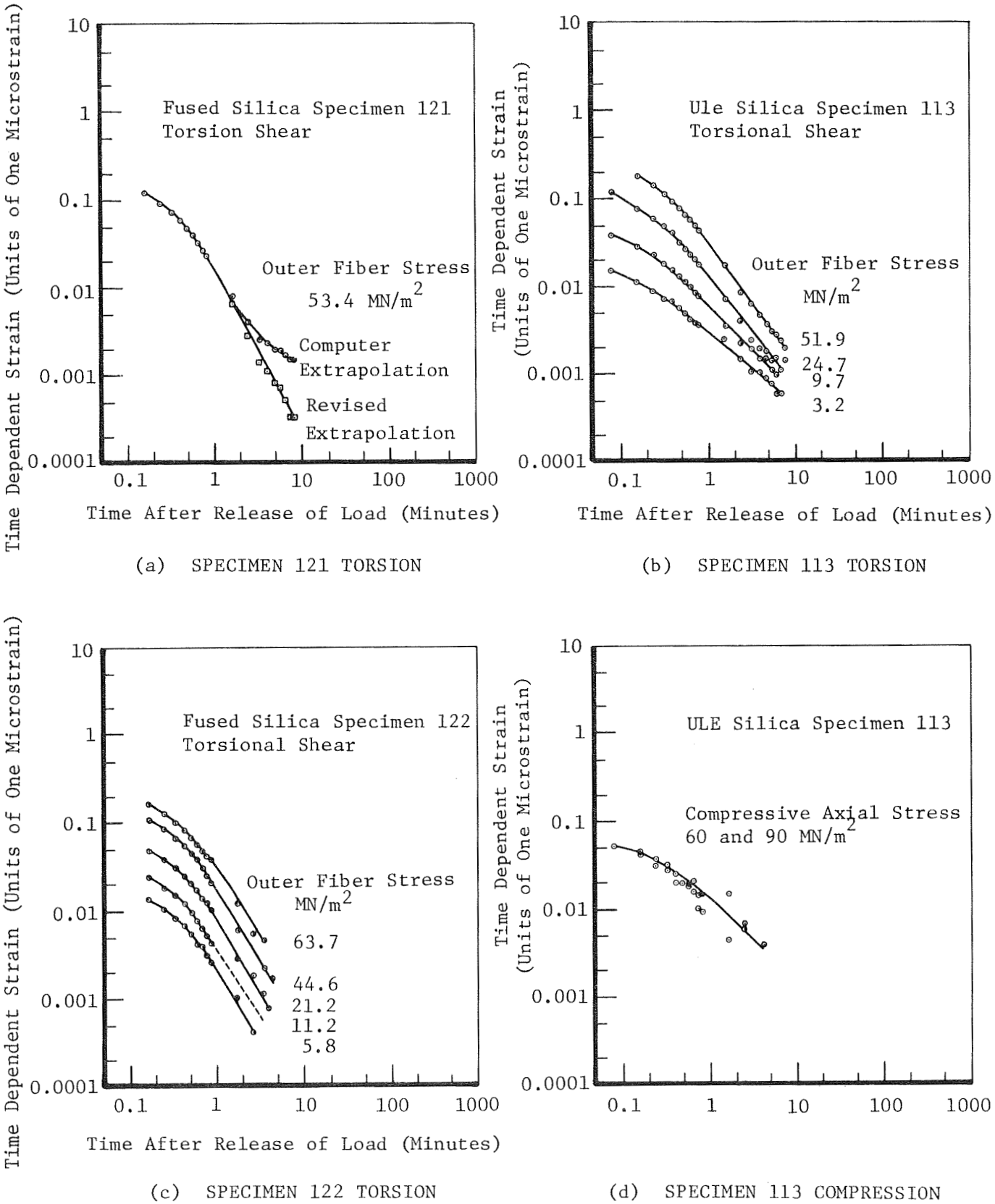


Figure 22: SILICA TIME DEPENDENT STRAIN

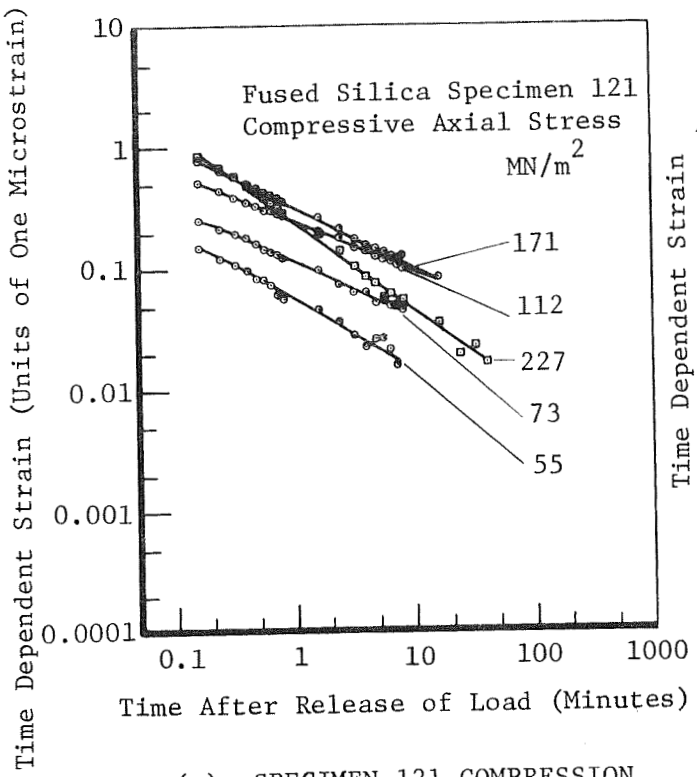


(e) SPECIMEN 121 COMPRESSION

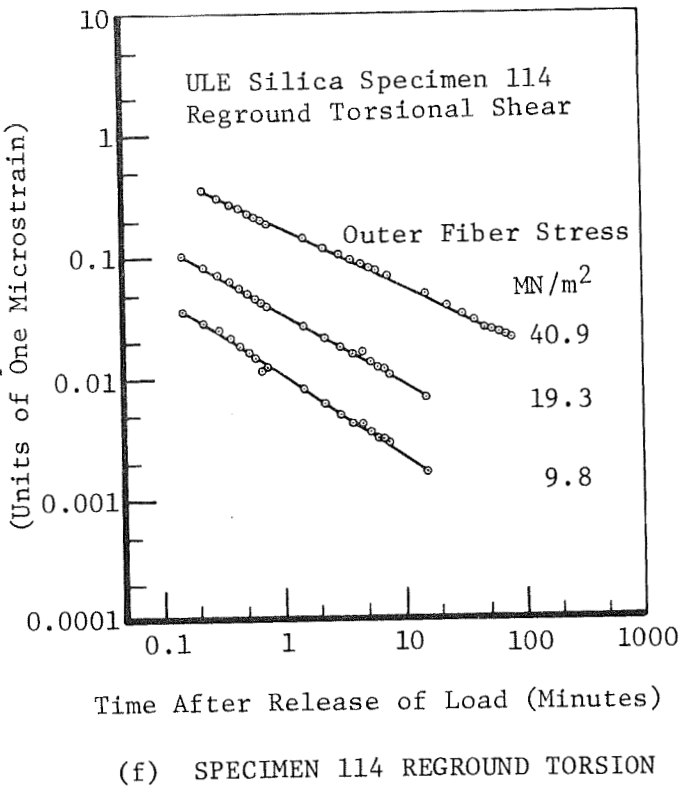


(f) SPECIMEN 114 REGROUND TORSION

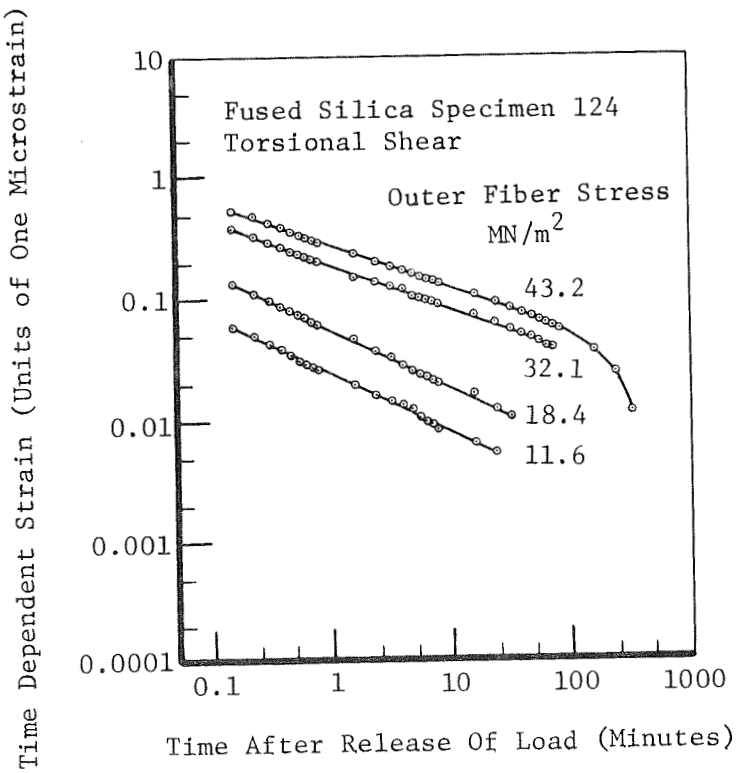


(g) SPECIMEN 124 REGROUND TORSION

Figure 22: (CONCLUDED)

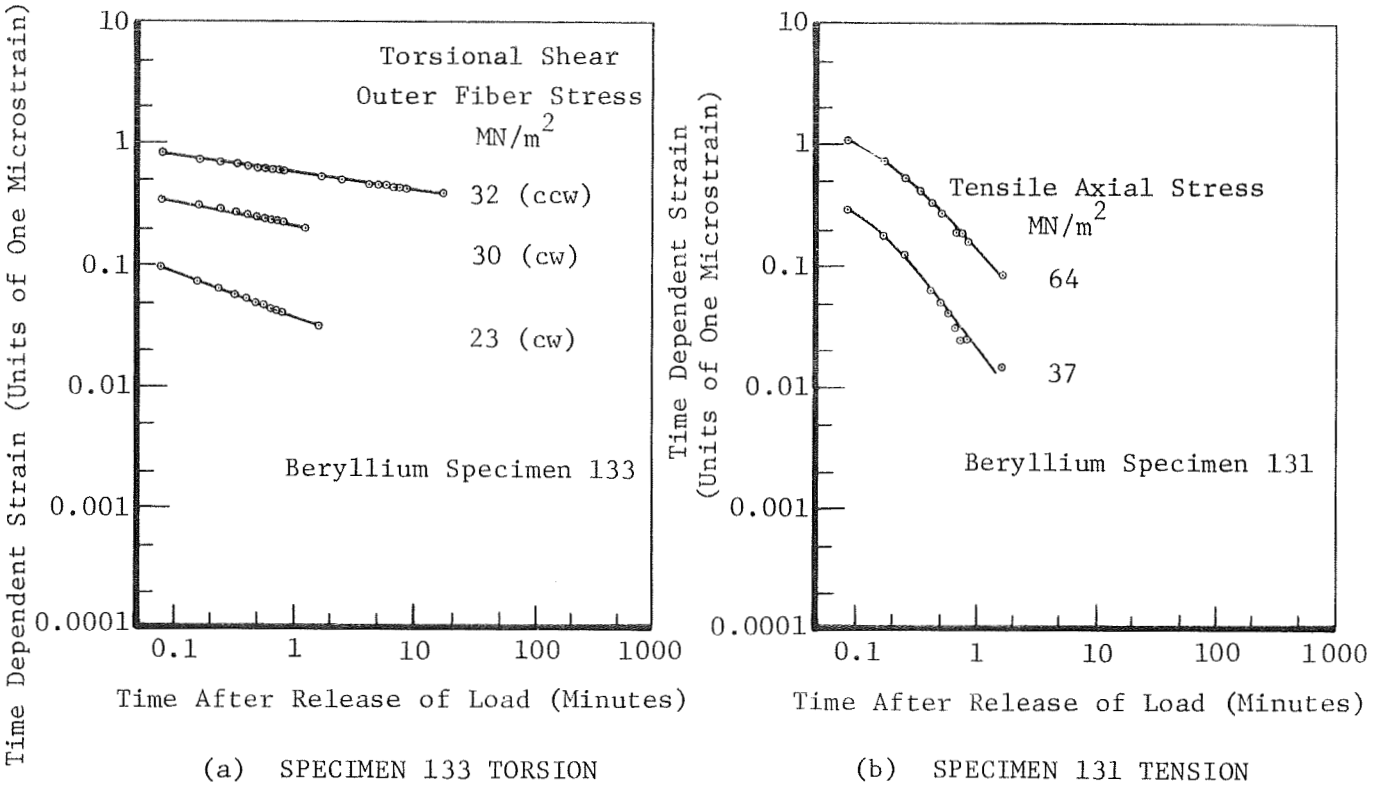


(a) SPECIMEN 133 TORSION

(b) SPECIMEN 131 TENSION

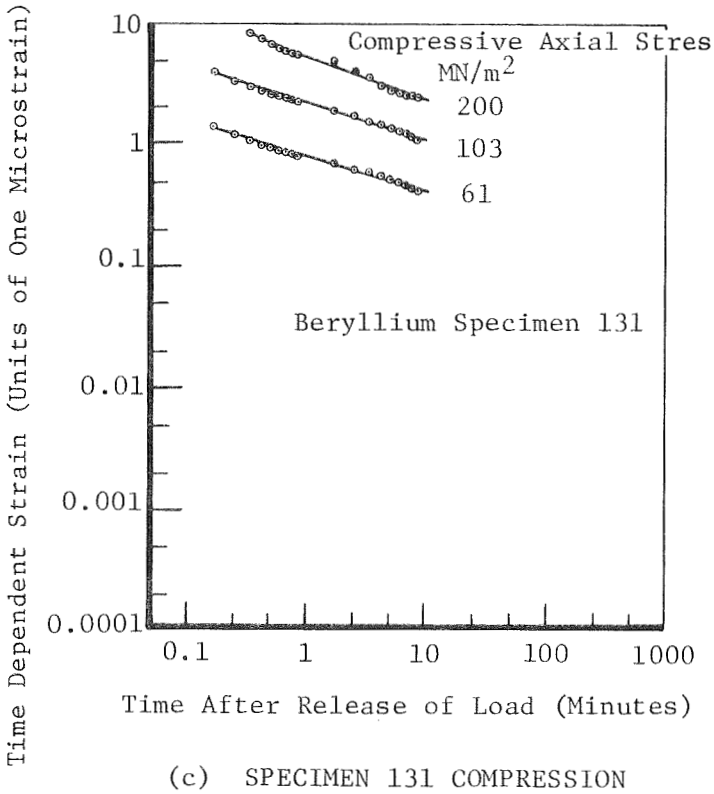


(c) SPECIMEN 131 COMPRESSION

Figure 23 : BERYLLIUM TIME DEPENDENT STRAIN

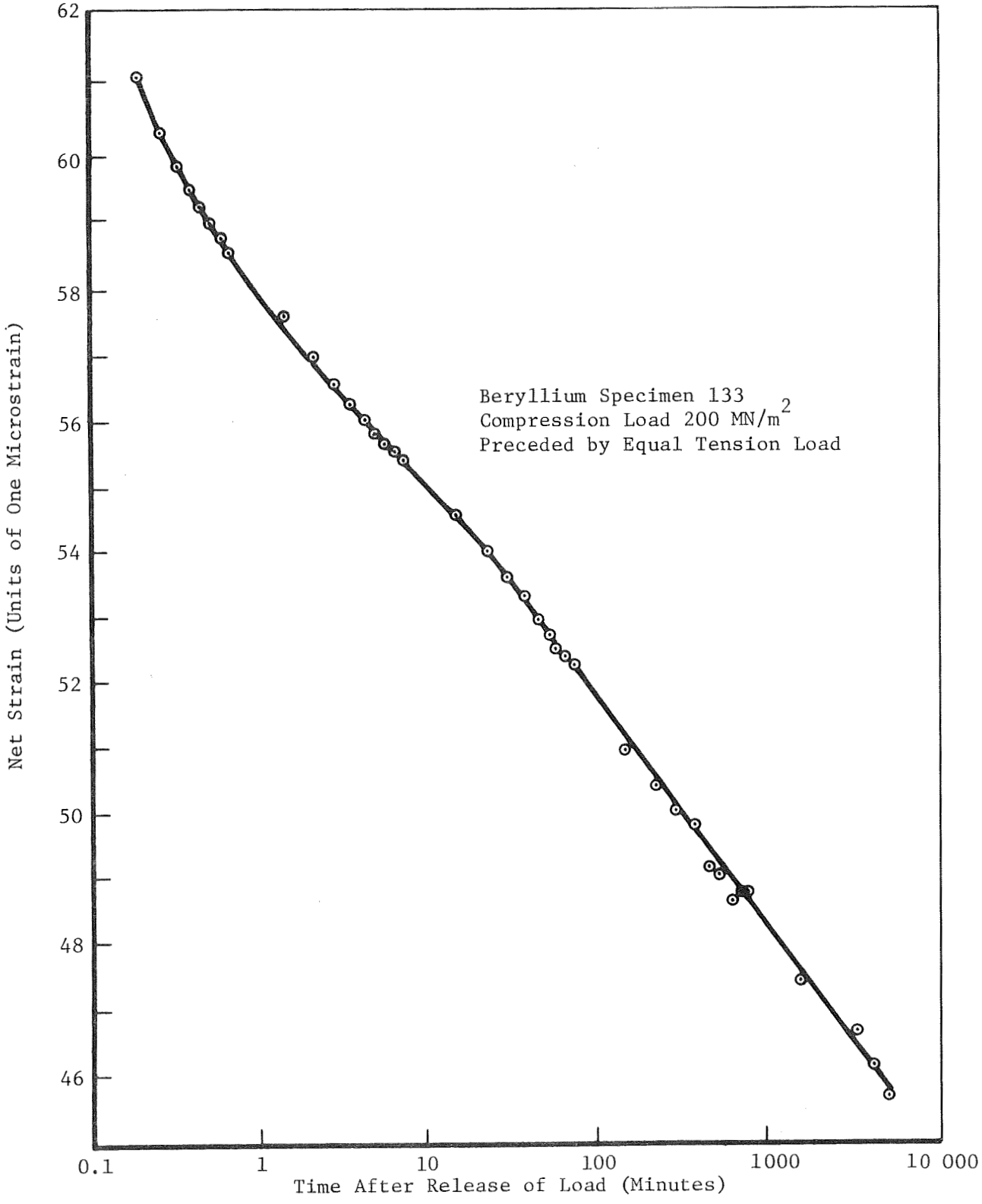


(d) SPECIMEN 133 AXIAL-LONG TERM

Figure 23: (CONCLUDED)

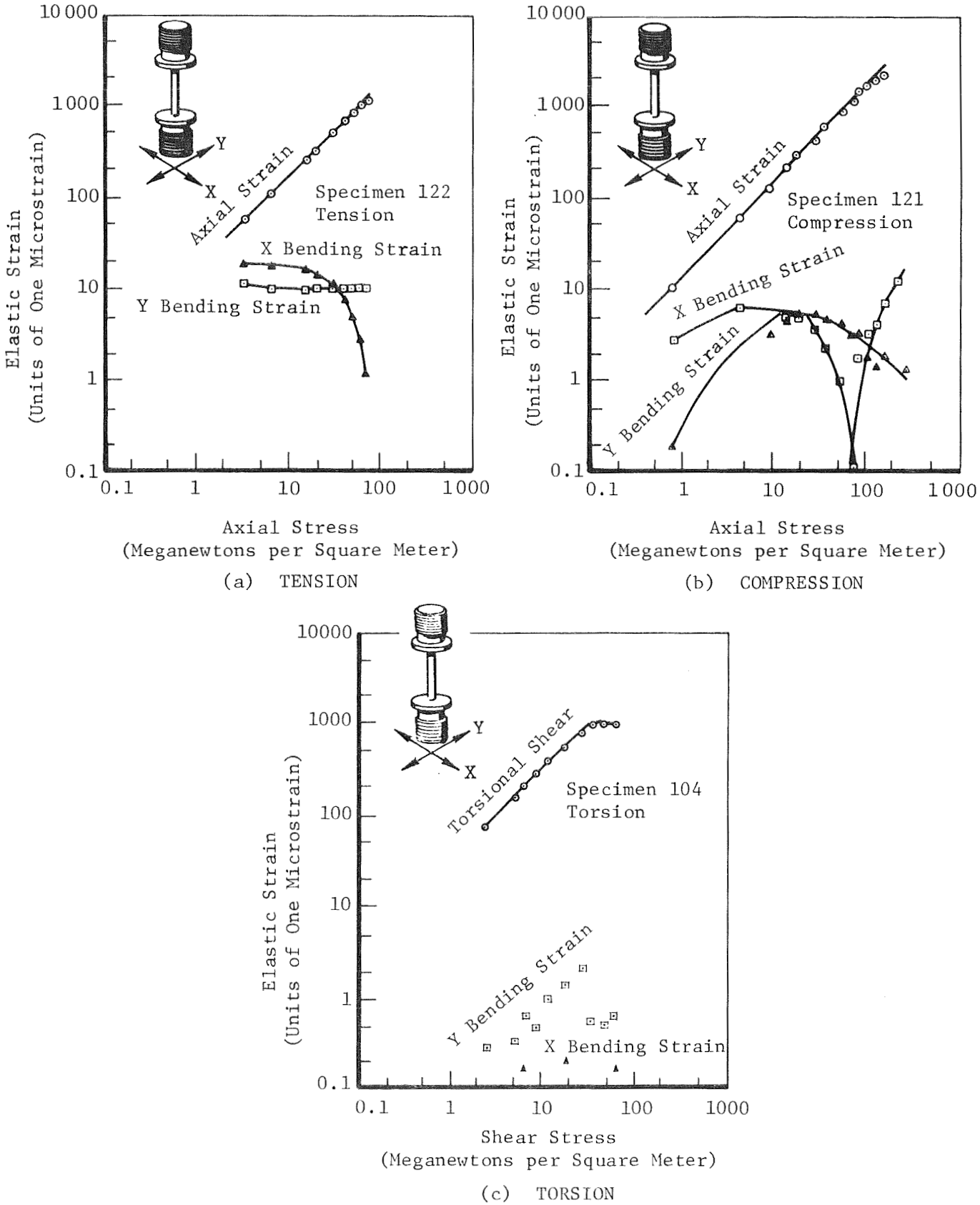


Figure 24: SPECIMEN BENDING STRAIN

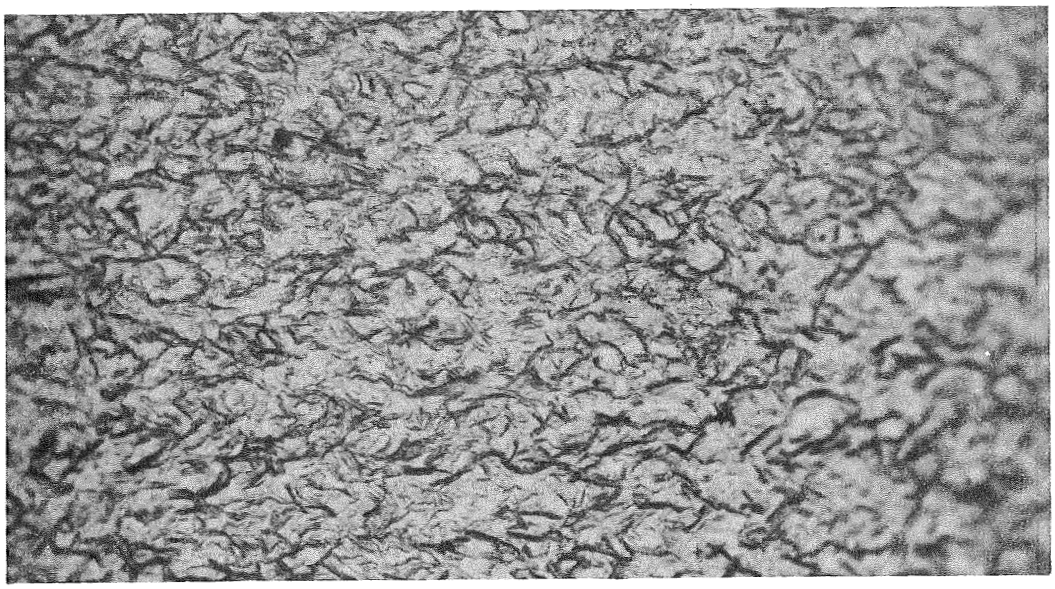

A. Before Etch

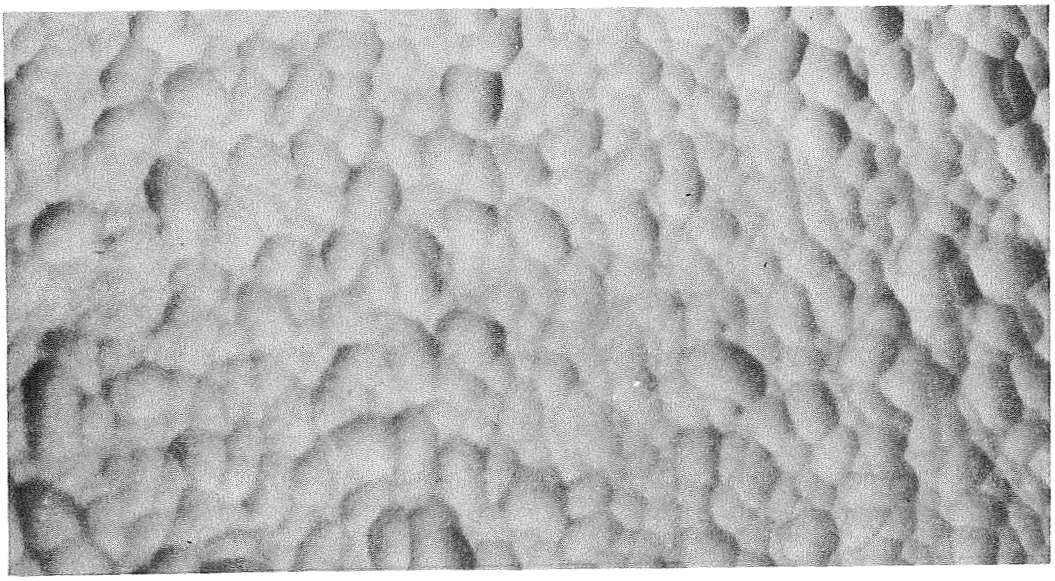

B. After Etch

Figure A.1: CER-VIT SURFACE CHARACTERISTICS
MAGNIFICATION 130X
0.1 mm SURFACE REMOVAL

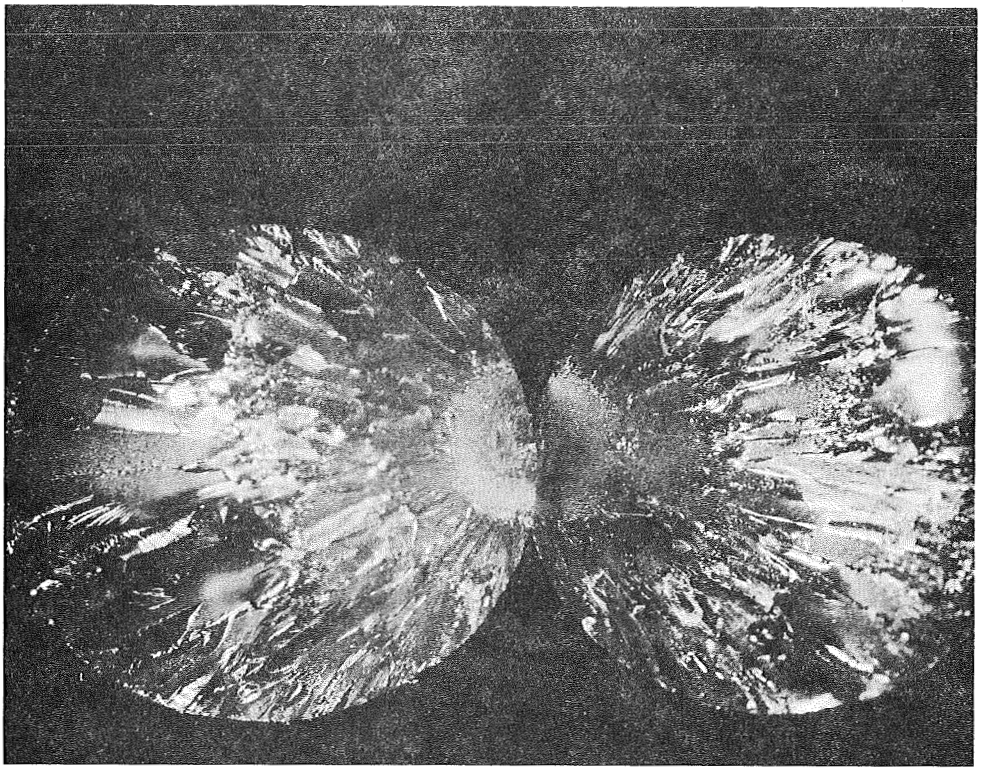

a. Fracture Orientation

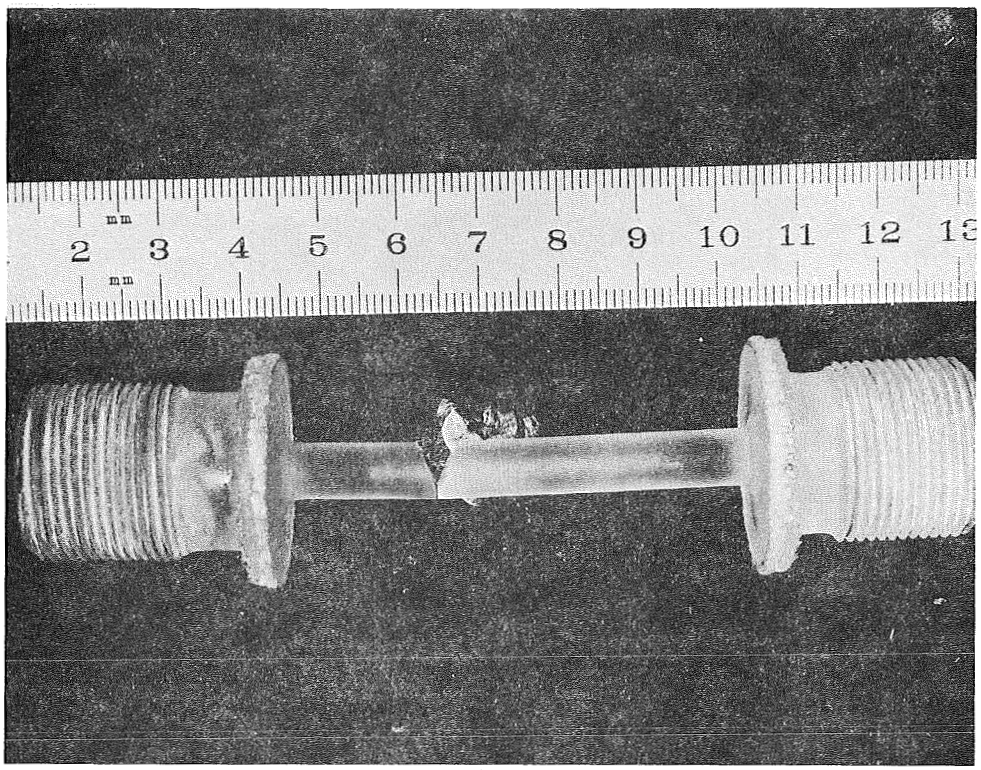


b. Fracture Pattern

Figure A.2: CER-VIT TENSILE FRACTURE

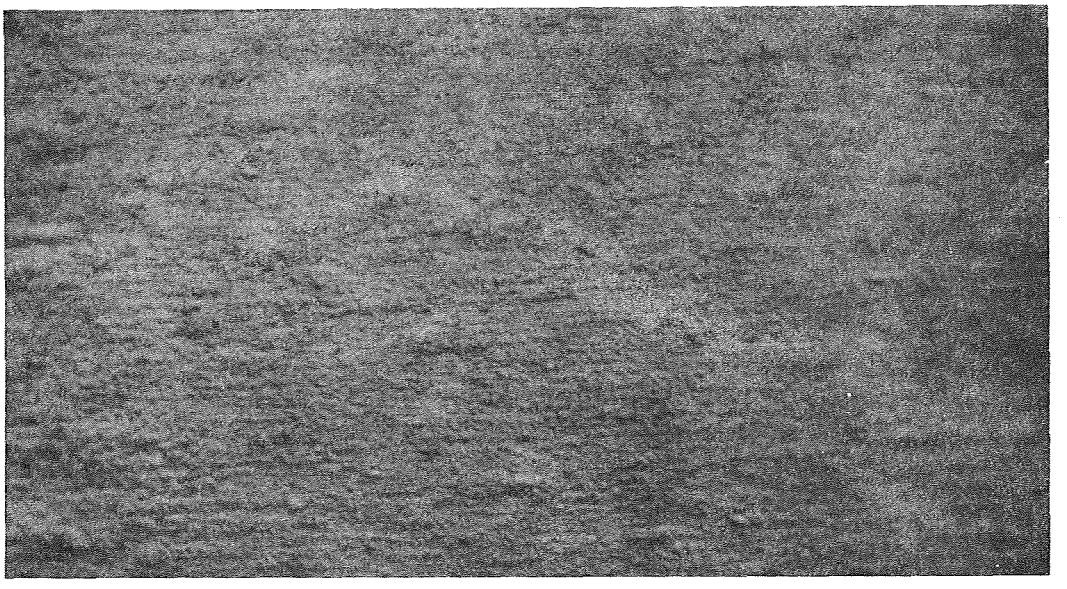

A. Before Etch

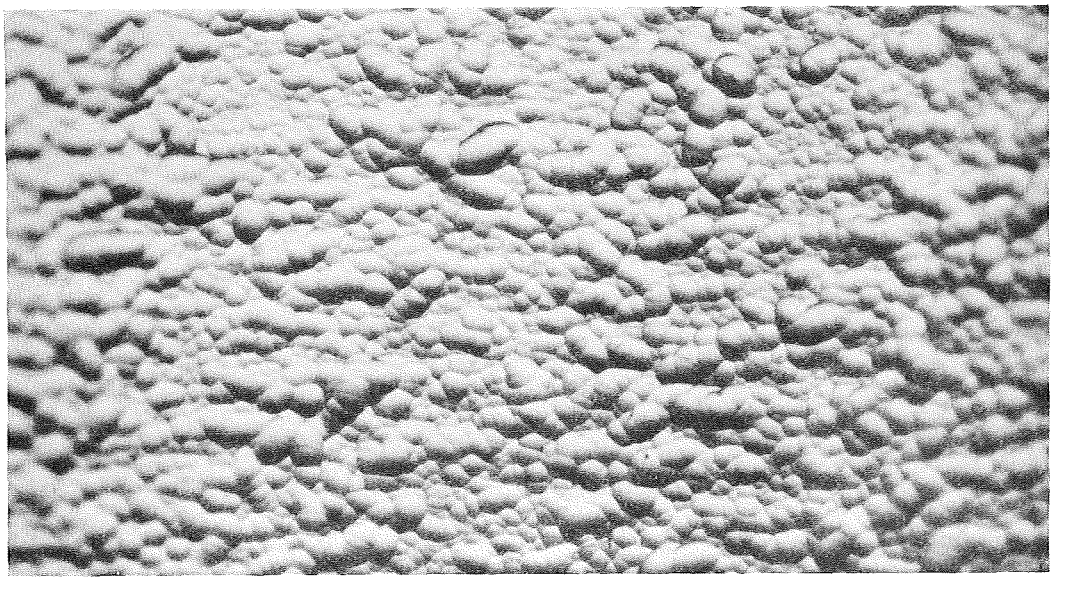

B. After Etch

Figure A.3: SILICA SURFACE CHARACTERISTICS
MAGNIFICATION 130X
0.1 mm SURFACE REMOVAL

Photomicrographs
100 X

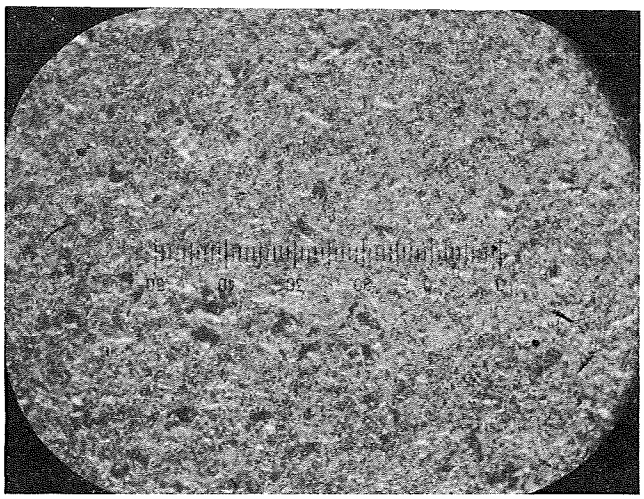

Code #7940 Fused Silica
Surface as Received

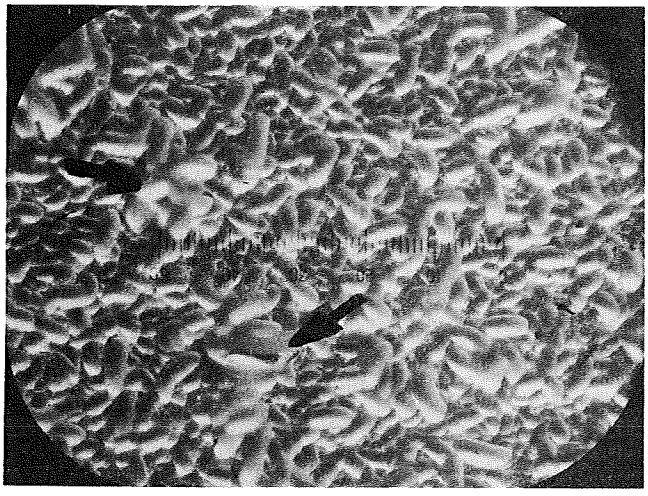

10 Minutes @50% HF
Glass Removal - .0008 inches[1]
Note Deep Checks

(1) 0.0008 inches = 0.02 mm

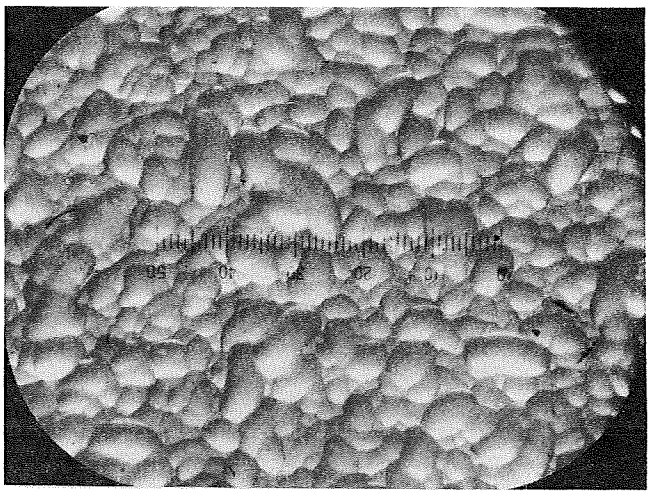

20 Minutes @50% HF
Glass Removal - .0016 inches[2]
Complete Fortification

(2) 0.0016 inches = 0.04 mm

Figure A.4: SILICA SURFACE CHARACTERISTICS
(Photos and Captions Courtesy of Corning Glass)

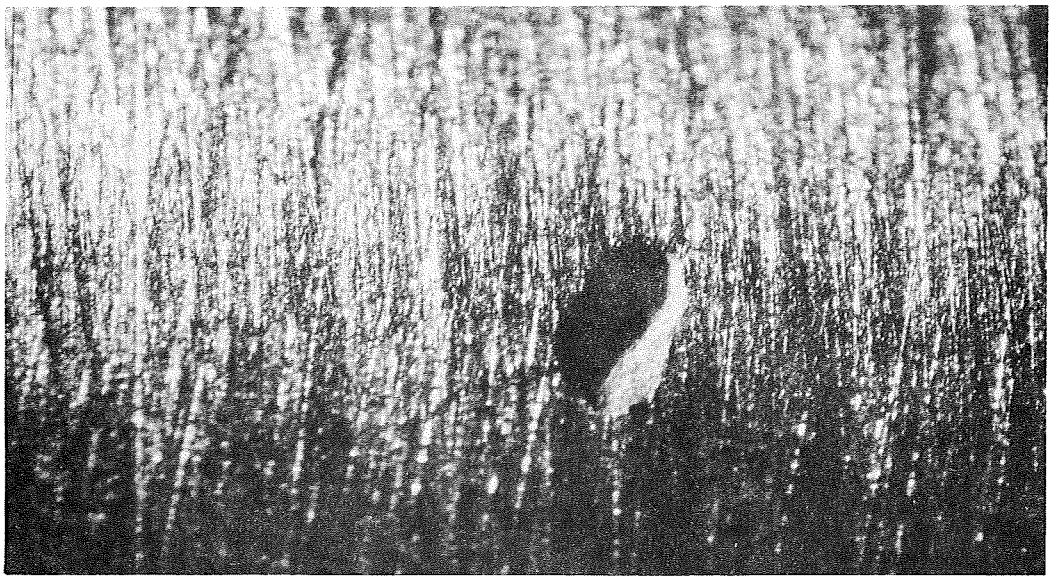

A. Before Etch

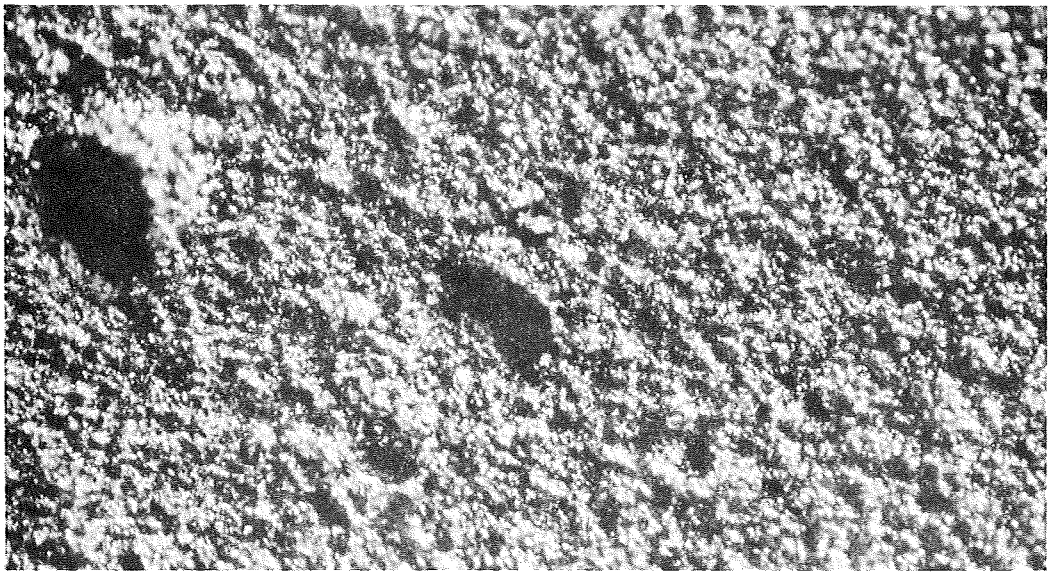

B. After Etch

Figure A.5: BERYLLIUM SURFACE CHARACTERISTICS
MAGNIFICATION 130X
0.25 mm SURFACE REMOVAL